University of Calgary

PRISM Repository **https://prism.ucalgary.ca**

The Vault Open Theses and Dissertations

2015-04-20

Non-invasive Cardiovascular Magnetic Resonance Imaging in Patients with Ischemic Heart Disease

Luu, Judy Mai

Luu, J. M. (2015). Non-invasive Cardiovascular Magnetic Resonance Imaging in Patients with Ischemic Heart Disease (Doctoral thesis, University of Calgary, Calgary, Canada). Retrieved from https://prism.ucalgary.ca. doi:10.11575/PRISM/27116

http://hdl.handle.net/11023/2147

Downloaded from PRISM Repository, University of Calgary

UNIVERSITY OF CALGARY

Non-invasive Cardiovascular Magnetic Resonance Imaging in Patients with Ischemic Heart Disease

by

JUDY MAI LUU

A THESIS

SUBMITTED TO THE FACULTY OF GRADUATE STUDIES

IN PARTIAL FULFILMENT OF THE REQUIREMENTS FOR THE

DEGREE OF DOCTOR OF PHILOSOPHY

CARDIOVASCULAR SCIENCE

CALGARY, ALBERTA

MARCH, 2015

© JUDY MAI LUU 2015

Abstract

Cardiovascular disease remains a significant cause of premature death and disability in developing nations, with an increasing need for early and accurate diagnosis to limit downstream adverse events. By exploiting intracapillary deoxygenated haemoglobin to generate its signal, oxygenation-sensitive cardiovascular magnetic resonance (OS-CMR) or commonly referred to as Blood-Oxygen Level Dependent CMR (BOLD-CMR), is a non-invasive imaging technique that does not require contrast agents or radiation. Therefore, the purpose of this thesis was to build upon the understanding of myocardial oxygenation using CMR in the assessment of ischemic heart disease.

By studying a population that included 34 patients with coronary artery, 32 participants with only coronary risk factors but no established clinical disease, and 11 young, healthy volunteers, we demonstrated that the OS-CMR signal intensity percent changes (ΔSI%) in response to adenosine-induced vasodilation may be a function of both advancing age and decreasing diastolic blood pressure. Furthermore, for the first time, we showed differential features of ΔSI% in the distinctive layers of myocardium using OS-CMR, whereby ΔSI% was much less in the subendocardium compared to the subepicardium in both patients with coronary artery disease (CAD) and in individuals with only risk factors for cardiovascular disease.

From there, we compared this imaging approach to the reference standard of fractional flow reserve (FFR) in 37 patients with suspected or known CAD. OS-CMR did identify abnormal myocardium supplied by coronary arteries with hemodynamically limiting stenoses, confirming a role for OS-CMR in the evaluation of myocardial

ischemia. Complementary comparisons of OS-CMR to the measures of stenosis diameter by QCA and myocardial perfusion by CMR showed weaker correlations.

Finally, in 34 patients with stable CAD, we sought to determine the impact of revascularization plus medical therapy (n=10 patients) versus medical therapy alone (n= 24 patients) on myocardial oxygenation at one-month follow-up. We demonstrated evidence to suggest that percutaneous coronary intervention (PCI) plus medical therapy may increase myocardial oxygenation as measured by OS-CMR. Conversely, patients treated with medical therapy exhibited reduced ΔSI% at the repeat scan, which was most profound in the subendocardium.

Overall, our results suggest that OS-CMR measures of myocardial oxygenation may reflect alterations or dysfunction of the microcirculation and its vasodilatory capacity to compensate in the face of increasing oxygen demands, which may potentially be used as a marker for myocardial ischemia. Further research is needed to demonstrate the prognostic role of OS-CMR in the long-term.

Preface

The layout of the following thesis follows a manuscript-based template, instead of the traditional format. The first chapter will introduce the scope of the thesis and provide a review of the literature as a background for the reader. The second chapter outlines the overarching hypothesis and objectives of the thesis. The three results chapter are presented as individual manuscripts, each with the basic components of an abstract, background, methods, results, discussion/conclusion, and references. The methodology, while similar for each manuscript, is separately written and at times can be repetitive, in order to adhere to the manuscript-based format. Finally, the last two chapters present a general discussion and concluding remarks to unify the overall findings of the thesis.

Acknowledgements

It is with the utmost gratitude and reverence that I begin by thanking my two great mentors and supervisors, Dr. Matthias Friedrich and Dr. Henk ter Keurs. For without their support, guidance, and persistence, I would not be able to accomplish this feat in a timely manner. Your wisdom and approaches to clinical science have taught me far more than I could ever have imagined. For everything and more, thank you.

I must also thank the supportive members of my supervisory committee, including Dr. John Tyberg and Dr. Andrew Howarth, for their strong encouragement and understanding of the various obligations I had throughout this journey. Having reached this point, I would not recommend completing medical school in the midst of a PhD. However, all of you kept pushing me forward, keeping me on track, and advocated for my success. I would also like to extend my gratitude to the rest of the members of my examining committee – Dr. Paolo Raggi and Dr. Hamid Banijamali. Thank you for taking the time to read my thesis and for offering your very welcomed wisdom and experience.

Finally, I would like to thank all my family, friends, co-workers, and Leaders in Medicine team who were always very supportive and understanding. You never once complained for periods when I was stuck working away and needed to reschedule for the third time. I hope you are proud of me after all, thank you.

Table of Contents

Preface iv
Acknowledgements v
Table of Contents vi
List of Tables ix
List of Figures and Illustrations x
List of Symbols, Abbreviations and Nomenclature xii
Epigraph xiii

Chapter One: BACKGROUND 1
1.1 INTRODUCTION 1
1.2 REVIEW OF LITERATURE 2
1.2.1 Myocardial Ischemia 2
1.2.1.1 Mechanism of myocardial ischemia 2
1.2.1.2 Consequence of chronic ischemia 5
1.2.1.3 Clinical implications of myocardial ischemia 6
1.2.2 Cardiac imaging for assessment of Coronary Artery Disease 7
1.2.2.1 Stress Testing 8
1.2.2.2 Mechanisms of Adenosine 10
1.2.2.3 Dobutamine Echocardiography 11
1.2.2.4 Thallium SPECT imaging 11
1.2.2.5 PET, CT, and X-Ray Coronary Angiography 13
1.2.3 Coronary blood flow 14
1.2.3.1 Autoregulation of Coronary Blood Flow 14
1.2.3.2 Measurements of Coronary Flow Reserve 17
1.2.3.3 Derivation of Fractional Flow Reserve from Coronary Flow Reserve 18
1.2.3.4 FFR as the standard for functional assessment of coronary stenosis 20
1.2.4 Cardiovascular Magnetic Resonance for Coronary Artery Disease 21
1.2.4.1 Basics of MR Physics 22
1.2.4.2 Generation of MRI Signal 24
1.2.4.3 Basic Imaging Sequences 26
1.2.4.4 Blood Oxygen Level Dependent (BOLD) contrast 32
1.2.4.5 Steady State Free Precession (SSFP) 34
1.2.4.6 Current CMR Protocol for Hypoxia Assessment 35
1.2.4.7 Limitations of CMR myocardial perfusion 36
1.2.4.8 Oxygen-Sensitive Cardiovascular Magnetic Resonance 37
1.3 References 48

Chapter Two: HYPOTHESES AND OBJECTIVES 59

Chapter Three: RESULTS – FIRST MANUSCRIPT 60
3.1 Title: Regional Assessment of Myocardial Oxygenation using Oxygen-Sensitive Cardiovascular Magnetic Resonance 60
3.2 Abstract 61
3.3 Abbreviations: 63

3.4 Background 64
3.5 Methods 65
3.5.1 Study population 65
3.5.2 CMR imaging protocol 66
3.5.3 Analysis of Oxygenation-Sensitive Images 67
3.5.4 Statistical Analysis 69
3.6 Results 70
3.6.1 Myocardial Oxygenation in Different Myocardial Layers 74
3.6.2 Inter- and Intra-observer Variability 76
3.6.3 Correlation Analyses and Multiple Stepwise Regression 78
3.7 Discussion 84
3.7.1 Role of Age and Diastolic Blood Pressure in Myocardial Oxygenation 85
3.7.2 Oxygen-sensitive CMR for the evaluation of microvascular dysfunction 88
3.7.3 Limitations 91
3.8 Conclusion 92
3.9 References 93

Chapter Four: RESULTS – SECOND MANUSCRIPT 97
4.1 Title: Relationship of Vasodilator-Induced Changes of Myocardial Oxygenation with the Severity of Coronary Artery Stenosis – a Study using Oxygenation-Sensitive Cardiovascular Magnetic Resonance 97
4.2 Abstract 98
4.3 Abbreviations: 100
4.4 Background 101
4.5 Methods 102
4.5.1 Study population 102
4.5.2 CMR imaging protocol 103
4.5.3 Analysis of Oxygenation-Sensitive Images 104
4.5.4 Analysis of First-Pass Perfusion and Late-Gadolinium Enhancement Imaging 105
4.5.5 Assessment of Fractional Flow Reserve (FFR) 105
4.5.6 Quantitative Coronary Angiography 106
4.5.7 Statistical Analysis 107
4.6 Results 108
4.6.1 Relationship of Vasodilator-Induced Myocardial Oxygenation Changes with FFR 111
4.6.2 Relationship of Myocardial Oxygenation with Conventional QCA, CMR First-Pass Perfusion Imaging, and Late Enhancement 114
4.6.3 Association of FFR Values with Inducible Increases of Myocardial Oxygenation 117
4.6.4 Diagnostic Performance of Oxygenation-Sensitive CMR for Detecting Coronary Artery Stenosis With an FFR of <0.80 118
4.7 Discussion 120
4.7.1 OS-CMR as a Marker for Myocardial Ischemia 120
4.7.2 Limitations of FFR 123
4.7.3 Exploring the Components Contributing to Tissue Oxygenation 125
4.7.4 Limitations 126

4.8 Conclusion 127
4.9 References 128

Chapter Five: RESULTS – THIRD MANUSCRIPT 132
5.1 Title: Impact of Medical Management with or without Percutaneous Coronary Intervention on Myocardial Oxygenation as assessed by OS-CMR 132
5.2 Abstract 133
5.3 Abbreviations 135
5.4 Background 136
5.5 Methods 137
5.5.1 Study population 137
5.5.2 Coronary Angiography Recommendation 138
5.5.3 CMR imaging protocol 138
5.5.4 Analysis of Oxygenation-Sensitive Images 139
5.5.5 Statistical Analysis 140
5.6 Results 141
5.7 Discussion 148
5.7.1 Evidence for Benefit of PCI plus Optimal Medical Therapy 148
5.7.2 OS-CMR for the Evaluation of Stable CAD 149
5.7.3 Limitations 152
5.8 Conclusion 153
5.9 References 154

Chapter Six: DISCUSSION 157
6.1 Synopsis 157
6.2 A Case for Dysfunctional Autoregulation or Vasodilatory Capacity 158
6.2.1 Confounders of Oxygen-Sensitive Contrast 160
6.3 Relation of the Present Work to Previously Published Studies 162
6.4 Troubleshooting 164
6.4.1 BOLD-CMR at Higher Field Strengths 165
6.5 Future Directions 167
6.6 References 170

Chapter Seven: CONCLUSION AND CLOSING REMARKS 173

Chapter Eight: APPENDIX 174

List of Tables

Table 3-1: Patient Demographics and Baseline CMR parameters. 70

Table 3-2: Participant Risk Factors for Coronary Artery Disease 72

Table 3-3: Patient Baseline Medications..... 73

Table 3-4: Pearson's Correlations between whole myocardial, subepicardial, and subendocardial BOLD ΔSI% to patient demographic characteristics..... 80

Table 4-1: Patient Demographics and Baseline Clinical Data. 110

Table 5-1: Patient Demographics and Baseline CMR parameters. 143

Table 5-2: Patient Coronary Risk Factors and Medications. 144

Table 5-3: OS-CMR signal intensity percent changes baseline and one-month follow-up CMR scans for patients recommended for medical management. 145

Table 5-4: OS-CMR signal intensity percent changes baseline and one-month follow-up CMR scans for patients recommended for and proceeded with PCI plus medical management. 146

Figure 6-1: Example of the effect of shimming in short-axis slice of a patient with CAD. 167

List of Figures and Illustrations

Figure 1-1: Pressure-flow diagram depicting concept of coronary flow reserve. 15

Figure 1-2: Theoretical derivation of FFR. 19

Figure 1-3: MRI Signal Generation. 25

Figure 1-4: T1 and T2 Decay curves. 28

Figure 1-5: Spin Echo using an 180° refocusing pulse. 29

Figure 1-6: Gradient echo with field gradients 31

Figure 1-7: Effect of deoxygenated hemoglobin on magnetic field and resultant signal. 33

Figure 1-8: The BOLD effect is governed by T2* decay. 34

Figure 1-9: Illustration of the origins of the BOLD effect in fMRI. 38

Figure 1-10: Blood T2* reflects volume percent of deoxygenated hemoglobin. 40

Figure 1-11: Hypothetical construct of the effect of pharmacological vasodilation on BOLD signal intensity. 42

Figure 1-12: Hypothetical construct of the effect of stenosis on BOLD signal intensity. 43

Figure 3-1: Manual tracing of contours for automatic computer generated signal intensity extraction. 68

Figure 3-2: Mean OS-CMR signal intensity percent changes in the whole myocardium, subepicardium and subendocardium in study participants. 75

Figure 3-3: Bland Altman graphical illustration of interobserver variability between two readers (R1 and R2) with Y-axis lines representing mean differences±1.96 x SD. 76

Figure 3-4: Bland Altman graphical illustration of intraobserver variability with Y-axis lines representing mean differences±1.96 x SD. 77

Figure 3-5: Correlation of independent predictive variable of age to signal intensity percent change in the subendocardium. 81

Figure 3-6: Correlation of the independent predictive variable, diastolic blood pressure, to signal intensity percent change in the subendocardium. 82

Figure 3-7: Correlation of the independent predictive variable, BMI, to signal intensity percent change in the subendocardium..... 83

Figure 4-1: Flow of patients through the study. 109

Figure 4-2: OS-CMR versus FFR ranges. 111

Figure 4-3: Relationship of OS-CMR to FFR, with or without CTOs..... 113

Figure 4-4: OS-CMR versus QCA. 115

Figure 4-5: Patient image example. 116

Figure 4-6: Relationship of FFR to OS-CMR, using threshold cut-off of 4.8%..... 119

Figure 5-1: OS-CMR signal intensity percent changes at baseline and one-month follow-up CMR scans..... 147

Figure 6-1: Example of the effect of shimming in short-axis slice of a patient with CAD. 167

Figure A-1: Absolute OS-CMR signal intensity changes from baseline to hyperemia in whole myocardium (See Figure 3-2 in Chapter 3 Results – Regional assessment of myocardial oxygenation using Oxygen-Sensitive Cardiovascular CMR)..... 174

Figure A-2: Absolute OS-CMR signal intensity changes from baseline to hyperemia in subendocardium (See Figure 3-2 in Chapter 3 Results – Regional assessment of myocardial oxygenation using Oxygen-Sensitive Cardiovascular CMR). 175

Figure A-3: Absolute OS-CMR signal intensity changes from baseline to hyperemia in subepicardium (See Figure 3-2 in Chapter 3 Results – Regional assessment of myocardial oxygenation using Oxygen-Sensitive Cardiovascular CMR). 176

Figure A-4: Absolute OS-CMR signal intensity changes from baseline to hyperemia in subendocardium correlated to predictive variable, age (See Figure 3-5 in Chapter 3 Results – Regional assessment of myocardial oxygenation using Oxygen-Sensitive Cardiovascular CMR). 177

Figure A-5: Absolute OS-CMR signal intensity changes from baseline to hyperemia in subendocardium correlated to predictive variable, diastolic blood pressure (See Figure 3-6 in Chapter 3 Results – Regional assessment of myocardial oxygenation using Oxygen-Sensitive Cardiovascular CMR). 178

Figure A-6: Absolute changes from baseline to hyperemia of OS-CMR signal intensity as a function of FFR ranges (see Figure 4-2; Chapter 4 Results: Relationship of Vasodilator-Induced Changes of Myocardial Oxygenation with the Severity of Coronary Artery Stenosis…). 179

List of Symbols, Abbreviations and Nomenclature

Symbol	Definition
ATP	Adenosine Triphosphate
BOLD	Blood Oxygen Level Dependent
CAD	Coronary Artery Disease
CFR	Coronary Fractional Reserve
CMR	Cardiovascular Magnetic Resonance
CT	Computed Tomography
DeoxyHb	Deoxygenated Hemoglobin
DE	Delayed Enhancement
Echo	Echocardiography
FFR	Fractional Flow Reserve
fMRI	Functional Magnetic Resonance Imaging
LGE	Late-Gadolinium Enhancement
LV	Left Ventricle/Ventricular
NADH	Nicotinamide Adenine Dinucleotide Hydride
OS-CMR	Oxygen(ation)-sensitive Cardiovascular Magnetic Resonance
PCI	Percutaneous Coronary Intervention
PCr	Creatine phosphate
PET	Positron Emission Tomography
SPECT	Single-Photon Emission Computed Tomography
SSFP	Steady State Free Precession

Epigraph

"And, when you want something [enough],

all the universe conspires in helping you to achieve it."

–Paulo Coelho, *The Alchemist*

Chapter One: BACKGROUND

1.1 INTRODUCTION

According to most recent Canadian statistics, cardiovascular disease is the second leading cause of death[1] and within every seven minutes, a person will die from heart disease or stroke. In 2008, over half of all cardiovascular deaths were due to ischemic heart disease and by 2020, it is projected to be the number one cause of death worldwide[2]. The term *ischemic heart disease* covers a large spectrum that includes clinical presentations varying from stable angina to sudden cardiac death. It can be caused by atherosclerosis of the coronary arteries, called coronary artery disease (CAD) and if left untreated, the condition can lead to acute myocardial infarction, with eventual mortality from complications due to heart failure and late cardiac damage[3].

With the increasing lifespan and the concurrent rise of diabetes type II seen in developing nations, the incidence of cardiovascular disease and deaths due to ischemic heart disease will become an even greater economic burden, with costs currently accumulating over $20 billion per year[2]. Therefore, the appeal of finding accurate, yet cost-effective diagnostic modalities for assessment of CAD becomes evermore necessary. Fortunately, the assessment for CAD is now done much more readily with an armamentarium of imaging tools that can evaluate the severity of CAD at different mechanistic levels. This present work examines the role of Oxygen-Sensitive Cardiovascular Magnetic Resonance imaging (OS-CMR) as a non-invasive tool to evaluate ischemic heart disease.

1.2 REVIEW OF LITERATURE

1.2.1 Myocardial Ischemia

1.2.1.1 Mechanism of myocardial ischemia

The heart is a well-perfused organ with a highly dense microvasculature that is able to achieve 65-75% maximal oxygen extraction at basal levels. With an oxygen consumption requirement of 8-10 ml O_2/100 g per min, resting coronary blood flow per gram of myocardium is about ten times greater than the whole-body average[4]. Considering there is little oxygen left in reserve (in the blood), any further change in metabolic demand is remarkably matched by linear increases with coronary flow; at even higher demands, oxygen extraction may rise too[5,6]. During periods of maximal exercise, the cardiac output can increase 4 to 6 times greater than normal through vasodilation of the coronary arteries[2], with oxygen consumption reaching 30-40 ml/100g per minute and aerobic adenosine triphosphate (ATP) production reaching 15-20mmol ATP/100 g per minute[4].

ATP is the primary source of energy for the heart and in normal cellular respiration, aerobic metabolism maintains adequate ATP production through oxidative phosphorylation. It can also be oxidatively regenerated using a variety of metabolic substrates, including 60-90% from fatty acids, and 10-40% from glucose and lactate. Normal myocardium, unlike skeletal muscle, is able to oxidize lactate, which becomes useful during periods of exercise when lactate is released into the bloodstream[5]. Within each minute, the normal myocardium produces approximately 33 mmol of ATP[7].

However, in ischemic heart disease, the lumen of coronary arteries can become occluded from atherosclerotic complications, leading to inadequate blood flow or perfusion. This ultimately leads to ischemia, which is defined as restriction of oxygen supply and substrate transport as a result of reduced organ perfusion[8], limiting the removal of metabolic waste products [4].

Within 8-15 seconds of acute coronary occlusion, obvious decline in the heart's performance can be seen[4,8]. The cascade proceeds with a decline in contractile function, as systolic segment shortening and wall thickening reduces (hypokinesis), followed by a complete termination of wall thickening (akinesis). With prolonged ischemia from 30 seconds to two minutes, paradoxical bulging and thickening (dyskinesis) will be present[9-11].

During this critical period in the first few contractions, myocardial energy production can still be maintained via aerobic metabolism. However, by one minute, there are serious functional impairments[12], as the myocardial oxygen reserve dissolved in both the myocardium and bound to myoglobin gets used up. The reduction in coronary flow and aerobic metabolism results in depletion of creatine phosphate (PCr) levels as this high-energy phosphate is rapidly converted into ATP to maintain normal energy conditions.

Glycolysis, normally a minor source of ATP in physiological conditions, becomes a more significant source through anaerobic metabolism, as the dependence of energy from fatty acids decreases and glycogen breakdown to glucose is activated immediately[13]. The switch from fatty acid utilization to anaerobic metabolism via glycolysis will provide some ATP, but this is highly inefficient[4,8,12]. Concurrent with

prolonged ischemia after 30 minutes, the metabolic products of NADH, lactate, and H^+ accumulate, as they can neither be completely oxidized nor washed out of the tissue due to low coronary flow. Furthermore, during periods of hypoxia, the myocardium will switch from lactate consumption to lactate production, further exacerbating the intracellular acidosis[5]. The accumulation of these metabolic products eventually leads to the inhibition of the glycolytic pathway and progressively diminishes tissue ATP[14]. The subsequent decrease in intracellular pH from proton accumulation leads to intracellular acidosis and reduced LV function[15].

Studies done to induce periods of myocardial ischemia by reducing total coronary flow and oxygen consumption in isolated perfused rat hearts have shown that within 30 minutes, irreversible damage of the ventricular myocardium occurs, with approximately 50-100% of the severely injured cells dying by 40 and 60 minutes, respectively[16].

Along this cascade, the Na^+/K^+ ATPase is compromised, resulting in a greater efflux of potassium into the extracellular space with an increase in intracellular sodium. A decrease in the Na^+ gradient across the cell membrane reduces Ca^{2+} extrusion. Proton accumulation during ischemia also leads to Na^+ accumulation via the Na^+/H^+ exchanger. Intracellular calcium continues to rise as the Na^+/Ca^{2+} exchanger starts extruding sodium. Eventually, progressive calcium overload and accumulation of metabolites will compromise cell membrane function, leading to myocyte death[2,17,18].

1.2.1.2 Consequence of chronic ischemia

During the first moments of acute coronary narrowing, contractile function declines. In some instances, the instability between energy supply and demand may eventually reach a steady state, where contractile dysfunction is proportional to reduction in blood flow, termed perfusion-contraction matching[9]. Studies done in anaesthetized swine hearts have shown within 5-10 minutes of ischemia, subendocardial PCr and ATP typically decline and lactate accumulation climbs dramatically to 300% of control. However, by 60 minutes, PCr and lactate levels returned to normal, while LV wall thickening and ATP remain depressed[19]. It is now believed that following the transient phase of imbalance between supply-demand during early myocardial ischemia, active down-regulation of myocardial energy requirements may occur as a protective means to preserve myocardial tissue at a lower metabolic level[9,19].

This condition, termed hibernating myocardium, is a manifestation of chronic ischemia, with function improving following reperfusion. Rahimtoola first noticed that patients with CAD and chronic LV dysfunction had improved contractility following revascularization by coronary bypass surgery[20]. Later, Braunwald popularized the concept of hibernating myocardium when he distinguished it from myocardial stunning[21].

Hibernating myocardium may be considered more severe than transient myocardial ischemia, as there are changes seen at the structural level. These characteristic features include replacement of sarcomeres (contractile material) by glycogen, loss of sarcoplasmic reticulum and Transverse (T)-tubules, disruption of the

cytoskeleton proteins titin and alpha-actinin, alteration of size and shape of mitochondria[22-24], and increased interstitial fibrosis[25].

Despite ongoing chronic ischemia, the ability of the human heart to adapt and compensate may be demonstrated to a certain degree through development of the coronary collateral circulation by providing increased blood flow to the jeopardized region. However, they are often not sufficient during increased times of oxygen demands, such as during exercise. It has been shown that coronary collateral development helps mitigate the effects of myocardial ischemia, keeping myocytes viable during coronary narrowing, and may also limit the degree of necrosis during myocardial infarctions[26,27]. By studying two hundred coronary arteriograms, researchers showed preservation of normal to mildly impaired myocardial contractility with adequate collateralization. The study also showed the stimulation of angiographically-visible collateral vessels is associated with luminal narrowing greater than 90% or chronic total occlusions[28]. Recent data, however, suggests that other factors may influence collateral growth in addition to degree of coronary stenosis, including duration of occlusion (in chronic total occlusions) and duration of symptoms[29].

1.2.1.3 Clinical implications of myocardial ischemia

To better understand the clinical implications of myocardial ischemia, it is important to recognize the spectrum of CAD, which includes the acute manifestations of myocardial infarctions, usually caused by occlusion of coronary arteries. In the long term following revascularization of infarcted myocardium, end-stage manifestations of CAD can be

seen in congestive heart failure patients with late systolic and/or diastolic dysfunction. More commonly, there can also be chronic phases of CAD, in which symptomatic, stable angina persists from chronic ischemia. In these patient populations, risk assessment of myocardial ischemia is important to determine appropriate treatment management based on medical therapy with or without revascularization[30].

It is also important to understand that while CAD mostly affects the epicardial coronary arteries, impairments in the coronary microcirculation may also play a role in the disease process related to myocardial ischemia. Clinically, coronary microvascular disease (CMVD) remains poorly understood as the smaller vessels are difficult to image and features classically related to CAD, such as alterations in myocardial contractility, are often absent altogether. Evidence of ischemia in CMVD tend to be shown more easily in the subendocardium or appear patchy throughout the myocardium[31].

A large, multi-centre trial has confirmed the benefit of ischemia reduction, where it was shown that patients with reduced ischemia achieved by optimal medical therapy and percutaneous coronary intervention (PCI) had lower rates of death and myocardial infarctions[32]. Therefore, there have been significant research efforts to develop non-invasive cardiac imaging for the timely diagnosis and evaluation of CAD[33,34].

1.2.2 Cardiac imaging for assessment of Coronary Artery Disease

For the evaluation of CAD, cardiac imaging modalities are broadly utilized for two main purposes—to assess myocardial viability i.e. hibernating myocardium or LV dysfunction caused by irreversible damage, and/or to evaluate evidence of inducible

ischemia in patients with stable CAD. The most common clinical modalities for functional assessments of patients suspected with CAD include echocardiography (Echo), Single-Photon Emission Computed Tomography (SPECT), Positron Emission Tomography (PET), Computed Tomography (CT), X-ray coronary angiography, and Cardiovascular Magnetic Resonance (CMR).

1.2.2.1 Stress Testing

Current diagnostic procedures often include a stress test coupled with an imaging modality to determine the significance of the lesion in the artery. Stress tests are performed through exercise or administration of a pharmacological agent (alternative for those who cannot exercise) to cause the vessels in the heart to dilate. The degree of arterial dilation between baseline (rest) and during pharmacologically induced hyperemia allow for detection of abnormalities in cardiac perfusion[3].

Over the last 50 years, exercise and pharmacological stress testing has developed as an important means to evaluate patients with known or suspected CAD. For instance, stress testing is frequently used to predict future coronary events among individuals with recorded CAD, prior history of myocardial infarction, or a history of unstable angina. In addition, patients identified as being at greater risk of death are considered candidates for coronary angiography and subsequent coronary revascularization. In contrast, studies using stress testing have shown that coronary interventions are of little benefit in low risk subgroups that have excellent prognosis[35].

Stress testing combines either exercise or pharmacologic agents with an imaging

modality such as nuclear perfusion or echocardiography. Treadmill or bicycle exercise is the preferred form of stress because it provides the most information concerning patient symptoms, cardiac function, and the hemodynamic responses during daily activities. The symptoms experienced upon exertion can be linked to the location, extent, and severity of abnormal perfusion[3].

Dunker and colleagues have consistently shown that exercise is the greatest physiological stimulus for increased myocardial oxygen demand[36]. Under exercise conditions, the increased oxygen requirement of muscle creates a necessity for an augmented blood flow response. The heart needs to increase its cardiac output and will subsequently raise the three main determinants of myocardial oxygen demand: heart rate, myocardial contractility, and ventricular systolic pressure. Generally, a heart rate increase of 85% or above the age-predicted maximum is considered adequate for exercise stress testing[35]. Already alluded to before, the approximate six-fold increase in oxygen demands of the LV during heavy exercise is met through proportional increases in coronary blood flow, since haemoglobin concentration and oxygen extraction (which is already 65-75% at rest) can increase not much further in most animal species[36].

However, for those patients unable to attain a sufficient level of exercise, pharmacological stress agents can be used to induce coronary hyperemia. The pharmacologic agents are commonly of two categories, an adrenergic agent such as dobutamine, or a vasodilator such as adenosine or dipyridamole[3].

1.2.2.2 Mechanisms of Adenosine

Adenosine is a molecule that powerfully regulates blood flow in many organ beds, including the coronary circulation. The general mechanism whereby adenosine produces its arteriolar vasodilatory effects is through binding of adenosine A_{2a} receptors on smooth muscle cells, which stimulates vascular relaxation[3]. More specifically, the binding of the adenosine receptors on smooth muscle cells leads to enhanced production of adenylate cyclase, which increases cyclic adenosine monophosphate levels (cAMP). cAMP is a secondary messenger molecule used for intracellular signal transduction that causes protein kinase activation to open ATP-sensitive potassium channels, resulting in membrane potential hyperpolarization and smooth muscle relaxation[37,38]. Generally, it has been shown that an infusion of 140 μg/kg/min induces maximal coronary hyperemia, with no further increase in coronary blood flow at higher doses. In a study performed by Ogilby et al. in 33 patients with CAD and 12 patients without CAD, intravenous infusion of adenosine of 140 μg/kg/min for six minutes resulted in slight increases in heart rate and cardiac output, with a minor decrease in systemic pressure and blood pressure.

Dipyridimole, also a coronary arteriolar vasodilator, works by blocking the intracellular reuptake and breakdown of adenosine. Therefore, dipyridimole is an indirect coronary vasodilator, as it functions to increase intracellular and interstitial concentrations of adenosine[3]. Dipyridimole is administered at 142 μg/kg/min (maximum 0.56 mg/kg) to achieve maximum effect.

1.2.2.3 Dobutamine Echocardiography

Echo and SPECT are imaging modalities that assess regional wall motion abnormalities and myocardial perfusion (characteristics of CAD), respectively, under conditions at rest and during stress using exercise or a pharmacological agent (predominantly dobutamine)[34]. Dobutamine stress echocardiography (DE) utilizes ultrasound to examine the heart[3] and aims to determine the presence or absence of inducible ischemia secondary to obstructive coronary artery disease based on systolic wall motion abnormalities. This protocol is based on the concept that the contractile function of myocardium perfused by stenotic arteries will be diminished following an ionotropic and chronotropic agent, and thus regions of ischemic myocardium will be revealed as wall motion abnormalities[39,40]. Dobutamine is a man-made catecholamine that targets beta-1 adrenergic receptors. Its main effect increases both contractility and heart rate, which increases the myocardial oxygen demand, thus mimicking the effects of exercise[37,41]. At low doses, the effect is an increase in contractility through adrenergic stimulation. With higher doses, heart rate and blood pressure will increase steadily, thus the increase in contractility and oxygen demand will stimulate an increase in coronary blood flow[3].

1.2.2.4 Thallium SPECT imaging

SPECT is a nuclear medicine imaging technique that utilizes gamma rays to provide 3D information both for myocardial perfusion and viability. Using radioisotope injections such as thallium-201 (^{201}Tl) or technetium Tc 99m (sestamibi and tetrofosmin), myocyte

membrane integrity and intact mitochondrial function are demonstrated[42]. Thallium-201 is biologically similar to potassium, therefore the myocardial uptake of thallium-201 is an active process dependent on the intact sarcolemmal membrane Na+/K+ ATPase activity[42,43].

The regional distribution of blood flow to the heart is measured and sampled after several hours[3]. The principle of myocardial perfusion imaging relies on the tight relationship between oxygen requirements and coronary blood flow, as previously mentioned. SPECT relies on stress-induced vasodilation to discern regions of diseased myocardium that receive less blood flow than normal myocardium. Areas with decreased radioactive uptake reflect ischemic heart muscle. This is true for the initial injection of thallium, where the uptake of the radioactive tracer is dependent on myocardial blood flow. Information about myocardial viability can also be assessed following 3 to 4 hours, where the retention of the tracer is an active process dependent on preserved cell membrane integrity and tissue viability[44].

SPECT imaging has been shown to have a wide range in sensitivity (63-93%) and specificity (10-90%) compared to X-ray angiography[45]. SPECT studies are limited by low spatial resolution and patient risk from exposure to radioactive material[33,46]. It has now been shown that the radiation is not only harmful to patients, but health care personnel working with patients who undergo SPECT imaging can also be exposed to radiation[47]. Another problem for SPECT imaging is the looming shortage of available radioisotopes. In 2009, the world's largest medical isotope provider was shut down for extended maintenance periods, leaving a sudden 30% shortfall for medical hospitals and institutes. With only five major sites providing the vast majority of the world's supply of

molybdenum-99, the shortage of nuclear isotopes is inevitable[48]. Thus, advancing the field of non-nuclear based cardiac imaging becomes evermore important.

1.2.2.5 PET, CT, and X-Ray Coronary Angiography

PET and CT are not routinely used for evaluation of CAD at our local hospital site. However, in brief, PET nuclear imaging provides assessment for both perfusion and ischemic metabolism, as myocardial uptake of a glucose analog, fluorine-18 labeled deoxyglucose (FDG), is reflective of the ischemia-induced shift of preferential metabolism of fatty acids to glucose[42]. Uren et al. have demonstrated the non-invasive ability of PET to both quantify myocardial blood flow and flow reserve in single-vessel diseased patients, and to assess the functional significance of coronary artery stenoses[49].

CT angiography utilizes X-rays to visualize the coronary arterial lumen, particularly for detection of atherosclerosis and calcium deposit[40].

X-ray coronary angiography is the most accurate method to investigate luminal anatomy of epicardial arteries with high temporal and spatial resolution. The technique relies on the insertion of a thin catheter into the vessels of the heart[3,50]. However, this method is invasive with often limited correlation between the narrowing of the artery to coronary perfusion, contractility, and degree of ischemia[51].

1.2.3 Coronary blood flow

1.2.3.1 Autoregulation of Coronary Blood Flow

To counter the limitations of X-ray coronary angiography, recent advances have emerged with a procedure called fractional flow reserve (FFR), whereby a pressure wire is inserted into the lumen of epicardial coronary arteries to determine the functional significance of a stenotic lesion. To better understand this critical concept, the physiology of coronary blood flow will first be explored.

In 1964, Mosher and colleagues performed a series of experiments on 22 mongrel dogs to study the concept of autoregulatory control of coronary blood flow, featuring the pressure-flow diagram that describes coronary flow reserve (Figure 1) [52,53].

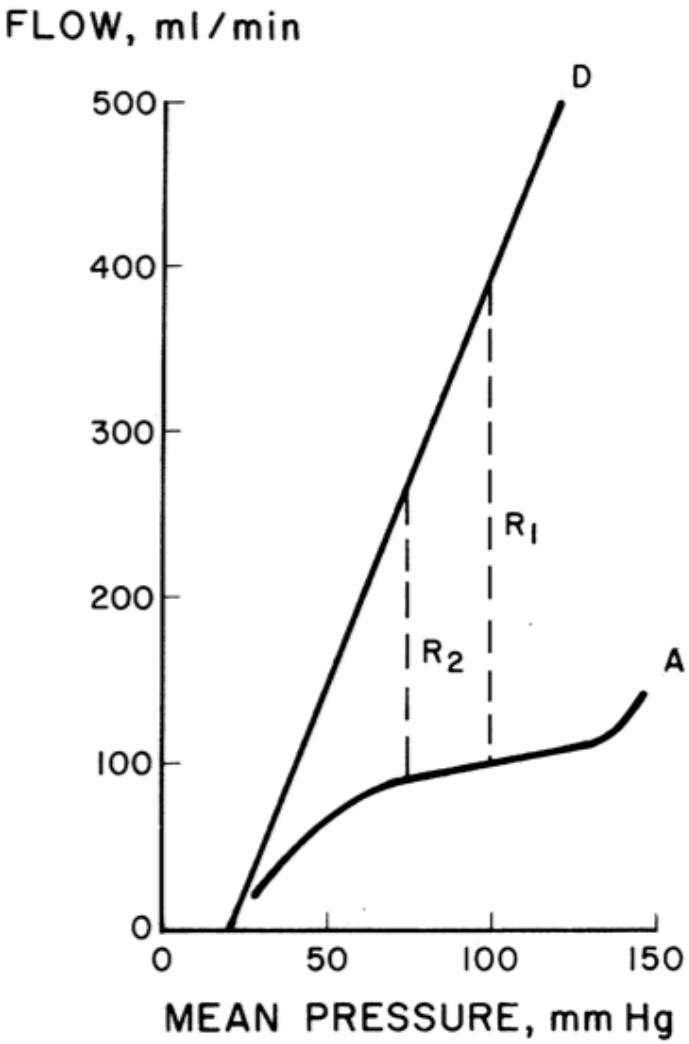

FIGURE 1. Diagram of pressure-flow relationships in normal left ventricle during autoregulation (A) and maximal vasodilatation (D). R_1 and R_2 are the coronary flow reserves at mean coronary perfusing pressures of 75 and 100 mm Hg when aortic pressure and heart rate are constant.

Figure 1-1: Pressure-flow diagram depicting concept of coronary flow reserve.

Taken from Hoffman JI. Maximal coronary flow and the concept of coronary vascular reserve. Circulation. 1984; 70: 153-159.

Intuitive to this discussion is the basic understanding of coronary flow as a function of the driving pressure and resistance (Flow = Change in pressure (P) / resistance (R))[54]. By cannulating the coronary vessels and using an extracorporeal circuit, Mosher and colleagues were able to change coronary perfusion pressures while maintaining constant aortic pressure. The experiments demonstrated that within physiologic range of arterial blood pressures, coronary blood flow is relatively independent of coronary perfusion pressures. Below this autoregulatory range at approximately 70 mmHg, coronary flow decreases greatly when perfusion pressure decreases. By injecting the dogs with nitroglycerin, near maximal vasodilation was induced and autoregulatory mechanisms gave way to mechanical factors. Above the upper range of about 130 mmHg, coronary flow rises markedly as vasoconstrictive mechanisms can no longer regulate flow[53]. Current literature indicates that autoregulation is controlled through the myogenic response of arterial vessels, mediated by stretch-activated channels and maintained through enzymes responsible for calcium sensitization[5]. The resistance vessels, comprised of the terminal arterioles, vasodilate in order to reduce the resistance and increase local blood flow. Conversely, vasoconstriction on the arterioles decreases the local blood flow. Capillaries, although part of the microcirculation, do not actively play a role in autoregulation, as they lack smooth muscle and only passively increase or decrease vessel width[5].

1.2.3.2 Measurements of Coronary Flow Reserve

As depicted in Figure 1, the difference between flow in the autoregulated range and maximal vasodilation is the coronary flow reserve[52,55]. This value represents the ability of the coronary vessels to increase blood flow in response to raised oxygen demands or decreased oxygen carrying capacity[56].

Coronary flow has been shown to increase above resting level in physiological conditions such as exercise, but also following coronary arterial occlusion via reactive hyperaemia[57] or with injection of vasodilating agents[58]. In past decades, researchers have measured coronary flow reserve in humans to obtain information about the coronary vascular bed and functional severity of a stenosis[52]. In anesthetised dogs under resting conditions, coronary flow is not altered until a stenosis with diameter of 85% is present. In contrast, under conditions of coronary hyperaemia, Gould et al. demonstrated that maximal coronary flow is limited by constriction as small as 30%[56]This was a pivotal finding, as the flow response to a hyperaemic stimulus was proven to be an effective measure to assess the hemodynamic significance of coronary lesions.

However, the assessment and interpretation of coronary flow reserve is difficult to make in patients, where values are defined as maximal flow divided (normalized) by control flow at rest. Coronary reserve is a function of perfusion pressure[52], thus if perfusion is high, as seen in hypertensive patients, the absolute coronary reserve may be normal or elevated. Absolute coronary flow reserve can also be influenced by changes in aortic pressure and heart rate (conditions that can alter cardiac work load), impacting the baseline and maximal coronary blood flow. Therefore, the clinical application of

coronary flow reserve may not reliably represent the functional severity of stenoses, as it may be altered by physiological factors unrelated to the lesion geometry[59].

1.2.3.3 Derivation of Fractional Flow Reserve from Coronary Flow Reserve

Nearly 15 years after the development of clinical measurements of coronary flow reserve, another assessment of functional stenosis severity emerged based on measurements of pressure. Pijls and colleagues first described the theoretical and experimental basis for fractional flow reserve (FFR) measurements in 1993[60].

In the physiological state, there is minimal pressure along the length of the vessel, even at maximal hyperaemia. For epicardial coronary arteries, the driving pressure across the coronary bed or myocardial perfusion pressure is the difference between the aortic and central venous pressure (or right atrial pressure)[61]. Experiments by Gregg and Shipley demonstrated a negligible influence of central venous pressure on coronary flow[62], since the central venous or right atrial pressure are relatively small in magnitude[54]. Thus, for normal coronaries, the perfusion pressure can be approximated by the aortic pressure alone. In the case of stenotic epicardial coronary arteries, the distal coronary pressure determines the myocardial perfusion in the diseased vessel.

Taking the above into account, FFR can be conceptualized as a percentage of "normal" flow and is a derivation of a ratio of two perfusion pressures—maximal myocardial blood flow in a diseased artery (distal coronary pressure) to the maximal flow of the same artery if it were normal (aortic pressure). Therefore, although FFR is a

ratio of two flows, the ratio can be derived from two pressure measurements[50] (Figure 2).

1. FFR is a ratio of myocardial blood flow in the stenotic territory (S) to normal (N) myocardial blood flow under hyperaemic conditions.

$$FFR = \frac{Flow_S}{Flow_N}$$

2. Since flow is a ratio of the pressure (P) difference across the coronary system divided by resistance (R), flow can then be substituted.

$$FFR = \frac{(P_d - P_v) / R_S}{(P_a - P_v) / R_N}$$

3. As measurements are obtained during maximal hyperemia, resistances are minimal and thus equal, allowing the venous pressures to theoretically to cancel out.

$$FFR = \frac{P_d - P_v}{P_a - P_v}$$

4. Venous pressure (P_v) is equal to right atrial pressure and can be considered negligible in comparison to P_a or P_d, therefore:

$$FFR = \frac{P_d}{P_a}$$

Figure 1-2: Theoretical derivation of FFR.

Image depicting how 2 flow measurements can equate to 2 pressure measurements. Diagram adapted from De Bruyne and Sarma, 2008. Pd, distal coronary pressure; Pa, aortic pressure; R_S, resistance in the stenotic territory; R_N, resistance in the normal territory.

In addition, the model proposed by Pijls et al. holds that the relationship between coronary pressure and flow is linear, as long as the resistances in the coronary circulation remain constant. Thus, measurements for FFR need to be done at maximal vasodilation[50,60,63]. An FFR measurement can be calculated separately for the epicardial artery, myocardium, and for the collateral circulation[60]. For the purpose of this thesis, the focus will be on the FFR measured for the myocardium.

1.2.3.4 FFR as the standard for functional assessment of coronary stenosis

Studies have shown that FFR takes collateral circulation into account[60,64] and indeed, a FFR value of <0.75 represents the threshold for detecting a physiologically significant lesion[64]. Furthermore, the value of FFR to guide the decision for revascularization has been in shown in patients with multivessel disease. When compared to SPECT, disconcordance was seen in many patients with no perfusion defect in regions supplied by arteries with total occlusions or FFR <0.75[65]. In these cases, SPECT was found to underestimate the extent of coronary artery disease in all myocardial territories[65,66]. Initial studies comparing relative CFR to FFR have shown correlation[67], while others have shown disconcordance due to basic coronary pathophysiology. This may be related to the pathological state influenced by focal versus diffuse atherosclerotic disease, rather than limitations of the clinical modalities themselves[66,68].

In a major study conducted in 20 medical centers in the United States and Europe, 1005 patients with multivessel CAD were randomly assigned to undergo PCI with drug-eluting stents guided either by angiography alone or angiography guided by

FFR measurements. Patients assigned to angiography-guided PCI underwent stenting of all indicated lesions, whereas those patients assigned to FFR-guided PCI underwent stenting in lesions with FFR <0.80. The primary end points were the rate of death, nonfatal myocardial infarction, and repeat revascularization at 1 year. Results showed that the 1-year event rate was significantly higher (91 patients) in the angiography group compared to the FFR group (67 patients). The researchers were able to conclude that routine measurements of FFR in patients with multi-vessel disease results in significantly better outcomes[69], even after two-year follow-up[70].

The FAME (Fractional flow reserve versus angiography in multivessel evaluation) trial showed superiority of FFR as a predictor of therapeutic success over angiographic assessment of coronary stenoses, especially in patients with multivessel disease[71]. Results from the DEFER (Deferral Versus Performance of PTCA in Patients Without Documented Ischemia) trial have further shown excellent five-year outcomes for patients deferred from PCI for an intermediate coronary stenosis based on a normal FFR >0.75 encountered less than 1% risk of cardiac death or myocardial infarction[72].

For the work of this thesis, FFR will be used as the reference standard for functional significance of coronary stenoses in comparison to CMR.

1.2.4 Cardiovascular Magnetic Resonance for Coronary Artery Disease

The clinical utility of cardiovascular magnetic resonance (CMR) has evolved tremendously over the last decade and now consists of a range of techniques for the evaluation of ischemic heart disease. CMR allows for non-invasive assessment of

function, perfusion, infarction, coronary angiography, and edema without the use of ionizing radiation[73,74]. To better understand the basis of CMR, a brief discussion of MR physics will first be explored.

1.2.4.1 Basics of MR Physics

All physical elements are made up of atoms with hydrogen, commonly found in water, being the most abundant atom in the human body. A single atom comprises of a nucleus spinning on its axis in the centre with negatively charged electrons orbiting around the nucleus. The mass of the nucleus is made up of positively charged protons and non-charged neutrons that are usually balanced in proportion, such that the atom has an even mass number[75]. According to theories of Quantum Mechanics, paired subatomic particles (such as neutrons and protons) will each spin at equal rates, but in opposite directions to each other so as to occupy different positions at any given time. Therefore, in nuclei with even mass numbers, the pairs of subatomic particles will spin in opposite directions to effectively form a nucleus with no net spin. However, in atoms of elements with odd mass numbers (called isotopes), having slightly more or fewer protons than neutrons create a situation where the spins are not equal and opposite, resulting in a nucleus that has a net spin or angular momentum. The foundation of MRI is henceforth, based on Nuclear Magnetic Resonance, nuclear as the MRI signal is derived from the nuclei of MR active atoms characterized by odd mass numbers. With that, the Laws of Electromagnetic Induction first outlined by Michael Faraday state that electrical charges in motion would induce a magnetic field. Therefore, in MR active nuclei, positively

charged protons when spinning in motion, will induce a nuclear-sized magnetic field that tends to align with an external magnetic field[75].

The isotope of the hydrogen nucleus with a single proton (protium) is the MR active nucleus commonly used in clinical MRI. The hydrogen nucleus behaves like a tiny magnet with a north and south pole represented by a magnetic moment that has vector properties of size and direction, often referred to as spins. At first, the magnetic moments of the hydrogen nuclei in our bodies are randomly orientated in the absence of an external magnetic field. However, during an examination, the patient is brought into a high-strength magnetic field and the magnetic moments in the human body become aligned in either of two possible energy states of the hydrogen atom, parallel (low energy state) or anti-parallel (high energy state) to the long-axis (z-axis) of the external magnetic field, B_0. The parallel orientation is slightly favoured over the anti-parallel position, creating an excess difference in spins along the parallel orientation. Those excess spins represent the ones that will yield a detectable net magnetization to create the images we see on screen[76,77]. At higher magnetic field strengths, there is an even greater number of excess spins as fewer spins have enough energy to align themselves in opposition to the external field, creating an overall greater signal[75].

Furthermore, while each hydrogen nucleus naturally spins on its axis, there can be an additional wobble of the magnetic moment influencd by the external magnetic field, B_0, referred to as precession. With precession, the magnetic moments follow a circular path around B_0 with a specific precessional frequency called the Lamour Frequency, governed by the Larmour Equation ($\omega_0 = \gamma \beta_0$). This equation states that precessional frequency, ω_0, is proportional to the external magnetic field strength, β_0,

and to the gyromagnetic ratio, γ (representation of the relationship between the magnetic moment of a spinning charged particle to its angular momentum)[75]. The gyromagnetic ratio is a constant value specific to each MR active nuclei. The energy of the speed of the hydrogen spins corresponds to the radiofrequency (RF) range of the electromagnetic spectrum. By applying a RF pulse of energy for a few milliseconds that matches that of the Larmour Frequency, spins undergo resonance or oscillation through absorption of energy. The excitation by the RF pulse causes the alignment of the spins to be perturbed at a specific flip-angle, away from the z-axis of the B_0. Hence, the term resonance in Nuclear Magnetic Resonance, as the RF pulse needs to be *on-resonance* with the rotational speed of the spins[76,77].

1.2.4.2 Generation of MRI Signal

The excitation of the spins by the RF pulse can be deconstructed into a vector that includes longitudinal magnetization (aligned with the z-axis) and transverse magnetization (perpendicular to z-axis). As alluded to above, when a patient is placed into an MRI scanner, an RF pulse (usually 90 degree) is first applied, which will allow the spins to have enough energy to tilt from the longitudinal magnetization (M_z) into the transverse or xy-plane. Next, the RF pulse is turned off and following excitation, the magnitude of longitudinal magnetization will increase and eventually recover to the axis of the external magnetic field (z-axis), as this is energetically most stable. Equally, this can be thought of as a relaxation process by which the hydrogen protons lose energy after the RF pulse was applied to them, which can be seen as a decrease in the transverse

magnetization. Referring back to Faraday's Laws of Electromagnetism, the MR signal is generated when the precessing spin in the tranverse plane produces magnetic field fluctuations inside the receiver coil to produce electrical voltage. The electrical voltage is then processed into the MRI signal. Importantly, the magnitude of the MR signal relies on the amount of magnetization in the transverse plane. As the transverse magnetization decreases, so does the amount of voltage induced by the receiver coil and this can be referred to as the Free Induction Decay (FID) signal[75]. After one RF pulse, one FID is received. However, the signal does not provide any information about the location in space. In order to acquire spatial information in the 3D plane (x, y, and z coordinates), multiple RF pulses are used with varying gradient coils to receive multiple FIDs or signals. The time between each successive RF pulse is called the repetition time (TR). All the information will then be used to construct the image (Figure 1-3)[76].

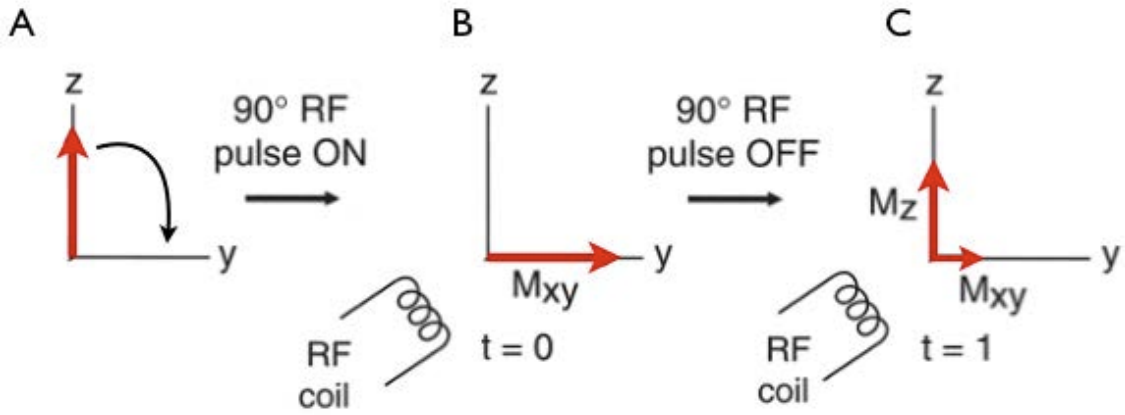

Figure 1-3: MRI Signal Generation.

Adapted from Hashemi et al, 2010. A) Longitudinal magnetization (M_z) at prior to start of scan. B) At time = zero after RF excitation, the longitudinal magnetization is completely tipped onto the xy-plane (M_{xy}) and signal is at its maximum C). After a period of time, M_z recovers by a certain amount while M_{xy} has decayed by a different amount. The oscillating excitation along the xy-plane induces a signal picked up by the receiver coil[78].

The time it takes for the longitudinal magnetization to recover fully is referred to as T1-relaxation. The tissue-specific T1 time constant is known as the time at which longitudinal magnetization has recovered 63% of its original value, hence it is often referred to as T1-recovery curve. Similarly, following excitation, the transverse magnetization will decrease and eventually decay to zero. The time it takes for the transverse magnetization to decay fully is referred to as T2-relaxation. Similarly, the tissue-specific T2 time constant is known as the time at which transverse magnetization has lost 63% of its original value. The T1 and T2 relaxations play a major role in producing various image contrasts in MR imaging. The T1 relaxation mechanism is affected by the energy exchange between the spins and the surrounding environment; hence T1 relaxation can be referred to as the spin-lattice relaxation. The T2 relaxation mechanism depends on the spin-spin interactions when the spins dephase to different rotational angles as a result of increasing randomness[76].

The relaxation mechanism affected by both the interaction between spins (T2) and additional inhomogenities in the magnetic field is referred to as T2*[76,77]. Of importance, paramagnetic substances such as deoxyhemoglobin, methemoglobin, and gadolinium are examples of magnetic field inhomogeneities that shorten the T1 and T2 relaxation times of imaged tissues[75].

1.2.4.3 Basic Imaging Sequences

As mentioned above, the time it takes between each successful RF pulse excitation is referred to as the TR. A combination of RF pulses at varying times is referred to as a

pulse sequence. The echo time (TE) refers to the time it takes in miliseconds to reach the peak of the induced signal measured in the receiver coil. Importantly, TR dictates how much longitudinal magnetization occurs in between each RF pulse and TE dictates the amount of transverse magnetization that occurs. For instance, a tissue will have a greater signal if there is a large component of transverse magnetization remaining at time TE because there will be a greater amplitude of signal received by the coil. Such tissues will tend to appear brighter on MRI images. Effectively, by varying the TR and TE times, pulse sequences are achieved such that they are favoured more towards T2-weighting or T1-weighting[75].

All tissues have different molecular makeups and will have varying T1 and T2 times. For instance, the T1 and T2 time of fat is shorter than that of water. Since TR controls the amount of recovery in the longitudinal vector, with a short enough TR, neither the T1 of fat or water will have time to fully recover. With the next RF excitation pulse, the difference in their longitudinal magnetization will be translated to a notable difference in the transverse plane and T1-weighted imaging is achieved, with contrast dependent predominately on the difference between the tissues T1 values. Therefore, for T1-weighting, TR must be short. Conversely, T2-weighting is where image contrast is predominately dependent on the difference in the T2 values of the tissues. TE controls the amount of time the T2 decay of the tissue occurs before the signal is read by the receiver coil. With a long enough TE, the T2 times of tissues can decay fully to express a difference in contrast in T2-weighted images (Figure 1-4)[75].

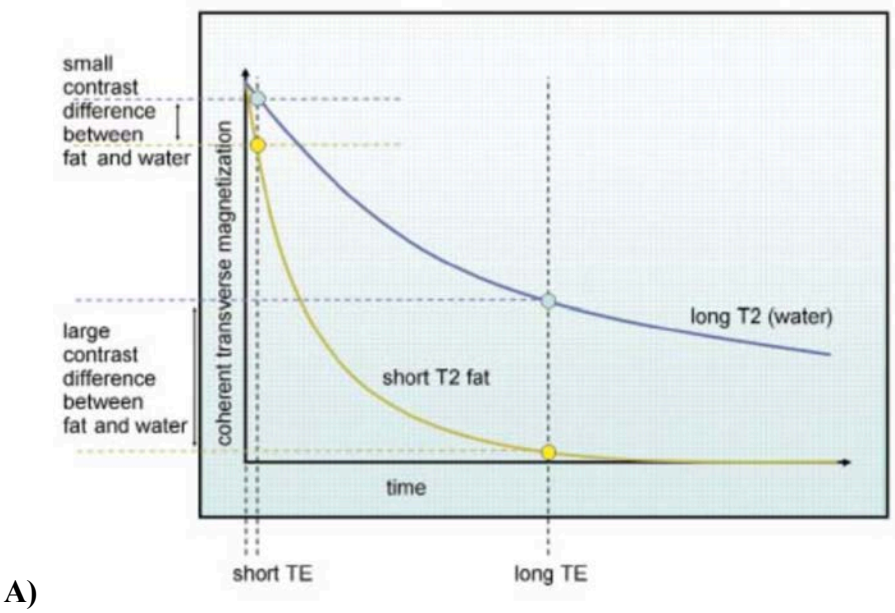

A)

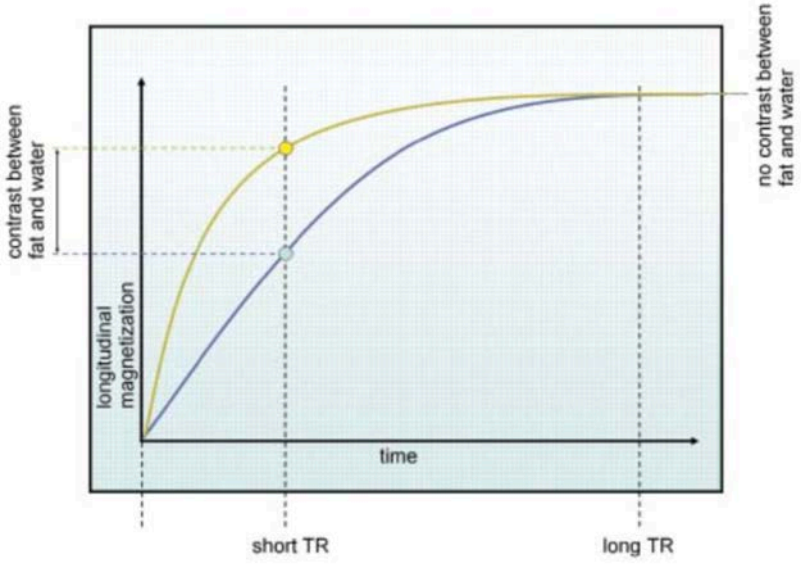

B)

Figure 1-4: T1 and T2 Decay curves.

(Taken from Westbrook et al, 2011) A) T2 decay of fat and water, illustrating with a long enough TE, there will be a discernable difference in their T2 times such that T2-weighted contrast is achieved. B) T1 recovery curve of fat and water, illustrating with a short enough TR, there will be a measureable difference in their T1 times such that T1-weighted contrast imaging is achieved.

MRI pulse sequences rely on two basic methods to regenerate the signal for good image contrast. As previously mentioned, following the initial 90° RF pulse, spins quickly dephase as result of T2* inhomogeneities in the magnetic field. Spin echo pulse sequences rely on an 180° refocusing pulse to rephase the spins to a maximal transverse magnetization and therefore, a maximum signal called a spin echo is induced in the receiver coil (Figure 1-5).

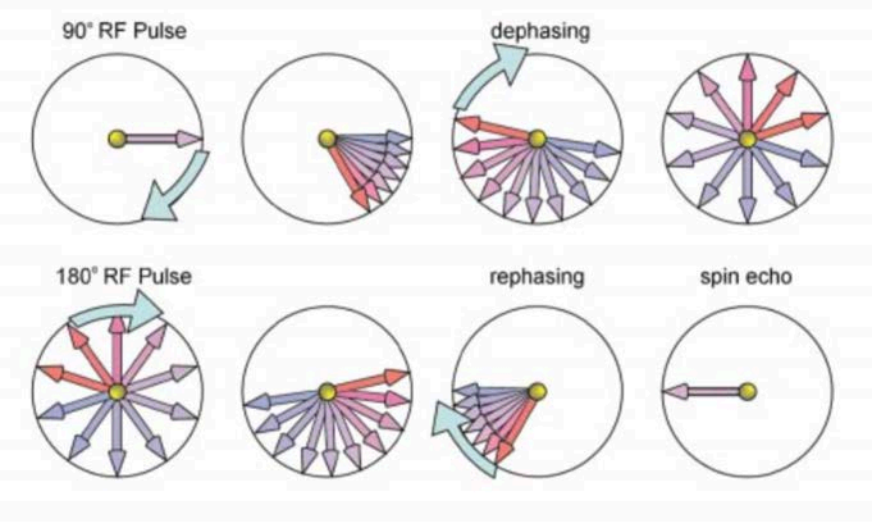

Figure 1-5: Spin Echo using an 180° refocusing pulse.

(Taken from Westbrook et al, 2011) Spin echo pulse sequences rely on the 180° refocusing pulse to rephase the spins for signal regeneration, essentially negating any T2* effects caused by local field inhomogeneities.

Gradient echo pulse sequences manipulate the local magnetic field strength within the magnetic bore to cause precession at various frequencies based on the application from the Larmour equation, whereby the precession frequency of spins is proportional to the magnetic field strength. When the initial magnetic field gradient is applied, the spins in the tissue quickly dephase at various frequencies along the gradient. A second magnetic field gradient of equal, but opposite direction is applied which will effectively re-phase the spins to generate a maximum signal in the receiver coil called a gradient echo. Unlike spin echos, gradient echos do not compensate for the rapid dephasing of the magnetic inhomogeneities and are therefore, more susceptible to the field inhomogeneities caused by T2* decay. T2-weighting in gradient echo imaging is hence, more commonly referred to as T2* weighed imaging[75,79].

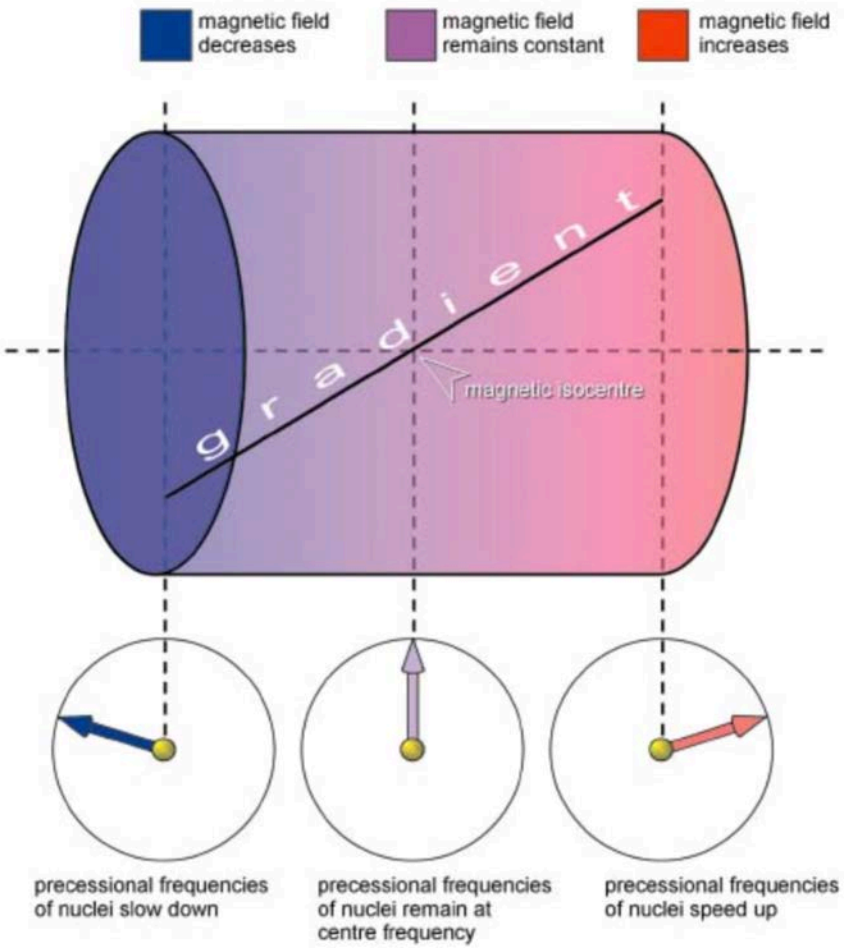

Figure 1-6: Gradient echo with field gradients

(Taken from Westbrook et al, 2011) Gradient echo pulse sequences rely on variations of the magnetic field to cause different precessional frequencies in the spins. RF pulses of varying angles are used to rephase the spins for signal regeneration and in general, gradient echo sequences tend to have faster image acquisition.

1.2.4.4 Blood Oxygen Level Dependent (BOLD) contrast

In T2-weighted images that are sensitive to the BOLD effect, the signal intensity is influenced by the paramagnetic properties of deoxygenated haemoglobin, which causes local distortions in the magnetic field. The longevity of the signals used to produce MR images is dependent on the uniformity of the magnetic field. The less uniform the magnetic field, the greater the difference between the precessing frequencies of the protons in the tissue sample, and thus, the faster the overall signal decay. Therefore, by using an appropriate MR sequence which is sensitive to local field inhomogeneities caused by the presence of deoxygenated haemoglobin, tissue pathology is reflected by the rapid signal decay governed by T2* (Figures 7 and 8).

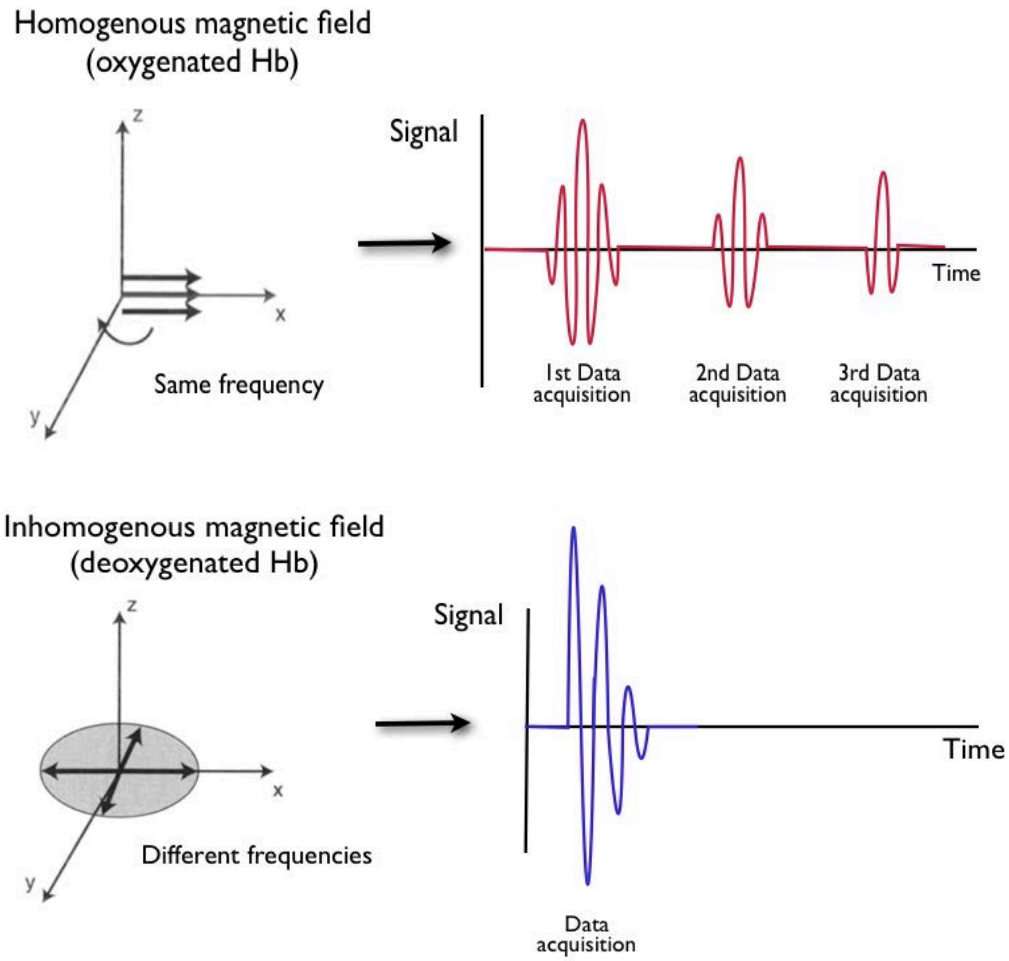

Figure 1-7: Effect of deoxygenated hemoglobin on magnetic field and resultant signal.

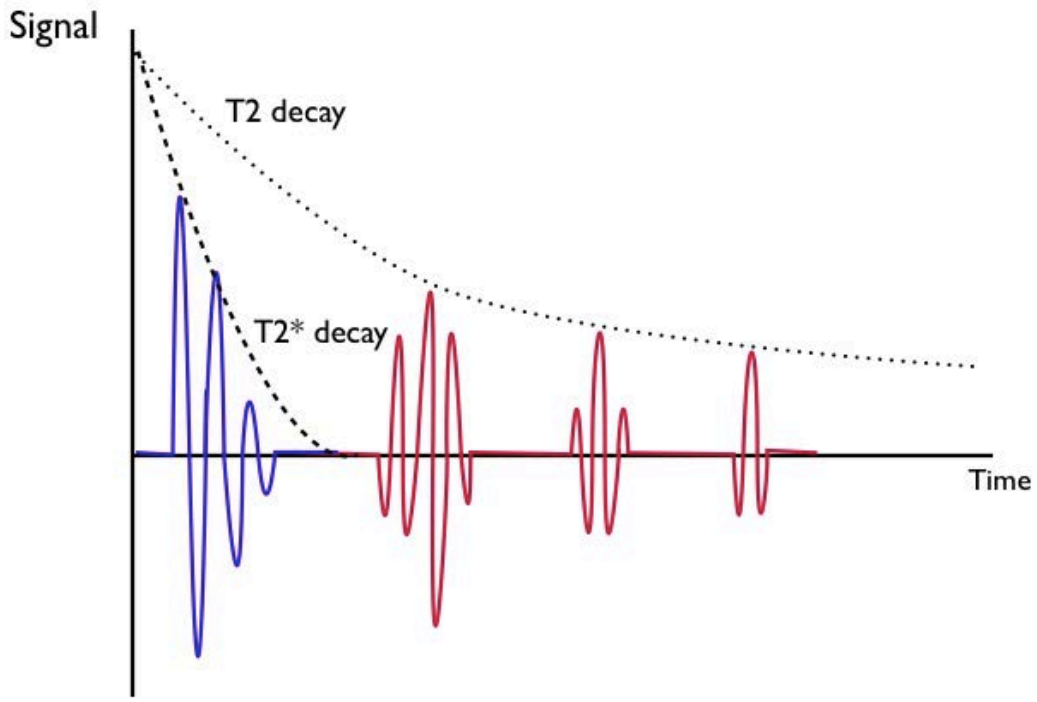

Figure 1-8: The BOLD effect is governed by T2* decay.

Note that the graph is a combination of both the signal decay curves from Figure 5 superimposed on one another to demonstrate the rapid decay as a result of local field inhomogeneities caused by deoxyHB.

1.2.4.5 Steady State Free Precession (SSFP)

For the present thesis, oxygen-sensitive contrast was achieved using a steady state free precession (SSFP) based sequence designed by Frahm in 1986[80] with capabilities of dynamic visualization of the cardiac phases, so called *cine* imaging[81]. While the advanced technical aspects of the sequence development are beyond the scope of this thesis, a brief discussion of the concept related to SSFP is warranted.

The excitation sequence allowed a balanced gradient echo that sampled the resonant magnetic field signal (called Signal from hereon) at steady state. The steady

state implies that the longitudinal and transverse magnetizations were constant and allows registration of both T1 and T2 tissue contrast. In order to achieve the steady state, trains of multiple refocusing radiofrequency (RF) pulses less than 90 degrees are used with relatively short times (TR) in between each repetition. As a result, the transverse magnetization does not have time to fully decay between each pulse sequence and carries over to the next sequential pulse repetitions. Rather than de-phasing the magnetic moments using a a so-called spoiler excitation pulse, which destroys any residual transverse magnetization prior to the next pulse sequence, our sequence used a so-called balanced SSFP approach that uses excitation gradients of equal but opposite polarities to fully re-phase the magnetic moments at the end of each sequence. Therefore, with the next RF pulse, the residual transverse magnetization is carried over and becomes superimposed on the current transverse magnetization being generated. Over a period of the trains of RF pulses, the Signal becomes a combination of previous successive runs and generates a greater signal to noise ratio (SNR) [82].

1.2.4.6 Current CMR Protocol for Hypoxia Assessment

The current protocol for evaluation of CAD includes assessment of ischemia and myocardial viability for identification of scar associated with myocardial infarction. The evaluation of ischemia is made using two different techniques, first-pass myocardial perfusion imaging (perfusion CMR) and detection of inducible wall motion abnormalities done under pharmacological stress testing. This is similar to the assessment of contractile reserve in response to dobutamine using echocardiography[44,83].

Scar is assessed using late-gadolinium enhancement (LGE), with the ability to image microvascular obstruction (no-reflow) [84,85].

It has been shown that CMR using the first-pass method, coupled with stress agents, was successful in assessing myocardial perfusion in correlation to CAD[86,87]. First-pass perfusion imaging relies on the monitoring of an injection of a contrast agent (usually gadolinium chelate) as it passes through the heart. Regions with poor blood flow will have lower signal than normally perfused regions[33,88]. CMR utilizes a radiation-free method to capture high-resolution images superior to both SPECT and echocardiography[34,89]. In a recent randomized, prospective study, researchers established a high diagnostic accuracy of a multi-parametric CMR protocol in 752 patients with coronary heart disease over that of SPECT, using X-ray coronary angiography as the reference standard[45].

1.2.4.7 Limitations of CMR myocardial perfusion

There are several aspects of CMR myocardial perfusion that can limit its performance. The gadolinium contrast has been implicated in the cause of some renal diseases. Because there are a significant number of patients with renal insufficiency that also suffer from CAD, there is a potential risk for this population when subjected to CMR perfusion imaging[90]. Moreover, the signal from the difference between the contrast medium and the heart muscle, reduced spatial resolution, and cardiac movement of the heart often lead to artefacts that mimic ischemia, causing difficulty in image analysis[33].

Each imaging modality has its own strengths and weaknesses[40], as they each attempt to exploit particular markers of myocardial ischemia. The hemodynamic significance of a stenotic artery and its impact on ischemia can be influenced by variables such as endothelial dysfunction and collateral circulation. CMR perfusion and the above-mentioned modalities for myocardial ischemia are still only surrogate tests that do not provide direct information about how the balance between supply and demand can alter tissue oxygenation[91].

1.2.4.8 Oxygen-Sensitive Cardiovascular Magnetic Resonance

In recent years, a more direct CMR technique for diagnosing ischemia has come forth with the possibility of BOLD-sensitive (Blood Oxygen Level Dependent) CMR imaging, which exploits the magnetic susceptibility effects of deoxygenated hemoglobin (deoxyHb) [92]. The paramagnetic properties of deoxygenated blood were first noted in the 1930s and have been applied in functional MRI studies of the brain[93-95]. When diamagnetic oxyhemoglobin loses its oxygen, the resulting deoxyHb, now with four unpaired electrons, becomes paramagnetic and causes a difference in magnetic susceptibility between the vessels and the surrounding tissues, dispersing the overall proton signal[96]. The effect of the dispersion (dephasing) caused by the deoxyHb reduces the signal intensity, making it appear dark in T2* or T2-weighted images[95,97] (Figure 9).

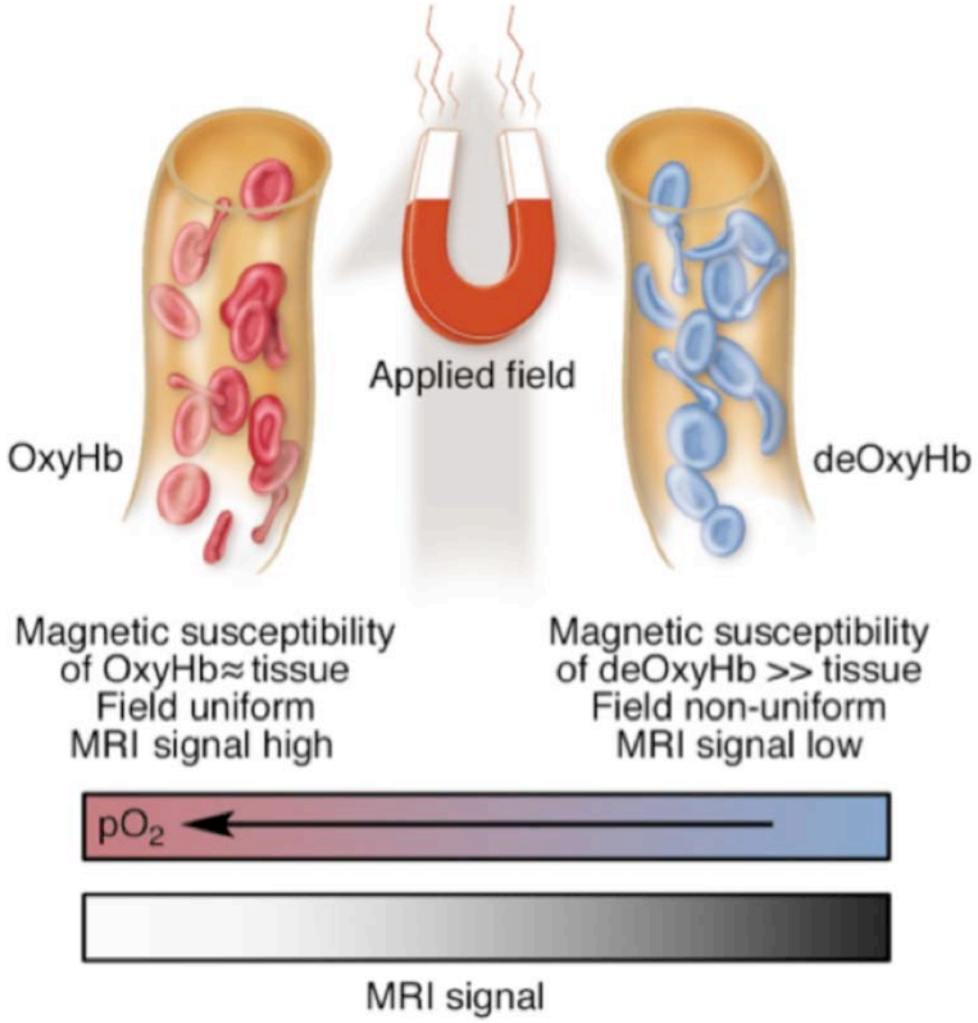

Figure 1-9: Illustration of the origins of the BOLD effect in fMRI.

Adapted from Gore, 2003. Principles and practice of functional MRI of the human brain. While arterial blood is similar in its magnetic properties to tissue, deoxygenated blood is paramagnetic and therefore, induces inhomogeneities within the magnetic field applied to the tissue of interest. The inhomogeneities in turn cause the MRI signal to decay more rapidly. Conversely, signal from tissue with more uniform magnetization increases[98].

Anatomical studies performed in pigs have provided an immense amount of information about the coronary circulation of humans, as both have relatively similar physiological structures. Based on pig studies, we know that the coronary system in its

entirety including epicardial arteries, arterioles, capillaries, venules, and veins, contains approximately 4.5mL of blood per 100g LV mass. A large portion of the myocardial blood volume resides in the microvessels, of which greater than 90% are highly dense capillaries measuring 6-7μm in diameter and ranging 2500 to 3500 per mm[399]. Holtz et al. have previously measured the intracapillary hemoglobin oxygen saturation in the myocardium in frozen tissue removed from thoracotomized dogs, with values ranging from 30-70%, averaging 41±19% in the subendocardim and 53±16% in the subepicardium[100]. Therefore, we can reasonably assume that the intracapillary deoxyHb saturation would likely range from 50-60%.

The BOLD technique derives its signal intensity from the amount of deoxyHb molecules in the blood, thus it is strongly correlated to oxygen metabolism and saturation. In five anesthesized pigs, Li et al. imaged regions in the descending aorta and inferior vena cava using a 1.5T gradient echo sequence at baseline and following ventilation manipulations to create various hemoglobin saturation levels. Signal intensities were measured from regions of interest drawn in the separate images of the aorta and vena cava. Blood samples taken from the artery and vein were also used to determine the blood oxygen saturation via pulse oximetry and T2* estimations (Figure 10). These researchers were able to demonstrate that the blood T2* correlated closely with the percentage of deoxyHb in the blood[101].

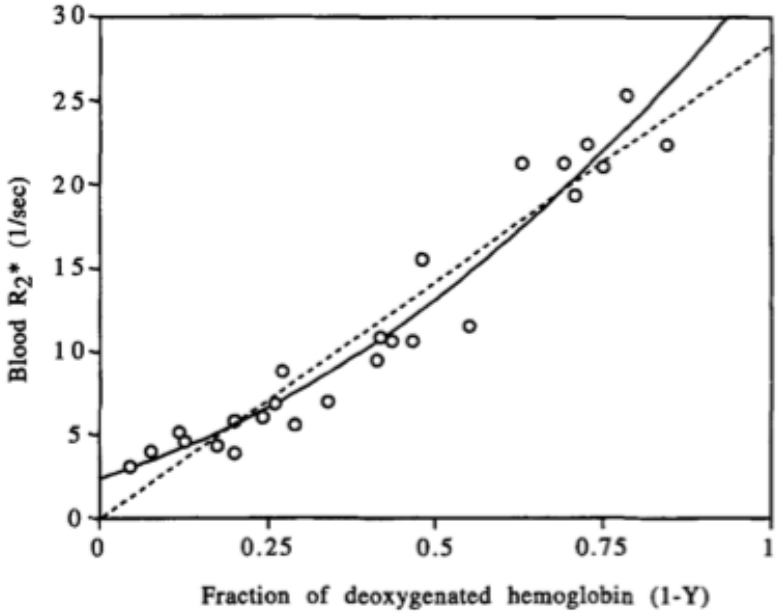

Figure 1-10: Blood T2* reflects volume percent of deoxygenated hemoglobin.

T2* was shown to be a linear function of hemoglobin saturation, whereby with increasing deoxygenated hemoglobin, T2* values decrease (dotted lines). Vice versa, with increasing oxygen saturation, T2* increases. R2* is a calculated quadratic function shown to represent 1/T2* (second-order, solid curve). Y = fractional blood oxygen saturation. Taken from Li et al, 1998[101].

An increase in oxygenated blood resulting in decreased deoxyHb saturation is associated with a greater MR signal[102]. Conversely, more deoxyHb is associated with a reduction in the MR signal[92]. This has been shown through studies performed on patients using administration of dipyridamole. Because the myocardium subtended by a stenotic coronary artery has a capillary bed that is already maximally vasodilated at rest, administration of dipyridamole resulted in a blunted hyperemic response in comparison to normal myocardium. Thus, areas with decreased signal intensity (higher levels of deoxyHb) indicated hypoperfused, ischemic myocardial territory[103-105]. From a physiological perspective, the decrease in signal intensity is expressed through the

following relationship, whereby flow is inversely proportional to the resistance and directly proportional to the perfusion pressure (Eq.4). Resistance in the coronary circulation is additive, whereby the total resistance equals the sum of the individual resistances in series. Figures 11 and 12 will illustrate this concept in further detail.

$$\text{Flow} = \frac{\text{Pressure}}{\text{Resistance}} \therefore \text{Flow} \propto \frac{1}{\text{Resistance}}$$

Eq.4

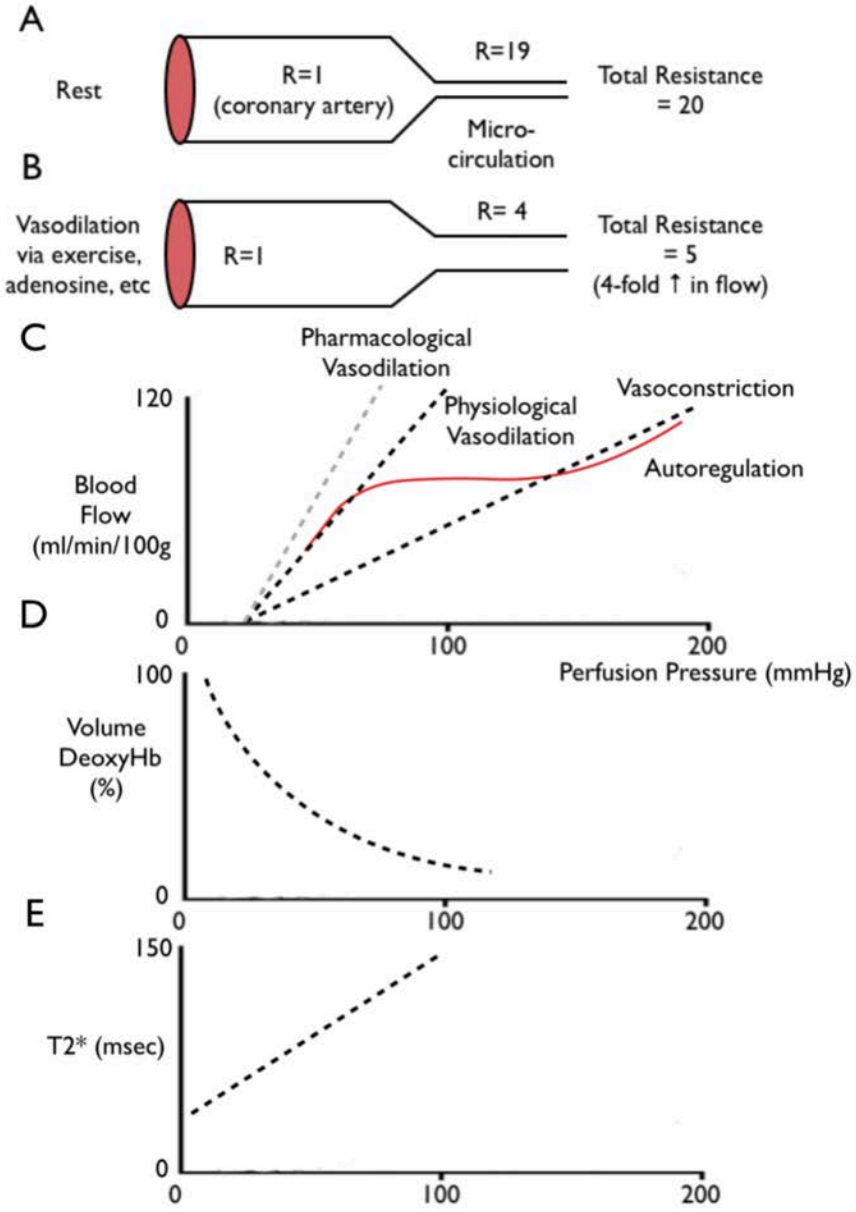

Figure 1-11: Hypothetical construct of the effect of pharmacological vasodilation on BOLD signal intensity.

(A) and (B) adapted from Levick et al, 2010 and (C) adapted from Westerhorf et al. [106]. Consider a healthy coronary vessel (A) which has resistance of 1 unit at rest and a resistance of 19 in the microcirculation, totalling 20 units. As a result of adenosine-mediated hyperemia, the microcirculation decreases resistance through vasodilation down to 4 units, reducing the total resistance by 4-fold (B). Flow, being inversely proportional to resistance, rises by 4-fold in comparison to physiological vasdodilation (grey dashed lines) (C). With no change in myocardial oxygen demand, adenosine-induced vasodilation increases T2* (E) secondary to elevated oxygenation saturation and decreased volume percentage of deoxyHb (D).

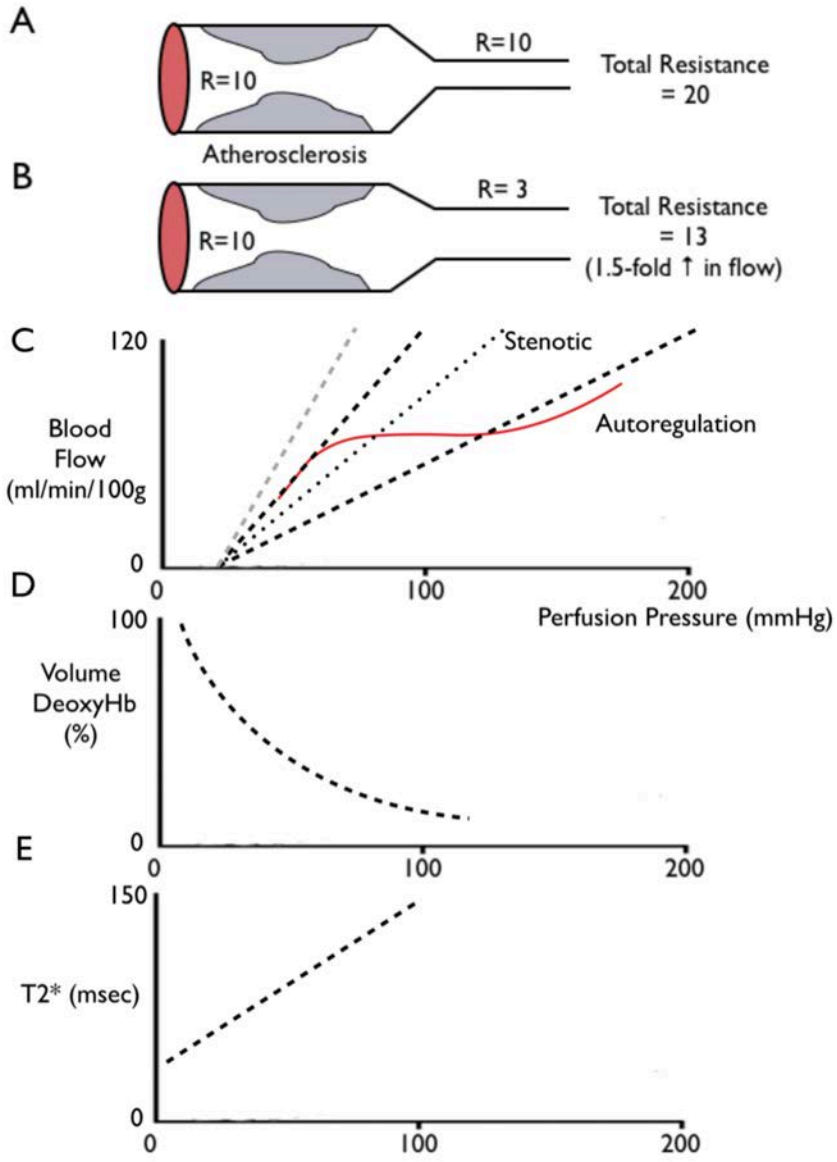

Figure 1-12: Hypothetical construct of the effect of stenosis on BOLD signal intensity.

(A) and (B) adapted from Levick et al, 2010. In a stenotic coronary artery (A), the resistance at baseline is 10 units at rest. In the microcirculation, resistance is decreased from 19 units (in a normal artery) to 10 units due to compensatory dilation. With adenosine-induced hyperemia, the reserve dilation of the coronary resistance vessels decreases the resistance further to 3 units (B). However, in the presence of a coronary stenosis (black dotted lines), the total resistance is 13 units, and therefore, flow is only augmented by 1.5 fold (20/13) compared to maximal pharmacologic vasodilation (black dashed lines) or physiological vasodilation (grey dashed lines) (C). The blunted hyperemic response resulted in a decreased T2* (E), secondary to relatively higher volume percentage of deoxyHB (D).

As described above, the relative change in signal intensity can be elicited through the administration of pharmacological vasodilator such as adenosine in clinical practice. Experimental studies performed in pigs and dogs have demonstrated that intracoronary adenosine infusion increases perfusion without increasing blood volume of myocardium or cardiac metabolic rate. In pig models, researchers have shown on average, T_2 increased 26% from baseline following intracoronary adenosine infusion of 100 μg/kg/min, while simultaneous T_1 measurements reflecting tissue blood volume remained constant. Within a minimum of 8% intravascular blood volume, Foltz et al. demonstrated that a 10% change in T2 values would be sufficient for detection between normal and hibernating myocardium. The 10% elevation in T2 following intracoronary adenosine infusion was associated with a 40% elevation in microcirculation oxygen saturation. Subsequently, the 40% increase in oxygen saturation was associated with a 3-fold increase in myocardial perfusion reserve. Therefore, the researchers demonstrated that BOLD-CMR is capable of detecting a 40% change in microcirculation oxygen levels, which is sufficient for differentiating between normal versus abnormal myocardium[107].

Furthermore, it has been shown that the BOLD signal intensity is not susceptible to changes in local blood flow and blood volume[91]. Here, magnetic susceptibility refers to the degree to which the magnitude of the signal intensity is altered by various components of the external magnetic field. Alluded to earlier, the presence of paramagnetic deoxyhemoglobin in red blood cells causes a difference in magnetic susceptibility between the blood and surrounding tissue, and is the key feature exploited in oxygen-sensitive CMR. Li et al. investigated the differential effects of coronary

vasodilation induced by dipyridamole (increased coronary flow but minimal change in oxygen consumption) to that induced by dobutamine administration (increased coronary flow with associated increased in oxygen consumption). With dipyridimole administration, myocardial venous oxygen saturation increases as oxygen supply (blood flow) exceeds demand (oxygen consumption). With dobutamine administration, cardiac work increases, leading to an increase in myocardial oxygen consumption and myocardial perfusion. The authors reasoned that with dobutamine, myocardial venous oxygen saturation tends to remain the same as the balance between oxygen supply and demand is maintained[108]. In normal volunteers (n=13), the BOLD signal response was measured when myocardial blood flow increased in excess of oxygen demand or when flow was increased in response to increased oxygen demand. The authors showed that the T2* signal intensity increased with dipyridamole but not with dobutamine, despite increased coronary blood flow with both administrations. This suggests that the T2* signal intensity is able to reflect altered myocardial oxygenation as a consequence of changes in the relationship between myocardial oxygen supply and demand. This also suggests that T2* signal intensity is not sensitive to changes in blood flow or blood volume and may reflect actual tissue oxygenation levels.

In previous studies, the oxygen-sensitive contrast generated by BOLD-CMR can be shown using various MRI sequences, such as a single breathhold, T2*-weighted segmented gradient echo pulse sequence that acquires 10 successive gradient echos per radiofrequency excitation[109], T2* weighted, gradient-echo echo planar imaging (EPI) [110], T2 prepared SSFP[111], or T2-mapping techniques using turbo spin-echo sequences[112]. The work of this thesis is based on an SSFP approach as discussed earlier. SSFP BOLD-

CMR has been used successfully in dog models. At 1.5T, Fieno et al. utilized a T2-prepared SSFP sequence to study oxygenation in coronary arteries. Maximal adenosine-induced vasodilation produced on average 28% increase in signal intensity compared to baseline, whereas image intensity in remote myocardium remained unchanged[97].

Moving forward from the proof-of-concept studies for BOLD-CMR in animals[101,113,114], there are now several studies published on the clinical utilization of this oxygenation-sensitive technique in patients suspected of CAD[46,103,104,111,112,115-119]. However, its use in clinical settings have been hampered by the fact that substantial changes in myocardial perfusion result in only relatively small variations in BOLD signal intensity. This was most evident in a critical study performed in 2003 by Friedrich et al., where the potential of oxygenation-sensitive CMR to identify myocardial ischemia in a clinical setting was used to assess patients with stress-induced angina[110]. In this investigation, change in BOLD signal with adenosine vasodilation was compared to change in adenosine nuclear SPECT and also to the degree of stenosis as indicated by coronary angiography. A BOLD SI change cut-off point of 1.2% identified stenoses ≥ 75% with 88% sensitivity and 47% specificity. Since then, improved pulse sequences have been developed[33,81,120,121] and recent studies performed on dogs by Vohringer et al. using the newer CMR sequences showed greater BOLD signal responses. The latter researchers demonstrated the strong correlation between myocardial oxygenation (indicated by coronary sinus oxygen saturation) with BOLD signal intensity changes when coronary flow increased with drug-induced hyperaemia[122].

The inherent problems encountered in studies done at 1.5T are related to low-signal to noise ratio, and subclinical image quality due to artefacts resulting from field inhomogenities and blood flow[46,109,116]. Furthermore, visual qualitative evaluations of BOLD-CMR images are currently limited by small percent changes that necessitate the use of spreadsheets for quantitative analysis. Recent studies have also shown the utility of BOLD-CMR at stronger magnetic field strengths using 3.0T scanners[119,123,124], stimulating continued BOLD-CMR development as a clinically feasible imaging modality providing qualitative data. With a higher magnetic field strength, the amount of excess spins available for magnetization will theoretically, allow for a higher BOLD sensitivity.

In summary, OS-CMR is a non-invasive approach for the assessment of ischemic heart disease that does not require contrast or radiation. Building on the foundation of previous experimental and clinical studies, further understanding of the oxygenation-sensitive contrast generation will be explored in the three manuscript-based chapters to follow.

1.3 References

1. Statistics Canada. Mortality, summary list of causes. Available at: http://www.statcan.ca/Daily/English/070427/d070427b.htm. Accessed 10/28, 2008.

2. Dymarkowski S, Bogaert J, Ni Y. Ischemic Heart Disease. In: Bogaert J, Dymarkowski S, Taylor AM, eds. Clinical Cardiac MRI. Berlin, Germany: Springer; 2005: 173-211.

3. Braunwald E, Libby P, Bonow R, Mann D, Zipes D. Braunwald's Heart Disease: A Textbook of Cardiovascular Medicine. 8th ed. Philadelphia, PA: Saunders Elsevier; 2008.

4. Gibbs CL. Cardiac energetics. *Physiol Rev.* 1978; 58: 174-254.

5. Levick J. Introduction to Cardiovascular Physiology. 5th ed. Great Britain: Hodder Arnold; 2010.

6. Crake T, Canepa-Anson R, Shapiro L, Poole-Wilson PA. Continuous recording of coronary sinus oxygen saturation during atrial pacing in patients with coronary artery disease or with syndrome X. *Br Heart J.* 1988; 59: 31-38.

7. Rosano GM, Fini M, Caminiti G, Barbaro G. Cardiac metabolism in myocardial ischemia. *Curr Pharm Des.* 2008; 14: 2551-2562.

8. Kubler W, Spieckermann PG. Regulation of glycolysis in the ischemic and the anoxic myocardium. *J Mol Cell Cardiol.* 1970; 1: 351-377.

9. Heusch G, Schulz R. Hibernating myocardium: a review. *J Mol Cell Cardiol.* 1996; 28: 2359-2372.

10. Theroux P, Ross J,Jr, Franklin D, Kemper WS, Sasyama S. Regional Myocardial function in the conscious dog during acute coronary occlusion and responses to morphine, propranolol, nitroglycerin, and lidocaine. *Circulation.* 1976; 53: 302-314.

11. Theroux P, Franklin D, Ross J,Jr, Kemper WS. Regional myocardial function during acute coronary artery occlusion and its modification by pharmacologic agents in the dog. *Circ Res.* 1974; 35: 896-908.

12. Wollenberger A, Krause EG. Metabolic control characteristics of the acutely ischemic myocardium. *Am J Cardiol.* 1968; 22: 349-359.

13. Stanley WC, Hall JL, Stone CK, Hacker TA. Acute myocardial ischemia causes a transmural gradient in glucose extraction but not glucose uptake. *Am J Physiol.* 1992; 262: H91-6.

14. Neely JR, Feuvray D. Metabolic products and myocardial ischemia. *Am J Pathol.* 1981; 102: 282-291.

15. Jacobus WE, Pores IH, Lucas SK, Weisfeldt ML, Flaherty JT. Intracellular acidosis and contractility in the normal and ischemic heart as examined by 31P NMR. *J Mol Cell Cardiol.* 1982; 14 Suppl 3: 13-20.

16. Neely JR, Rovetto MJ, Whitmer JT, Morgan HE. Effects of ischemia on function and metabolism of the isolated working rat heart. *Am J Physiol.* 1973; 225: 651-658.

17. Sambandam N, Lopaschuk GD. AMP-activated protein kinase (AMPK) control of fatty acid and glucose metabolism in the ischemic heart. *Prog Lipid Res.* 2003; 42: 238-256.

18. Vassalle M, Lin CI. Calcium overload and cardiac function. *J Biomed Sci.* 2004; 11: 542-565.

19. Arai AE, Pantely GA, Anselone CG, Bristow J, Bristow JD. Active downregulation of myocardial energy requirements during prolonged moderate ischemia in swine. *Circ Res.* 1991; 69: 1458-1469.

20. Rahimtoola SH. The hibernating myocardium. *Am Heart J.* 1989; 117: 211-221.

21. Braunwald E, Rutherford JD. Reversible ischemic left ventricular dysfunction: evidence for the "hibernating myocardium". *J Am Coll Cardiol.* 1986; 8: 1467-1470.

22. Ausma J, Cleutjens J, Thone F, Flameng W, Ramaekers F, Borgers M. Chronic hibernating myocardium: interstitial changes. *Mol Cell Biochem.* 1995; 147: 35-42.

23. Ausma J, Furst D, Thone F, Shivalkar B, Flameng W, Weber K, Ramaekers F, Borgers M. Molecular changes of titin in left ventricular dysfunction as a result of chronic hibernation. *J Mol Cell Cardiol.* 1995; 27: 1203-1212.

24. Schwarz ER, Schaper J, vom Dahl J, Altehoefer C, Grohmann B, Schoendube F, Sheehan FH, Uebis R, Buell U, Messmer BJ, Schaper W, Hanrath P. Myocyte degeneration and cell death in hibernating human myocardium. *J Am Coll Cardiol.* 1996; 27: 1577-1585.

25. Nagueh SF, Mikati I, Weilbaecher D, Reardon MJ, Al-Zaghrini GJ, Cacela D, He ZX, Letsou G, Noon G, Howell JF, Espada R, Verani MS, Zoghbi WA. Relation of the

contractile reserve of hibernating myocardium to myocardial structure in humans. *Circulation.* 1999; 100: 490-496.

26. Mills JD, Fischer D, Villanueva FS. Coronary collateral development during chronic ischemia: serial assessment using harmonic myocardial contrast echocardiography. *J Am Coll Cardiol.* 2000; 36: 618-624.

27. Charney R, Cohen M. The role of the coronary collateral circulation in limiting myocardial ischemia and infarct size. *Am Heart J.* 1993; 126: 937-945.

28. Levin DC. Pathways and functional significance of the coronary collateral circulation. *Circulation.* 1974; 50: 831-837.

29. Meier P, Schirmer SH, Lansky AJ, Timmis A, Pitt B, Seiler C. The collateral circulation of the heart. *BMC Med.* 2013; 11: 143-7015-11-143.

30. Schwitter J, Arai AE. Assessment of cardiac ischaemia and viability: role of cardiovascular magnetic resonance. *Eur Heart J.* 2011; 32: 799-809.

31. Lanza GA, Crea F. Primary coronary microvascular dysfunction: clinical presentation, pathophysiology, and management. *Circulation.* 2010; 121: 2317-2325.

32. Shaw LJ, Berman DS, Maron DJ, Mancini GB, Hayes SW, Hartigan PM, Weintraub WS, O'Rourke RA, Dada M, Spertus JA, Chaitman BR, Friedman J, Slomka P, Heller GV, Germano G, Gosselin G, Berger P, Kostuk WJ, Schwartz RG, Knudtson M, Veledar E, Bates ER, McCallister B, Teo KK, Boden WE, COURAGE Investigators. Optimal medical therapy with or without percutaneous coronary intervention to reduce ischemic burden: results from the Clinical Outcomes Utilizing Revascularization and Aggressive Drug Evaluation (COURAGE) trial nuclear substudy. *Circulation.* 2008; 117: 1283-1291.

33. Dharmakumar R, Arumana JM, Tang R, Harris K, Zhang Z, Li D. Assessment of regional myocardial oxygenation changes in the presence of coronary artery stenosis with balanced SSFP imaging at 3.0 T: theory and experimental evaluation in canines. *J Magn Reson Imaging.* 2008; 27: 1037-1045.

34. Miller DD, Shaw LJ. Coronary artery disease: diagnostic and prognostic models for reducing patient risk. *J Cardiovasc Nurs.* 2006; 21: S2-16; quiz S17-9.

35. D Weiner. UptoDate: Advantages and limitations of different stress testing modalities. Available at: http://www.uptodate.com/online/content/topic.do?topicKey=chd/34293&source=related_link#H20. Accessed April 20, 2010.

36. Duncker DJ, Bache RJ. Regulation of coronary blood flow during exercise. *Physiol Rev.* 2008; 88: 1009-1086.

37. Iskandrian AS, Verani MS, Heo J. Pharmacologic stress testing: mechanism of action, hemodynamic responses, and results in detection of coronary artery disease. *J Nucl Cardiol.* 1994; 1: 94-111.

38. Kleppisch T, Nelson MT. Adenosine activates ATP-sensitive potassium channels in arterial myocytes via A2 receptors and cAMP-dependent protein kinase. *Proc Natl Acad Sci U S A.* 1995; 92: 12441-12445.

39. Manning W. Stress echocardiography in the diagnosis and prognosis of coronary heart disease. In: Downey B, ed. UpTodate. Waltham, MA: UpToDate; 2012.

40. Howarth AG, Friedrich MG. Imaging as an End Point in Ischemia Trials. *Curr Cardiovasc Imaging Rep.* 2011; 4: 90-97.

41. Heller G. Dobutamine stress radionuclide myocardial perfusion imaging. In: Downey B, ed. UpToDate. Waltham, MA: UpToDate; 2012.

42. Soman P, Udelson JE. Assessment of Myocardial Viability by Nuclear Imaging in Coronary Heart Disease. In: Basow DS, ed. UpToDate. Waltham, MA: UpToDate; 2012.

43. Holly TA, Kansai P. Basic Properties of Myocardial Perfusion Agents. In: Basow DS, ed. UpToDate. Waltham, MA: UpToDate; 2012.

44. Buckley O, Di Carli M. Predicting benefit from revascularization in patients with ischemic heart failure: imaging of myocardial ischemia and viability. *Circulation.* 2011; 123: 444-450.

45. Greenwood JP, Maredia N, Younger JF, Brown JM, Nixon J, Everett CC, Bijsterveld P, Ridgway JP, Radjenovic A, Dickinson CJ, Ball SG, Plein S. Cardiovascular magnetic resonance and single-photon emission computed tomography for diagnosis of coronary heart disease (CE-MARC): a prospective trial. *Lancet.* 2011; .

46. Egred M, Waiter GD, Redpath TW, Semple SK, Al-Mohammad A, Walton S. Blood oxygen level-dependent (BOLD) MRI: A novel technique for the assessment of myocardial ischemia as identified by nuclear imaging SPECT. *Eur J Intern Med.* 2007; 18: 581-586.

47. Tsao CW, Frost LE, Fanning K, Manning WJ, Hauser TH. Radiation Exposure to Staff and the Public Following Myocardial Perfusion Imaging (MPI). 2011.

48. IAEA. Medical Isotopes Shortage Reveals Larger Issue. Available at: http://www.iaea.org/newscenter/news/2009/medicalisotopes.html. Accessed April 14, 2012.

49. Uren NG, Melin JA, De Bruyne B, Wijns W, Baudhuin T, Camici PG. Relation between myocardial blood flow and the severity of coronary-artery stenosis. *N Engl J Med.* 1994; 330: 1782-1788.

50. De Bruyne B, Sarma J. Fractional flow reserve: a review: invasive imaging. *Heart.* 2008; 94: 949-959.

51. Topol EJ, Nissen SE. Our preoccupation with coronary luminology. The dissociation between clinical and angiographic findings in ischemic heart disease. *Circulation.* 1995; 92: 2333-2342.

52. Hoffman JI. Maximal coronary flow and the concept of coronary vascular reserve. *Circulation.* 1984; 70: 153-159.

53. Mosher P, Ross J,Jr, McFate PA, Shaw RF. Control of Coronary Blood Flow by an Autoregulatory Mechanism. *Circ Res.* 1964; 14: 250-259.

54. Klocke FJ. Coronary blood flow in man. *Prog Cardiovasc Dis.* 1976; 19: 117-166.

55. Hoffman JI. A critical view of coronary reserve. *Circulation.* 1987; 75: I6-11.

56. Gould KL, Lipscomb K, Hamilton GW. Physiologic basis for assessing critical coronary stenosis. Instantaneous flow response and regional distribution during coronary hyperemia as measures of coronary flow reserve. *Am J Cardiol.* 1974; 33: 87-94.

57. Coffman JD, Gregg DE. Reactive hyperemia characteristics of the myocardium. *Am J Physiol.* 1960; 199: 1143-1149.

58. Aversano T, Becker LC. Persistence of coronary vasodilator reserve despite functionally significant flow reduction. *Am J Physiol.* 1985; 248: H403-11.

59. Gould KL, Kirkeeide RL, Buchi M. Coronary flow reserve as a physiologic measure of stenosis severity. *J Am Coll Cardiol.* 1990; 15: 459-474.

60. Pijls NH, van Son JA, Kirkeeide RL, De Bruyne B, Gould KL. Experimental basis of determining maximum coronary, myocardial, and collateral blood flow by pressure measurements for assessing functional stenosis severity before and after percutaneous transluminal coronary angioplasty. *Circulation.* 1993; 87: 1354-1367.

61. Cross CE, Rieben PA, Salisbury PF. Coronary driving pressure and vasomotor tonus as determinants of coronary blood flow. *Circ Res.* 1961; 9: 589-600.

62. Gregg DE, SHIPLEY RE. Studies of the venous drainage of the heart. *Am J Physiol.* 1947; 151: 13-25.

63. Lim MJ, Kern MJ. Coronary pathophysiology in the cardiac catheterization laboratory. *Curr Probl Cardiol.* 2006; 31: 493-550.

64. Pijls NH, Van Gelder B, Van der Voort P, Peels K, Bracke FA, Bonnier HJ, el Gamal MI. Fractional flow reserve. A useful index to evaluate the influence of an epicardial coronary stenosis on myocardial blood flow. *Circulation.* 1995; 92: 3183-3193.

65. Ragosta M, Bishop AH, Lipson LC, Watson DD, Gimple LW, Sarembock IJ, Powers ER. Comparison between angiography and fractional flow reserve versus single-photon emission computed tomographic myocardial perfusion imaging for determining lesion significance in patients with multivessel coronary disease. *Am J Cardiol.* 2007; 99: 896-902.

66. Schelbert HR. FFR and Coronary Flow Reserve: Friends or Foes? *JACC Cardiovasc Imaging.* 2012; 5: 203-206.

67. De Bruyne B, Baudhuin T, Melin JA, Pijls NH, Sys SU, Bol A, Paulus WJ, Heyndrickx GR, Wijns W. Coronary flow reserve calculated from pressure measurements in humans. Validation with positron emission tomography. *Circulation.* 1994; 89: 1013-1022.

68. Johnson NP, Kirkeeide RL, Gould KL. Is discordance of coronary flow reserve and fractional flow reserve due to methodology or clinically relevant coronary pathophysiology? *JACC Cardiovasc Imaging.* 2012; 5: 193-202.

69. Tonino PA, De Bruyne B, Pijls NH, Siebert U, Ikeno F, van't Veer M, Klauss V, Manoharan G, Engstrom T, Oldroyd KG, Ver Lee PN, MacCarthy PA, Fearon WF, FAME Study Investigators. Fractional flow reserve versus angiography for guiding percutaneous coronary intervention. *N Engl J Med.* 2009; 360: 213-224.

70. Pijls NH, Fearon WF, Tonino PA, Siebert U, Ikeno F, Bornschein B, van't Veer M, Klauss V, Manoharan G, Engstrom T, Oldroyd KG, Ver Lee PN, MacCarthy PA, De Bruyne B, FAME Study Investigators. Fractional flow reserve versus angiography for guiding percutaneous coronary intervention in patients with multivessel coronary artery disease: 2-year follow-up of the FAME (Fractional Flow Reserve Versus Angiography for Multivessel Evaluation) study. *J Am Coll Cardiol.* 2010; 56: 177-184.

71. Tonino PA, Fearon WF, De Bruyne B, Oldroyd KG, Leesar MA, Ver Lee PN, Maccarthy PA, Van't Veer M, Pijls NH. Angiographic versus functional severity of coronary artery stenoses in the FAME study fractional flow reserve versus angiography in multivessel evaluation. *J Am Coll Cardiol.* 2010; 55: 2816-2821.

72. Pijls NH, van Schaardenburgh P, Manoharan G, Boersma E, Bech JW, van't Veer M, Bar F, Hoorntje J, Koolen J, Wijns W, de Bruyne B. Percutaneous coronary intervention of functionally nonsignificant stenosis: 5-year follow-up of the DEFER Study. *J Am Coll Cardiol.* 2007; 49: 2105-2111.

73. Karamitsos TD, Dall'Armellina E, Choudhury RP, Neubauer S. Ischemic heart disease: comprehensive evaluation by cardiovascular magnetic resonance. *Am Heart J.* 2011; 162: 16-30.

74. Hombach V, Merkle N, Bernhard P, Rasche V, Rottbauer W. Prognostic significance of cardiac magnetic resonance imaging: Update 2010. *Cardiol J.* 2010; 17: 549-557.

75. Westbrook C, Roth C, Talbot J. MRI in Practice. Fourth Edition ed. West Sussex, UK: Wiley-Blackwell; 2011.

76. Aletras AH. Basic MRI Physics. In: Kwong RY, ed. Contemporary Cardiology: Cardiovascular Magnetic Resonance Imaging. Totowa, NJ: Humana Press Inc; 2008: 1-31.

77. Dymarkowski S, Bosmans H. Cardiac MRI Physics. In: Bogaert J, Dymarkowski S, Taylor AM, eds. Clinical Cardiac MRI. Berlin, Germany: Springer; 2005: 1-30.

78. Hashemi RH, William GB, Christopher JL. MRI - The Basics. 3rd ed. Philadelphia, PA: Lippincott Williams & Wilkins; 2010.

79. Ridgway JP. Cardiovascular magnetic resonance physics for clinicians: part I. *J Cardiovasc Magn Reson.* 2010; 12: 71-429X-12-71.

80. Frahm J, Haase A, Matthaei D. Rapid NMR imaging of dynamic processes using the FLASH technique. *Magn Reson Med.* 1986; 3: 321-327.

81. Dharmakumar R, Arumana JM, Larson AC, Chung Y, Wright GA, Li D. Cardiac phase-resolved blood oxygen-sensitive steady-state free precession MRI for evaluating the functional significance of coronary artery stenosis. *Invest Radiol.* 2007; 42: 180-188.

82. Plein S, Greenwood J, Ridgway J. Cardiovascular MR Manual. First Edition ed. London, UK: Springer; 2011.

83. Heydari B, Jerosch-Herold M, Kwong RY. Assessment of myocardial ischemia with cardiovascular magnetic resonance. *Prog Cardiovasc Dis.* 2011; 54: 191-203.

84. Bettencourt N, Chiribiri A, Schuster A, Nagel E. Assessment of myocardial ischemia and viability using cardiac magnetic resonance. *Curr Heart Fail Rep.* 2009; 6: 142-153.

85. Flett AS, Westwood MA, Davies LC, Mathur A, Moon JC. The prognostic implications of cardiovascular magnetic resonance. *Circ Cardiovasc Imaging.* 2009; 2: 243-250.

86. Wilke N, Simm C, Zhang J, Ellermann J, Ya X, Merkle H, Path G, Ludemann H, Bache RJ, Ugurbil K. Contrast-enhanced first pass myocardial perfusion imaging: correlation between myocardial blood flow in dogs at rest and during hyperemia. *Magn Reson Med.* 1993; 29: 485-497.

87. Arai AE. Magnetic resonance first-pass myocardial perfusion imaging. *Top Magn Reson Imaging.* 2000; 11: 383-398.

88. Plein S, Kozerke S, Suerder D, Luescher TF, Greenwood JP, Boesiger P, Schwitter J. High spatial resolution myocardial perfusion cardiac magnetic resonance for the detection of coronary artery disease. *Eur Heart J.* 2008; .

89. Soriano CJ, Ridocci F, Estornell J, Jimenez J, Martinez V, De Velasco JA. Noninvasive diagnosis of coronary artery disease in patients with heart failure and systolic dysfunction of uncertain etiology, using late gadolinium-enhanced cardiovascular magnetic resonance. *J Am Coll Cardiol.* 2005; 45: 743-748.

90. Kuo PH, Kanal E, Abu-Alfa AK, Cowper SE. Gadolinium-based MR contrast agents and nephrogenic systemic fibrosis. *Radiology.* 2007; 242: 647-649.

91. Friedrich MG. Testing for myocardial ischemia: the end of surrogates? *JACC Cardiovasc Imaging.* 2010; 3: 385-387.

92. Uludag K, Dubowitz D, Buxton R. Basical Principles of Functional MRI. In: Edelman R, Hesselink J, Zlatkin M, Crues J, eds. Clinical Magnetic Resonance Imaging. 3rd ed. Philadelphia, Pa: Saunders Elsevier; 2006: 249-287.

93. Pauling L, Coryell CD. The Magnetic Properties and Structure of Hemoglobin, Oxyhemoglobin and Carbonmonoxyhemoglobin. *Proc Natl Acad Sci U S A.* 1936; 22: 210-216.

94. Ogawa S, Lee TM, Kay AR, Tank DW. Brain magnetic resonance imaging with contrast dependent on blood oxygenation. *Proc Natl Acad Sci U S A.* 1990; 87: 9868-9872.

95. Ogawa S, Lee TM, Nayak AS, Glynn P. Oxygenation-sensitive contrast in magnetic resonance image of rodent brain at high magnetic fields. *Magn Reson Med.* 1990; 14: 68-78.

96. Thulborn KR, Waterton JC, Matthews PM, Radda GK. Oxygenation dependence of the transverse relaxation time of water protons in whole blood at high field. *Biochim Biophys Acta.* 1982; 714: 265-270.

97. Fieno DS, Shea SM, Li Y, Harris KR, Finn JP, Li D. Myocardial perfusion imaging based on the blood oxygen level-dependent effect using T2-prepared steady-state free-precession magnetic resonance imaging. *Circulation.* 2004; 110: 1284-1290.

98. Gore JC. Principles and practice of functional MRI of the human brain. *J Clin Invest.* 2003; 112: 4-9.

99. Kaul S, Jayaweera AR. Coronary and myocardial blood volumes: noninvasive tools to assess the coronary microcirculation? *Circulation.* 1997; 96: 719-724.

100. Holtz J, Grunewald WA, Manz R, von Restorff W, Bassenge E. Intracapillary hemoglobin oxygen saturation and oxygen consumption in different layers of the left ventricular myocardium. *Pflugers Arch.* 1977; 370: 253-258.

101. Li D, Waight DJ, Wang Y. In vivo correlation between blood T2* and oxygen saturation. *J Magn Reson Imaging.* 1998; 8: 1236-1239.

102. Chavhan GB, Babyn PS, Thomas B, Shroff MM, Haacke EM. Principles, techniques, and applications of T2*-based MR imaging and its special applications. *Radiographics.* 2009; 29: 1433-1449.

103. Egred M, Waiter GD, Al-Mohammad A, Semple SI, Redpath TW, Walton S. Blood oxygen level dependent (BOLD) MRI: A novel technique for the detection of myocardial ischemia. *Eur J Intern Med.* 2006; 17: 551-555.

104. Wacker CM, Bock M, Hartlep AW, Beck G, van Kaick G, Ertl G, Bauer WR, Schad LR. Changes in myocardial oxygenation and perfusion under pharmacological stress with dipyridamole: assessment using T*2 and T1 measurements. *Magn Reson Med.* 1999; 41: 686-695.

105. Wacker CM, Hartlep AW, Pfleger S, Schad LR, Ertl G, Bauer WR. Susceptibility-sensitive magnetic resonance imaging detects human myocardium supplied by a stenotic coronary artery without a contrast agent. *J Am Coll Cardiol.* 2003; 41: 834-840.

106. Westerhof N, Boer C, Lamberts RR, Sipkema P. Cross-talk between cardiac muscle and coronary vasculature. *Physiol Rev.* 2006; 86: 1263-1308.

107. Foltz WD, Huang H, Fort S, Wright GA. Vasodilator response assessment in porcine myocardium with magnetic resonance relaxometry. *Circulation.* 2002; 106: 2714-2719.

108. Li D, Dhawale P, Rubin PJ, Haacke EM, Gropler RJ. Myocardial signal response to dipyridamole and dobutamine: demonstration of the BOLD effect using a double-echo gradient-echo sequence. *Magn Reson Med.* 1996; 36: 16-20.

109. Wacker CM, Hartlep AW, Pfleger S, Schad LR, Ertl G, Bauer WR. Susceptibility-sensitive magnetic resonance imaging detects human myocardium supplied by a stenotic coronary artery without a contrast agent. *J Am Coll Cardiol.* 2003; 41: 834-840.

110. Friedrich MG, Niendorf T, Schulz-Menger J, Gross CM, Dietz R. Blood oxygen level-dependent magnetic resonance imaging in patients with stress-induced angina. *Circulation.* 2003; 108: 2219-2223.

111. Bernhardt P, Manzke R, Bornstedt A, Gradinger R, Spiess J, Walcher D, Rasche V, Hombach V. Blood oxygen level-dependent magnetic resonance imaging using T2-prepared steady-state free-precession imaging in comparison to contrast-enhanced myocardial perfusion imaging. *Int J Cardiol.* 2011; 147: 416-419.

112. McCommis KS, Goldstein TA, Abendschein DR, Herrero P, Misselwitz B, Gropler RJ, Zheng J. Quantification of regional myocardial oxygenation by magnetic resonance imaging: validation with positron emission tomography. *Circ Cardiovasc Imaging.* 2010; 3: 41-46.

113. Wendland MF, Saeed M, Lauerma K, de Crespigny A, Moseley ME, Higgins CB. Endogenous susceptibility contrast in myocardium during apnea measured using gradient recalled echo planar imaging. *Magn Reson Med.* 1993; 29: 273-276.

114. Reeder SB, Holmes AA, McVeigh ER, Forder JR. Simultaneous noninvasive determination of regional myocardial perfusion and oxygen content in rabbits: toward direct measurement of myocardial oxygen consumption at MR imaging. *Radiology.* 1999; 212: 739-747.

115. Egred M, Waiter GD, Semple SI, Redpath TW, Al-Mohammad A, Norton MY, Metcalfe MJ, Walton S. Blood oxygen level-dependent (BOLD) magnetic resonance imaging in patients with dypiridamole induced ischaemia; a PET comparative study. *Int J Cardiol.* 2007; 115: 36-41.

116. Wacker CM, Bock M, Hartlep AW, Bauer WR, van Kaick G, Pfleger S, Ertl G, Schad LR. BOLD-MRI in ten patients with coronary artery disease: evidence for imaging of capillary recruitment in myocardium supplied by the stenotic artery. *MAGMA.* 1999; 8: 48-54.

117. Niemi P, Poncelet BP, Kwong KK, Weisskoff RM, Rosen BR, Brady TJ, Kantor HL. Myocardial intensity changes associated with flow stimulation in blood oxygenation sensitive magnetic resonance imaging. *Magn Reson Med.* 1996; 36: 78-82.

118. Arnold JR, Karamitsos TD, Bhamra-Ariza P, Francis JM, Searle N, Robson MD, Howells RK, Choudhury RP, Rimoldi OE, Camici PG, Banning AP, Neubauer S, Jerosch-Herold M, Selvanayagam JB. Myocardial oxygenation in coronary artery disease: insights from blood oxygen level-dependent magnetic resonance imaging at 3 tesla. *J Am Coll Cardiol.* 2012; 59: 1954-1964.

119. Karamitsos TD, Leccisotti L, Arnold JR, Recio-Mayoral A, Bhamra-Ariza P, Howells RK, Searle N, Robson MD, Rimoldi OE, Camici PG, Neubauer S, Selvanayagam JB. Relationship between regional myocardial oxygenation and perfusion in patients with coronary artery disease: insights from cardiovascular magnetic resonance and positron emission tomography. *Circ Cardiovasc Imaging.* 2010; 3: 32-40.

120. Dharmakumar R, Hong J, Brittain JH, Plewes DB, Wright GA. Oxygen-sensitive contrast in blood for steady-state free precession imaging. *Magn Reson Med.* 2005; 53: 574-583.

121. Arumana JM, Li D, Dharmakumar R. Deriving blood-oxygen-level-dependent contrast in MRI with T2*-weighted, T2-prepared and phase-cycled SSFP methods: theory and experiment. *Magn Reson Med.* 2008; 59: 561-570.

122. Vohringer M, Flewitt JA, Green JD, Dharmakumar R, Wang J,Jr, Tyberg JV, Friedrich MG. Oxygenation-sensitive CMR for assessing vasodilator-induced changes of myocardial oxygenation. *J Cardiovasc Magn Reson.* 2010; 12: 20.

123. Manka R, Paetsch I, Schnackenburg B, Gebker R, Fleck E, Jahnke C. BOLD cardiovascular magnetic resonance at 3.0 tesla in myocardial ischemia. *J Cardiovasc Magn Reson.* 2010; 12: 54.

124. Jahnke C, Gebker R, Manka R, Schnackenburg B, Fleck E, Paetsch I. Navigator-gated 3D blood oxygen level-dependent CMR at 3.0-T for detection of stress-induced myocardial ischemic reactions. *JACC Cardiovasc Imaging.* 2010; 3: 375-384.

Chapter Two: HYPOTHESES AND OBJECTIVES

Hypothesis

Our group previously tested a T_2*-sensitive cine SSFP cardiovascular magnetic resonance sequence in animal experiments[1]. Using the present imaging approach, we hypothesized that OS-CMR is able to non-invasively assess myocardial oxygenation levels in patients suspected of having ischemic heart disease.

Objectives

1. Primary

Determine whether measurement of tissue oxygenation by OS-CMR can evaluate myocardial ischemia in patients suspected of having CAD. In comparison to:

a) functional significances of stenoses as assessed by Fractional Flow Reserve.

b) anatomical stenosis severity as assessed by Quantitative Coronary Angiography.

c) myocardial perfusion using qualitative CMR First-Pass Perfusion imaging.

2. Secondary

Determine whether OS-CMR can detect and quantify regional oxygenation changes throughout the myocardium in patients with coronary artery disease.

References

1. Vohringer M, Flewitt JA, Green JD, Dharmakumar R, Wang J,Jr, Tyberg JV, Friedrich MG. Oxygenation-sensitive CMR for assessing vasodilator-induced changes of myocardial oxygenation. *J Cardiovasc Magn Reson.* 2010; 12: 20.

Chapter Three: RESULTS – FIRST MANUSCRIPT

3.1 Title: Regional Assessment of Myocardial Oxygenation using Oxygen-Sensitive Cardiovascular Magnetic Resonance

Judy Luu, MD[1], Anna Schmidt, MD/PhDc[1], Jacqueline Flewitt, MSc.[1], Yoko Mikami, MD/PhD[1], Henk ter Keurs, MD/PhD[1], and Matthias G. Friedrich, MD.[2]

[1]Stephenson CMR Centre, Department of Cardiac Sciences, Libin Cardiovascular Institute of Alberta, [2]Philippa and Marvin Carsley Cardiovascular MR Centre at the Montreal Heart Institute/Université de Montréal, Montreal QC, Canada

Keywords: Transmural, regional myocardial gradient, coronary risk factors, ischemic heart disease, oxygenation-sensitive, cardiovascular magnetic resonance

3.2 Abstract

Background

OS-CMR exploits the inherent magnetic property of hemoglobin with the signal intensity (SI) in T2*-weighted images being dependent on its oxygenation status. The technique has been used to detect myocardial ischemia in patients with coronary artery disease (CAD). As ischemic myocardial damage occurs primarily in the subendocardium, we hypothesized that there is a transmural oxygenation gradient in patients with ischemic heart disease.

Methods

11 healthy volunteers, 34 patients with suspected or known CAD, and 32 controls with coronary risk factors but no history of ischemic heart disease (BMI and gender matched controls) were scanned on a clinical 1.5T MRI system using a cine SSFP T2*-weighted sequence. OS-CMR was performed at rest and during adenosine-induced coronary hyperemia in a single basal or mid-ventricular axis slice. A blinded reader traced inner and outer contours using CMR computer software (CVI^{42}, Circle Cardiovascular Imaging Inc, Calgary, AB). The relative mean change in OS-CMR signal intensity (ΔSI%) from rest to adenosine was calculated for the whole myocardium, epicardium, and endocardial regions. Multiple regression analysis was used to determine independent predictors of signal intensity percent changes in the myocardium.

Results

ΔSI% was homogenous throughout the myocardium in young, healthy subjects, whereas matched controls and patients with CAD had significantly reduced ΔSI% in the

subendocardium compared to the subendocardial segments. Patients with CAD and matched controls had an overall decreased ΔSI% across all myocardium layers when compared to young, healthy subjects ($p<0.05$). Multiple regression analysis identified only DBP and age as statistically significant predictors of signal intensity changes in the subendocardium.

Conclusion

OS-CMR can distinguish regional changes in myocardial oxygenation present in patients with known CAD that is not present in healthy subjects. However, segments from the matched controls with risk factors for CAD also exhibited differential regional changes, demonstrating the presence of abnormal oxygenation that may be explained by other co-morbidities. Decreasing DBP and increasing age were independent predictors of abnormal signal intensity response following adenosine-induced vasodilation. Therefore, the evaluation of regional myocardial oxygenation by OS-CMR may be further developed for assessment of patients at risk for CAD.

3.3 Abbreviations:

BMI:	Body Mass Index
BOLD:	Blood-Oxygen Level Dependent
CAD:	Coronary Artery Disease
CMD:	Coronary microvascular dysfunction
DBP:	Diastolic Blood Pressure
HTN:	Hypertension
ICC	Interclass Correlation Coefficient
LV:	Left Ventricular
LVEDVI:	LV end-diastolic volume index
LVEF:	LV ejection fraction
LVESVI:	LV end-systolic volume index
LVSVI:	LV stroke volume index
OS-CMR:	Oxygen-sensitive Cardiovascular Magnetic Resonance
SBP:	Systolic Blood Pressure
SI:	Signal Intensity
ΔSI%:	Mean signal intensity percent change from rest to stress
SSFP:	Steady State Free Precession

3.4 Background

It has long been known that the progression of ischemic heart disease in the myocardium is an inhomogenous process, whereby evidence for pre-existing cardiac damage can be found in the subendocardium of patients with angina pectoris but no associated infarction[1]. Additionally, evidence of early endothelial dysfunction in both epicardial and microvascular vessels has been demonstrated in patients having only risk factors for coronary artery disease (CAD), without any angiographic evidence of flow-limiting stenoses[2,3]. With the increasing prevalence of cardiovascular disease, significant research efforts have been devoted to the development of non-invasive cardiac imaging for the evaluation and timely diagnosis of ischemic heart disease.

Over the last several years, there has been a growing body of evidence to support the non-invasive approach for the assessment of myocardial oxygenation using cardiovascular magnetic resonance (CMR) as a marker for CAD[4]. Without the need for contrast agents or radiation, Oxygenation-Sensitive CMR (OS-CMR) exploits the inherent magnetic properties of deoxygenated hemoglobin such that signal intensity (SI) is directly dependent on tissue oxygenation in the myocardium[5,6]. Validated in the kidney cortex and skeletal muscle of rabbits, Dharmakumar et al. demonstrated the ability of OS-CMR to detect slight changes in the microcirculation, whereby the measured signal values were shown to be dependent on types of microcirculation with greater blood volume and on increased field strength at 3.0T compared to 1.5T[7]. As myocardial blood volume resides predominantly in the microcirculation, it is hypothesized that OS-CMR can detect alterations in myocardial oxygenation that may

provide useful diagnostic information for patients at increased risk for microvascular ischemia. Therefore, the purpose of the present study was two-fold: to determine whether OS-CMR can detect and quantify transmural regional changes in the subepicardial and subendocardial layers of the myocardium. Secondly, we sought to determine whether alterations in transmurality of tissue oxygenation could be predicted by key demographic characteristics or risk factors.

3.5 Methods

3.5.1 Study population

We prospectively recruited participants aged 18-70 for three study cohorts: 1) Patients with suspected or known CAD referred for clinically indicated diagnostic angiography 2) Individuals with no history or evidence of ischemic heart disease but having coronary risk factor(s) (also referred to as BMI and gender matched controls), including diabetes type II, current or previous smoker (pack year history was not recorded), dyslipidemia, family history, or hypertension (HTN) (defined as systolic blood pressure >140, diastolic blood pressure >90 or effectively controlled with usage of oral anti-hypertensives). Patients in this cohort were excluded if they had any history of valvular heart disease or known cardiomyopathies. 3) The third cohort included healthy individuals <40 years old, with no significant previous medical history and no history or evidence of ischemic heart disease. Exclusion criteria for all three cohorts included previous coronary bypass surgery as well as the presence of contraindications to MRI (morbid obesity, implanted metallic devices, severe claustrophobia), adenosine

vasodilating agent, or gadolinium contrast (renal dysfunction indicated by glomerular filtration rate < 60 ml/min). Xanthine or dipyridamole use within 24 hours of CMR scan was not permitted. Ethics approval was obtained from the University of Calgary Conjoint Health Research Ethics Board and full written informed consent was obtained from all subjects.

3.5.2 CMR imaging protocol

CMR was performed with the patient in supine position using 1.5T MRI System (Magnetom Avanto®, Siemens Healthcare, Erlangen, Germany) with a 32-channel cardiac coil. Image acquisition was performed during breath-holds, using retrospective electrocardiogram (ECG)-gated sequences. Steady state free precession (SSFP) cine images were initially acquired for left ventricular (LV) volume and functional scanning. Oxygenation-sensitive CMR images were acquired for the entire cardiac cycle in the short axis view at one regional slice (basal and/or mid) using a T2* oxygenation-sensitive, ECG-triggered SSFP sequence with a long repetition time, as previously reported [8]. Scan parameters were: field of view 400 x 400 mm; matrix size 128 x 128, bandwidth 273 Hz/Pixel, TR/TE = 5.4/2.7ms, flip angle 90°, slice thickness 15mm. Typical breath-hold length was 10-15 seconds. The data acquisition of OS-CMR images were repeated during intravenous administration (at least 2 minutes after starting the infusion) of 140mcg/kg/min adenosine.

3.5.3 Analysis of Oxygenation-Sensitive Images

CMR images acquired with the oxygenation-sensitive SSFP cine sequence were analysed offline by a blinded reader using certified software (CVI[42], Circle, Cardiovascular Imaging Inc., Calgary, Canada). One basal or mid ventricular slice was selected for analysis at end-systole. Images were excluded if they included the presence of significant partial volume effect, the presence of inhomogeneity artefact, or any other significant image problem such as discordance in slice position between rest and stress due to extensive respiratory motion during a breathhold. Epicardial and endocardial contours were manually drawn for the short axis slice. The software measured and outputted the signal intensities (SI) for the whole (total) myocardium, subepicardium, and subendocardium to Microsoft Excel (Version 2008, for Macintosh) spreadsheets for calculations (Figure 1). The change in mean signal intensity (ΔSI%; signal intensity percent change) was calculated as the SI at rest subtracted from SI at maximal hyperemia during adenosine infusion, divided by the SI at rest and expressed as a percentage.

$$\Delta\% = \frac{\text{mean SI (stress)} - \text{mean SI (rest)}}{\text{mean SI (rest)}} \times 100$$

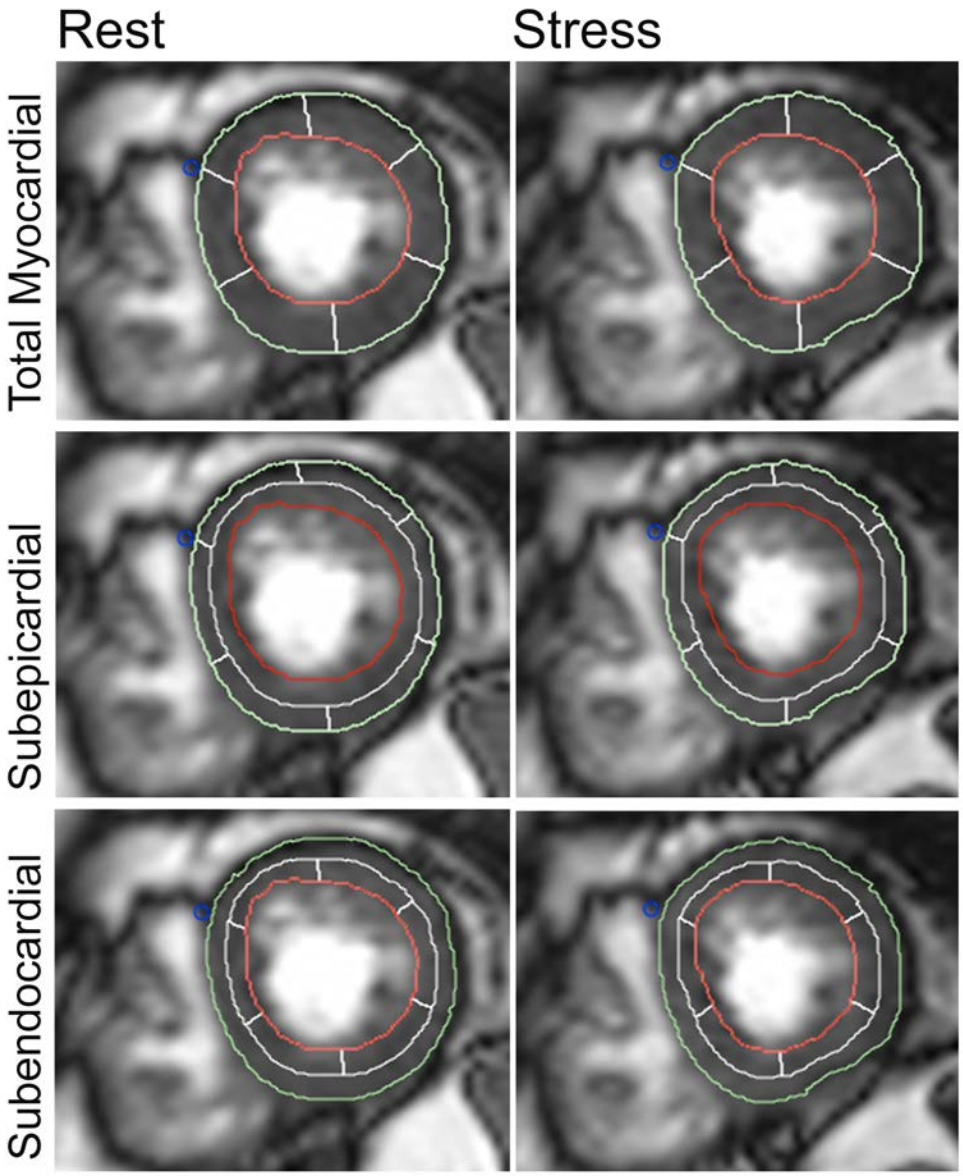

Figure 3-1: Manual tracing of contours for automatic computer generated signal intensity extraction.

Basal slices from a patient to represent the method used for image analysis. Contours were drawn for both rest and stress images. Contours were drawn around the epicardium (green) and around the endocardium (red) to isolate the actual myocardium, excluding trabeculations. The OS-CMR SI was computed for the region isolated within the red and green borders. Careful consideration was taken to avoid artefacts and the large cavity in the middle, which would affect the mean OS-CMR SI. Segmentation division was automatically drawn after the right ventricle insertion points were identified (blue dot). At 50% from the endocardium, the subepicardial region was marked and at 50% from the epicardium, the subendocardial region was marked.

3.5.4 Statistical Analysis

Data analysis was performed using statistical software (IBM SPSS Statistics for Mac version 20.0. Armonk, NY: IBM Corp). Continuous variables were presented as mean +/- 95% confidence intervals and categorical variables as percentages. Differences in the demographics and myocardial layers between cohorts were calculated using ANOVA (Analysis of Variance) and Bonferroni's correction for Post-Hoc analysis. Independent T-tests was used for differences within groups for the myocardial layers. Pearson's correlation was used to determine the strength of a linear relationship between the coronary risk factors to the different myocardial layers. Using multiple regression analysis with the stepwise method, independent predictors of the dependent variable, OS-CMR ΔSI%, were computed for demographic variables including age, Body Mass Index (BMI), systolic (SBP) and diastolic blood pressure (DBP), gender, past or present smoker, HTN, dyslipidemia, diabetes, family history, and previous history of CAD. The Interclass Correlation Coefficient (ICC) was used to measure inter- and intra-observer variability and the Bland Altman method was used to graphically depict the interobserver and intraobserver variability for 20 randomly selected, consecutive patients with known CAD between the quantitative outputs of two readers. Inter-reader reliability based on ICC values less than 0.40 is considered poor, between 0.40 and 0.59 is considered fair. Values between 0.60 and 0.74 are considered good and any values above 0.75 are considered excellent [9].

3.6 Results

In total, 11 healthy volunteers, 34 patients suspected or known to have coronary artery disease, and 32 controls with coronary risk factors but no history of ischemic heart disease (matched controls), completed the study protocol. Image quality was good in all participants. Patient demographics and baseline characteristics are listed in Table 1. In the participants with only coronary risk factors and previously diagnosed hypertension, blood pressures were all controlled with systolic <140mmHg and diastolic < 90mmHg. Patient coronary risk factors and medications are listed in Table 2 and Table 3.

Table 3-1: Patient Demographics and Baseline CMR parameters.

	Healthy Volunteers (n=11)	Controls with Coronary Risk Factors (n=32)	CAD Patients (n=34)	p-Value	Post-Hoc Analysis		
					p Value[1]	p Value[2]	p Value[3]
Age, years	29±4	52±9	60±7	p=0.000	p=0.000	p=0.000	P=0.040
Male	6 (55%)	24 (75%)	26 (76%)	p=NS	p=NS	p=NS	p=NS
BMI	22.8±2.6	27.4±4.0	29.1±5.7	p=0.019	p=0.001	p=0.001	p=NS
Systolic BP, mmHg	119±7	120±24	128±12	p=NS	p=0.024	p=NS	p=NS
Diastolic BP, mmHg	88±9	80±10	77±9	p=0.048	p=0.004	p=0.005	p=NS
CMR Baseline Parameters							
LVSVI, mL/m^2	49±6	48±23	45±7	p=NS	p=NS	p=NS	p=NS
LVEDVI, mL/m^2	74.5±9	85±16	88±17	p=NS	p=NS	p=NS	p=NS
LVESVI, mL/m^2	31.5±9	31.6±10	31.7±11	p=NS	p=NS	p=NS	p=NS

LVEF, %	64±4	60±5	59±8	p=NS	p=NS	p=NS	p=NS

Note: Values are presented as n (%) or mean ± SD.

Post-Hoc Analyses:

p Value[1]: Statistical significance between healthy volunteers and controls with coronary risk factors

p Value[2]: Statistical significance between healthy volunteers and CAD patients

p Value[3]: Statistical significance between controls with coronary risk factors and CAD patients

Table 3-2: Participant Risk Factors for Coronary Artery Disease

Cardiovascular Risk Factors, N (%)	Healthy Volunteers (n=11)	Controls with Coronary Risk Factors (n=32)	CAD Patients (n=34)	p value	Post-Hoc Analysis		
					p Value[1]	p Value[2]	p Value[3]
Past/present smoker	0	10 (31%)	18 (53%)	p=0.004	p=NS	p=0.004	p=NS
Hypertension	0	10 (31%)	16 (47%)	p=0.014	p=NS	p=0.012	p=NS
Dyslipidemia	0	14 (44%)	26 (76%)	p=0.000	p=0.016	p=0.000	p=0.009
Diabetes Mellitus	0	14 (44%)	7 (21%)	p=0.009	p=0.013	p=NS	p=NS
Family History	2 (18.2%)	18 (56%)	27 (79%)	p=0.001	p=NS	p=0.001	p=NS
Prior CAD	0	0	8 (24%)	p=0.014	p=NS	p=NS	p=0.027

Post-Hoc Analyses:

p Value[1]: Statistical significance between healthy volunteers and controls with coronary risk factors

p Value[2]: Statistical significance between healthy volunteers and CAD patients

p Value[3]: Statistical significance between controls with coronary risk factors and CAD patients

Table 3-3: Patient Baseline Medications

Medication, N (%)	Healthy Volunteers (n=11)	Controls with Coronary Risk Factors (n=32)	CAD Patients (n=34)	p Value[1]	Post-Hoc Analysis		
					p Value[1]	p Value[2]	p Value[3]
Antiplatelets	0	9 (28%)	33 (97%)	p=0.000	p=0.040	p=0.000	p=0.000
Beta-Blockers	0	1 (4%)	21 (54%)	p=0.000	p=NS	p=0.000	p=0.000
Calcium Channel Blockers	0	1 (3%)	1 (3%)	p=NS	p=NS	p=NS	p=NS
Statins	0	14 (44%)	33 (97%)	p=0.000	p=0.002	p=0.000	p=0.000
ACE inhibitors or ARBs	0	10 (32%)	18 (53%)	p=0.004	p=NS	p=0.004	p=NS
Diuretics	0	2 (6%)	6 (18%)	p=NS	p=NS	p=NS	p=NS

ACE Inhibitors: Angiotensin-converting-enzyme; ARBS: Angiotensin II receptor blockers

Post-Hoc Analyses:

p Value[1]: Statistical significance between healthy volunteers and controls with coronary risk factors

p Value[2]: Statistical significance between healthy volunteers and CAD patients

p Value[3]: Statistical significance between controls with coronary risk factors and CAD patients

3.6.1 Myocardial Oxygenation in Different Myocardial Layers

The relative BOLD ΔSI% for each cohort is illustrated in Figure 2 (See Appendix Figure A-1, A-2, A-3 for absolute changes). The mean ΔSI% for the whole myocardium of the young, healthy volunteers was 21.2% (CI 14.5 – 27.9%), which was statistically significant compared to the whole myocardium of the matched controls (9.7% CI 6.4 – 13.1%; $p<0.05$) and compared to the CAD patients (4.5% CI 2.1 – 6.9%; $p<0.001$). The whole myocardium of the matched controls was also statistically significant when compared to the CAD patients ($p<0.05$). When comparing the mean ΔSI% for the subepicardial layers for all three cohorts, there was statistical significance when comparing to the healthy volunteers (21.0% CI 14.8 – 27.1%; $p<0.05$). However, there was no statistical significance between the subepicardium of matched controls (12.4% CI 8.6 – 16.1%) and the CAD patients (8.1% CI 5.1 – 11.2%; $p=0.234$). Across all three cohorts, there was statistical significance ($p<0.05$) between the multiple comparisons of subendocardium of the healthy volunteers (21.9% CI 14.4 – 29.3%), matched controls (6.4% CI 3.2 – 9.5%), and CAD patients (1.1% CI -1.0 – 3.3%). Overall, in controls with coronary risk factors (matched controls) and CAD patients, there was a nearly 50% decrease in ΔSI% following adenosine-induced hyperemia across the whole myocardium, subepicardium, and subendocardium when compared to young, healthy subjects ($p<0.05$).

The ΔSI% was homogenous throughout the different myocardial layers in healthy subjects ($p=0.510$), whereas CAD patients had statistically significant reduced signal intensities within the subendocardium compared to the subepicardial segments

(p<0.001). A similar finding of reduced ΔSI% in the subendocardium compared to the subepicardium was also seen in the matched controls with coronary risk factors (p<0.001).

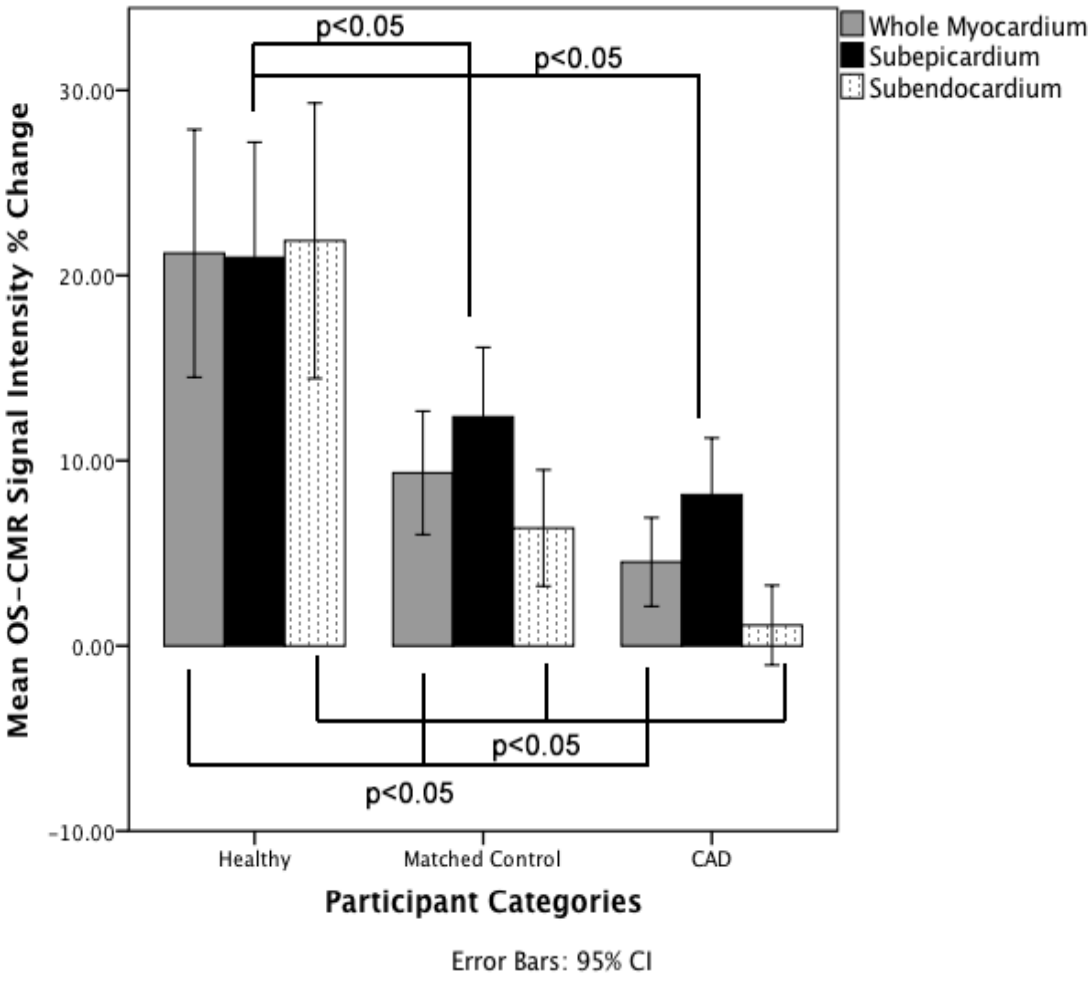

Figure 3-2: Mean OS-CMR signal intensity percent changes in the whole myocardium, subepicardium and subendocardium in study participants.

Not shown on the figure, ΔSI% for the subepicardium of the matched controls and CAD patients were not significant, p=NS.

3.6.2 Inter- and Intra-observer Variability

The interobserver variability of the OS-CMR measurements was small with an ICC for single measures of 0.931 (CI 0.900 – 0.952). The intraobserver variability was also small, with an ICC for single measure of 0.883 (CI 0.833 – 0.918). Bland Altman graphical depiction can be seen in Figure 3 and 4 with the mean difference representing the estimated bias between the two readings. The standard deviation around the mean difference represents the random fluctuations around the mean difference (Y-axis). The x-axis also demonstrates the scatter around the average of the two readings.

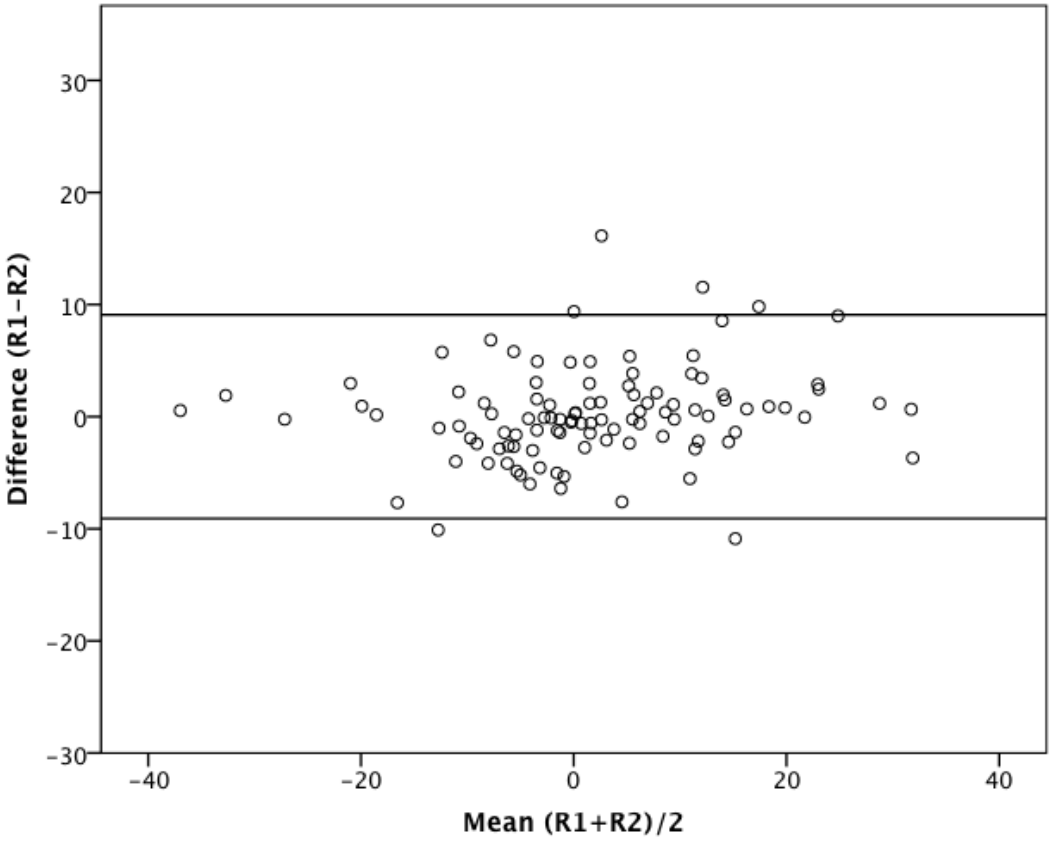

Figure 3-3: Bland Altman graphical illustration of interobserver variability between two readers (R1 and R2) with Y-axis lines representing mean differences±1.96 x SD.

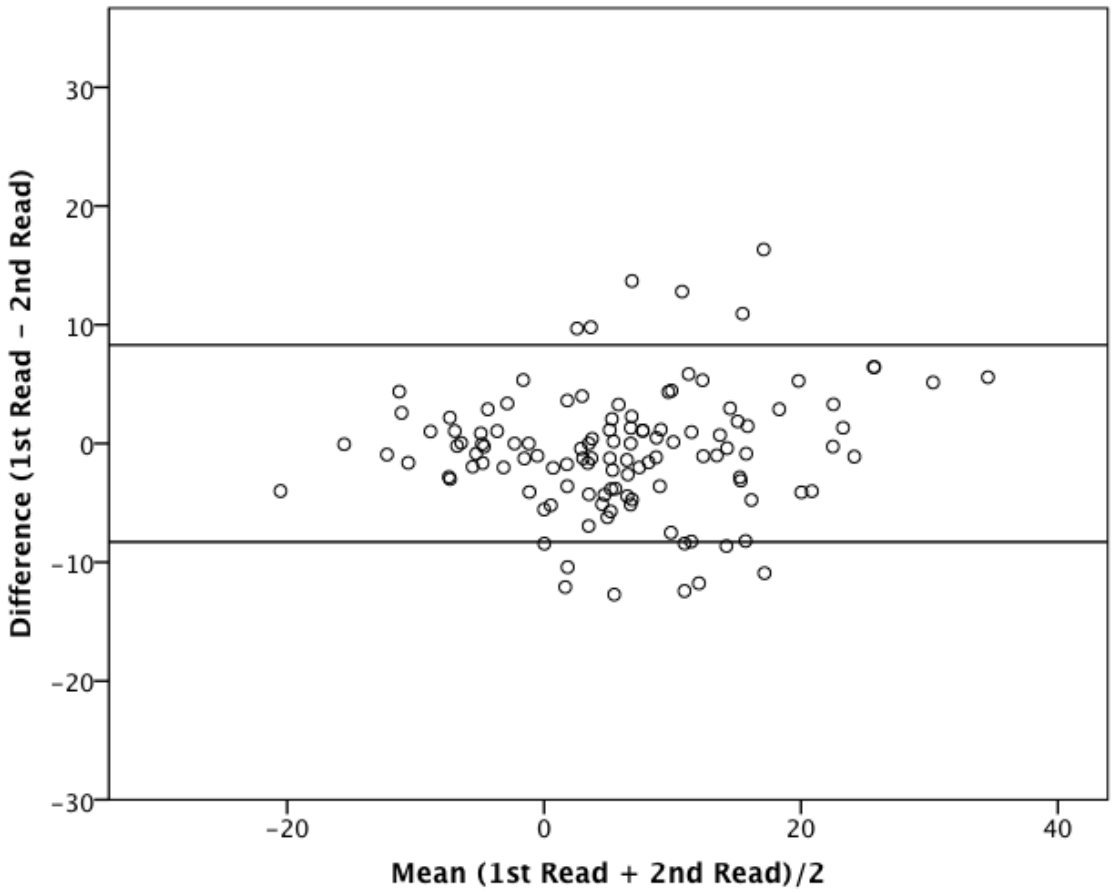

Figure 3-4: Bland Altman graphical illustration of intraobserver variability with Y-axis lines representing mean differences±1.96 x SD.

3.6.3 Correlation Analyses and Multiple Stepwise Regression

Data from all three participant groups (healthy volunteers, matched controls, and patients with CAD) were analysed together. Continuous variables of age, DBP, and BMI, as well as categorical variables of family history and dyslipidemia had the strongest correlations to alterations in BOLD ΔSI% in the different myocardial layers (Table 4). Any history of smoking, whether previous or current, was not significantly correlated to subepicardial signal intensity (Pearson = -0.159, p=0.111), but was significantly correlated to subendocardial signal intensity (Pearson = -0.236, p = 0.034). Similar patterns were seen with BMI and dyslipidemia, where although not significantly correlated to subepicardial signal intensity, the risk factors correlated significantly with subendocardial signal intensity (Table 4).

Using multiple regression analysis, DBP (Beta=0.335, p=0.004), age (Beta=-0.309, p=0.008), and family history (Beta=-0.223, p=0.047) were significant independent predictors of whole myocardial BOLD ΔSI%. The overall model fit was R=0.62 and R^2=0.39. Likewise, DBP (Beta=0.376, p=0.002) and family history (Beta=-0.310, p=0.009) were the only independent predictors of subepicardial BOLD signal intensity changes with an overall model fit R=0.54 and R^2=0.29. For subendocardial BOLD signal intensity, age (Beta=-0.468, p=0.000) (Figure 5) and DBP (Beta=0.324, p=0.003) (Figure 6) were independent predictors with an overall model fit of R=0.64 and R^2=0.41 (For additional figures illustrating absolute values, please refer to the Appendix Figure A-4 and A-5). BMI, while not a significant predictor in the model, was significantly correlated to subendocardial signal intensity (Pearson = -0.349, p=0.003) (Figure 7). The correlation between age, DBP, and BMI to subendocardial

signal intensity was non-significant when the young, healthy volunteers (mean age 29 years) were excluded. The presence of diabetes as a cardiovascular risk factor was not an independent predictor of BOLD ΔSI% in any of the myocardial layers.

Table 3-4: Pearson's Correlations between whole myocardial, subepicardial, and subendocardial BOLD ΔSI% to patient demographic characteristics.

	Pearson's Correlations					
	Whole Myocardium	**p Value**	**Subepi-**	**p value**	**Subendo-**	**p Value**
Age	-0.441	p=0.000	-0.314	p=0.007	-0.537	p=0.000
BMI	-0.283	p=0.014	-0.193	p=0.068	-0.349	p=0.003
DBP	0.481	p=0.000	0.461	p=0.000	0.459	p=0.000
Past/Present Smoker	-0.186	p=0.000	-0.159	p=0.111	-0.236	p=0.034
HTN	-0.025	p=0.003	0.043	p=0.372	-0.349	p=0.236
Dyslipidemia	-0.238	p=0.032	-0.154	p=0.118	-0.306	p=0.008
Diabetes Mellitus	-0.065	p=0.311	-0.016	p=0.450	-0.122	p=0.175
Family History	-0.356	p=0.002	-0.361	p=0.002	-0.307	p=0.008
Prior CAD	-0.106	p=0.041	0.013	p=0.461	-0.201	p=0.060

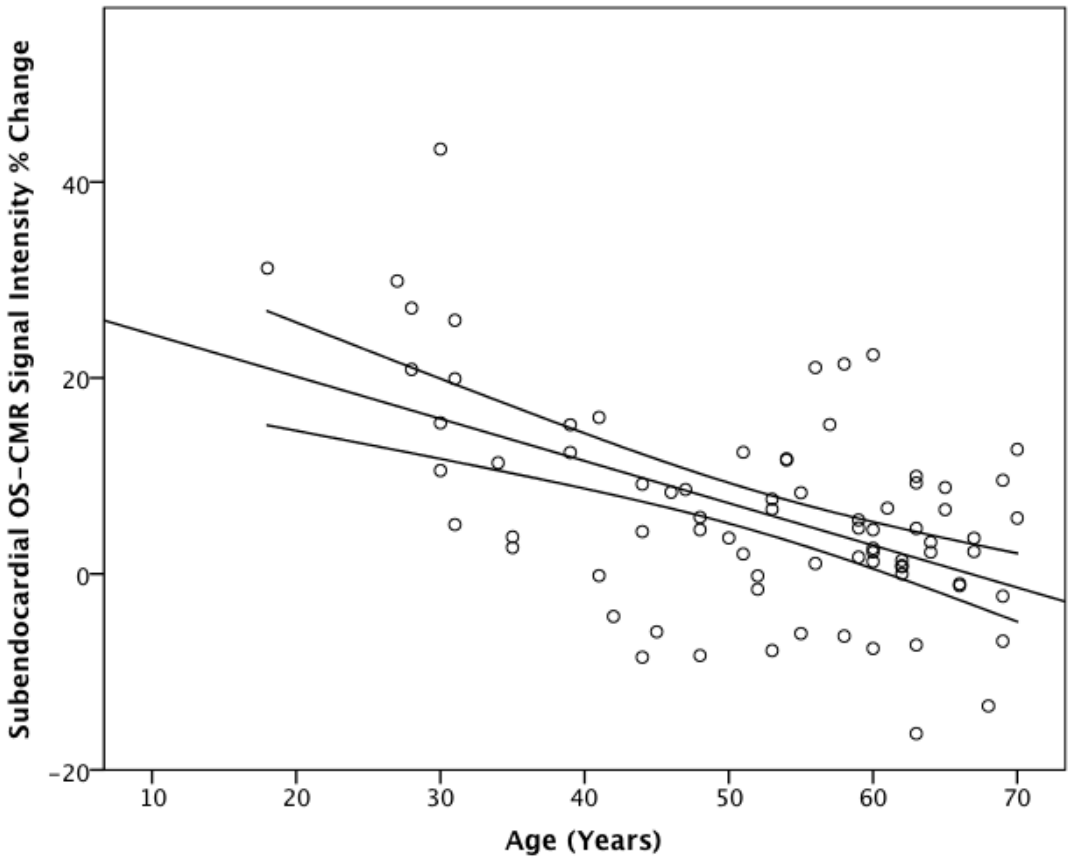

Figure 3-5: Correlation of independent predictive variable of age to signal intensity percent change in the subendocardium.

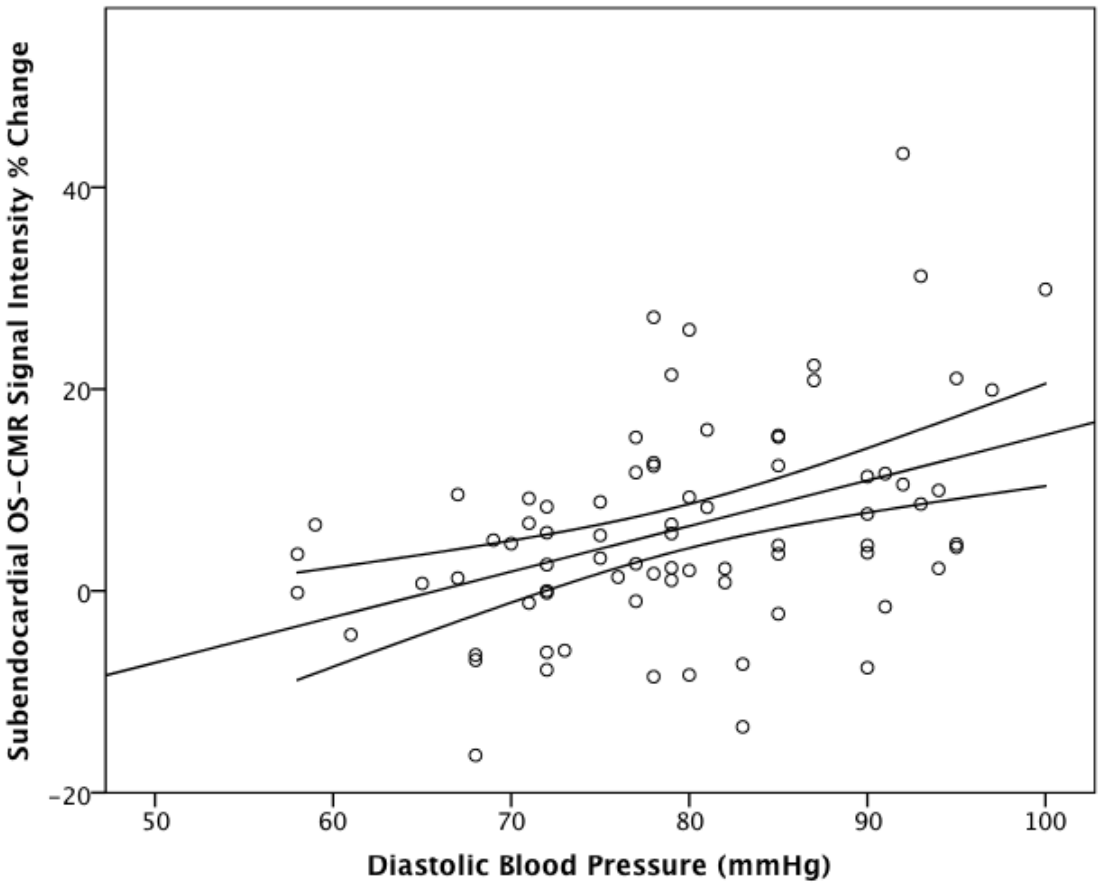

Figure 3-6: Correlation of the independent predictive variable, diastolic blood pressure, to signal intensity percent change in the subendocardium.

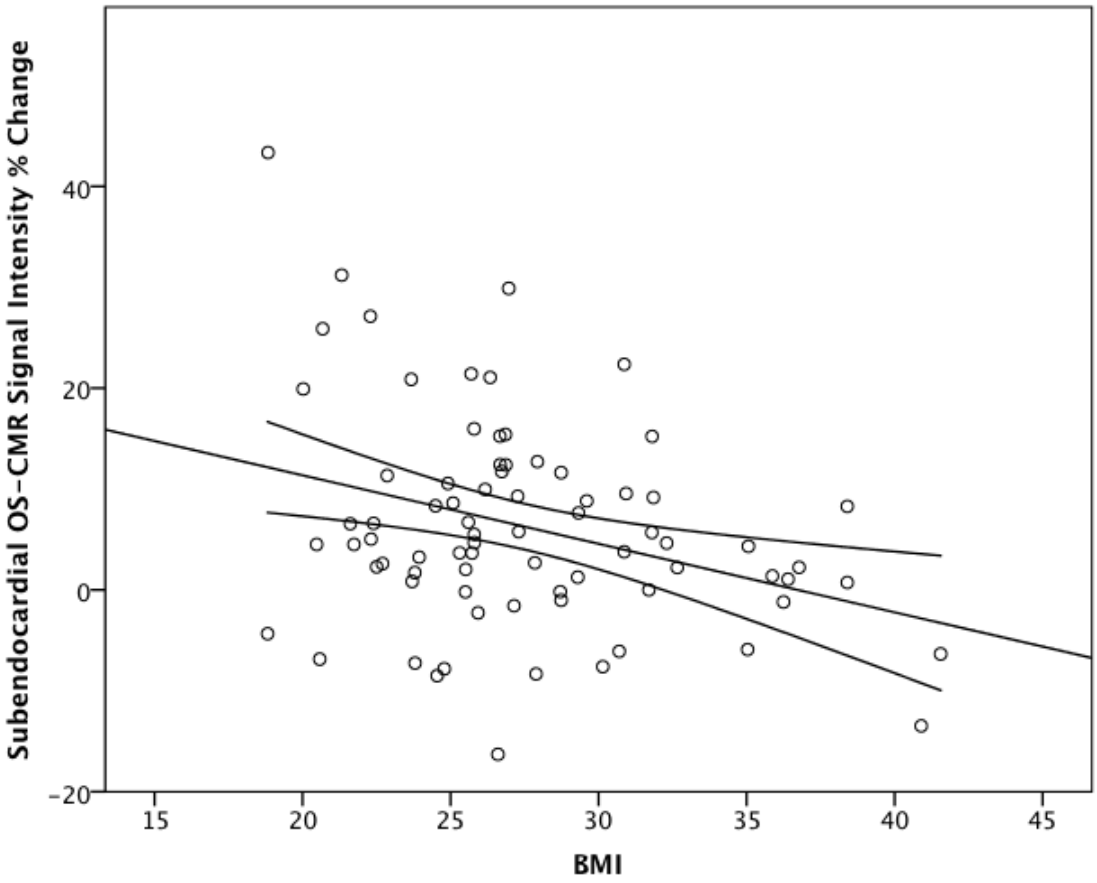

Figure 3-7: Correlation of the independent predictive variable, BMI, to signal intensity percent change in the subendocardium.

While not significant as an independent predictor, BMI was correlated to signal intensity percent change (Pearson's correlation = -0.349; $p<0.003$).

3.7 Discussion

Previous animal and clinical studies have shown the relative mean signal intensity from baseline to adenosine-induced hyperemia as measured by OS-CMR is a function of oxygen saturation and the volume percentage of deoxygenated hemoglobin in the capillary blood [4,10]. To our knowledge, our study is the first to examine the transmurality in the different myocardial layers using OS-CMR, demonstrating the presence of regional changes in the subendocardium compared to the subepicardium. Importantly, when compared to young, healthy individuals, there was a nearly fifty-percent blunted response following adenosine in both the CAD cohort and the matched controls with risk factors but no clinical evidence of CAD. In the latter cohort, we demonstrated the presence of subendocardial deoxygenation using OS-CMR that may be predicted by weak correlation with decreasing diastolic blood pressure and increasing age. From a clinical perspective, the study findings may have implications toward the evaluation of disease progression in ischemic heart disease.

Oxygenation-sensitive contrast is a measure of intracapillary deoxyhemoglobin blood content[11] and is neither influenced by capillary blood volume or blood flow, reflecting the relationship between myocardial oxygen supply and demand[12]. Our results further expand on these findings by exploring regional changes in the signal intensity in different layers of the myocardium. Since the endocardium is at greater risk for ischemic injury than the epicardium, we hypothesized that the tissue oxygenation would also be differentially affected.

Using the BOLD technique, Egred et al. showed that an impairment of vasodilation following dipyridamole infusion resulted in decreased mean BOLD ΔSI% from a concomitant increase of deoxyhemoglobin and reduced coronary perfusion in CAD patients with established three-vessel disease[13]. We too, found an overall decreased response by over one-half following adenosine-induced hyperemia in our CAD population with total myocardial ΔSI% of 4.5, and notably, even more decreased ΔSI% in the subendocardium at 1.1%. Previous data from our research group using the cine SSFP sequence has demonstrated that a BOLD ΔSI% of 4.8 or less is associated with functionally significant stenoses with FFR <0.80[8]. Therefore, at a mean ΔSI% of 1.1%, measurement of the tissue oxygenation of the subendocardium may better reflect disease severity in patients with CAD. While a mean difference of 1.1% may appear inadequate as a reliable measure, previous researchers have similarly found small differences can adequately predict coronary disease. Walcher et al. found that mean signal intensities ranging from 1.50% to 1.54% can predict segments supplied by normally perfused coronary arteries and mean signal intensities ranging as low as 0.90 - 1.08% can predict coronaries supplied by functionally significant stenosis[14].

3.7.1 Role of Age and Diastolic Blood Pressure in Myocardial Oxygenation

In our young, healthy participants, we found no evidence of regional differences between the subepicardial and subendocardial layers compared to the older participants (mean age 52-60 years), suggesting the impact of aging on BOLD ΔSI%. Indeed, aging, among other coronary risk factors, has been shown to play an important role in the

impairment of endothelial function in both the coronary epicardial arteries and microvasculature [2,3,15,16].

Adding to our understanding of tissue oxygenation, Arnold et al. showed a trend for smoking to increase the odds of an abnormal BOLD response, whereas the presence of late gadolinium enhancement, hypercholesteremia, and diabetes did not significantly change the odds of an abnormal BOLD response[17]. Referring to Figure 3-6, we also found that decreasing DBP was predictive of abnormal BOLD signal intensity following adenosine-induced vasodilation, albeit a weak correlation as there was a large scatter in plot. The scatter may be due the intrinsic inhomogeneity of the OS-CMR technique, as the T2*-sequence is more susceptible to influences in the surrounding tissue. However, in support of our findings, one previous study looked at blood pressure measurements of two large French cohorts of men composed of 15,561 men aged 20 to 82 years and 6,246 men aged 42 to 53 years, studied for a mean period of 13.5 years and 17 years, respectively. After adjustment for age or other major risk factors, the participants with increased systolic blood pressure and concomitant decreased blood pressure were shown to have the highest relative risk of cardiovascular mortality compared to subjects with no changes in either systolic of diastolic blood pressure (relative risk range from 2.07 to 2.16) [18]. Elevation in total peripheral vascular resistance is known to be associated with both high systolic and diastolic blood pressure. Stiffening of arteries, on the other hand, can paradoxically result in high systolic blood pressure due to reduced capacitance, and decreased diastolic blood pressure due to reduced elastic recoil supporting the diastolic pressure[19]. Arterial stiffness increases with age and atherosclerosis, where one hypothesis suggests that the repetitive cyclic stress over an individual's life span can

lead to degradation of the elastic fibers in the smooth muscles of arteries[20]. To support our speculations, we demonstrated decreased signal intensity following adenosine-induced hyperemia in the matched controls with no evidence of CAD (mean age 52) and CAD patients (mean age 60) in comparison healthy, younger volunteers.

Various pharmacological therapies including beta-blockers, ACE inhibitors and ARBs, have been shown to improve arterial stiffness[21]. We did not appreciate the effect of these medications on the improvement of the myocardial oxygenation in the CAD patients. In our study population, approximately 50% of the CAD patients were on these medications at the time of the scan. However, compliance was not recorded nor was duration of therapy, which may have confounded the data.

Although BMI was not a significant independent predictor, it was statistically significantly correlated to subendocardial BOLD ΔSI%. We suspect this is likely due various outliers that can be seen on Figure 7. BMI, however, is known to not be a reliable indicator of an individual's overall health or measure of obesity, as athletes may have the same BMI as individuals at risk for CAD, but overall much healthier body composition made up of less body fat and more muscle. Although not measured in our study, central obesity measured by waist circumference has been shown to be directly related to increased mortality in patients CAD (hazard ratio [HR]: 1.70, 95% confidence interval [CI]: 1.58 to 1.83). BMI, on the other hand, was inversely associated with mortality (HR: 0.64, 95% CI: 0.59 to 0.69)[22].

3.7.2 Oxygen-sensitive CMR for the evaluation of microvascular dysfunction

Coronary microvascular dysfunction (CMD) is a condition that affects the small coronary arterial network of the myocardium, limiting the microvascular vasodilator capacity of the microcirculation. Previous studies demonstrated the ability of CMR to examine oxygenation-sensitive contrast in the microcirculation found in the kidney cortex and skeletal muscle of rabbits, implicating the role of OS-CMR in evaluating microvascular disease [7]. In canine studies, Vohringer et al. also showed that OS-CMR is susceptible to changes induced by endothelial-dependent vasodilation using acetylcholine [10], in which an abnormal response to acetylcholine was shown in patients with endothelial dysfunction of the coronary microvasculature[2]. Using OS-CMR in patients with CAD, Arnold et al. compared BOLD signal intensity and PET myocardial perfusion imaging to coronary angiography. With quantitative coronary angiography as the reference standard, myocardial segments were labelled as "stenosed" if subtended by significantly stenotic vessels, "remote from ischemia" if supplied by vessels with minimal or no disease, and myocardial segments from normal volunteers were labelled "normal". During hyperemia in remote myocardial segments, these researchers demonstrated a range of signal intensities (ranging from -5% to 30%) and myocardial blood flow measurements in between values of the normal and stenosed segments. In previous PET studies, Uren et al. have also shown reduced coronary vasodilator reserve and altered metabolism in myocardium subtended by normal arteries that were remote from ischemic region, postulating the presence of diffuse microvascular dysfunction[17,23,24]. In our study, we demonstrated a nearly 50% blunted response in matched controls with only risk factors when compared to the young, healthy

volunteers. This is consistent with studies that have demonstrated in the presence of coronary risk factors, patients without evidence of angiographic limiting stenoses were shown to have a blunted response to endothelium-dependent vasodilation following acetylcholine infusion, indicating that there may be abnormalities in the microvasculature that are not detectable on conventional imaging modalities for CAD [25].

There are many risk factors that have been shown to be associated CMD, including diabetes, aging, hypertension, dyslipidemia, and insulin resistance [26]. In our study, we found that diabetes as a coronary risk factor was not a significant predictor of tissue oxygenation in the myocardium, particularly in the subendocardium. This may be attributed to the fact we had only 21 patients with diabetes, and of those, the duration of the condition ranged anywhere from newly diagnosed to greater than 10 years with diabetes. Arnold et al. also demonstrated that diabetes did not appear to have an influence on the oxygen-sensitive contrast, as the presence of diabetes did not significantly change the odds of an abnormal BOLD response[17]. This is further supported by a large randomized control trial that looked at screening CAD patients with diabetes type II (DMII) as a high risk for cardiac events. The study screened over 1000 patients and concluded that within the population of asymptomatic type 2 diabetes, use of myocardial perfusion imaging screening revealed no discernible effect of DMII on subsequent cardiac events[27]. Therefore, more likely contributing to the subendocardial deoxygenation may include other risk factors known to contribute to abnormal coronary circulation in the resistance vessels, including hypercholesteremia, smoking, and hypertension [3,15].

Interestingly, while CMD is a condition affecting the microcirculation throughout the myocardium, we demonstrated a greater decrease in BOLD ΔSI% in the subendocardium compared to the subepicardium. Other researchers have also shown similar findings. Using myocardial perfusion imaging by CMR, Panting et al. have previously demonstrated subendocardial hypoperfusion in comparison to the subepicardum during intravenous infusion of adenosine in patients with syndrome X, but no evidence of diabetes, hypertension, or LV hypertrophy[28]. Extending those findings, Lanza et al. provided evidence to support the presence of coronary microvascular dysfunction in patients with syndrome X by using dobutamine CMR perfusion imaging and transthoracic echo-Doppler recording. Lanza et al. demonstrated the evidence of perfusion defects localized to the subendocardium, in keeping with findings by Panting and colleagues. The perfusion defects detected by CMR were accompanied by impaired coronary microvascular dilatory function following adenosine, as assessed by echo-Doppler [29]. As to why the subendocardium was more preferentially affected than the subepicardium, one potential hypothesis may be that autoregulation of blood flow has different limits in the endocardium compared to the epicardium. While the heart is able to autoregulate over a wide range of perfusion pressures, differential compressive forces result in more constrained blood flow during systole in the endocardium. As a result, the resistance vessels (arterioles) must vasodilate to a larger extent in diastole to compensate for the reduced blood flow in systole. The lower limit of perfusion pressure for maximal vasodilation in the endocardium is 70mmHg, whereas it is 40mmHg in the epicardium. Therefore, in cases where blood flow to the heart is severely limited, the endocardium is more prone to

cardiac injury, with areas of necrosis generally larger in the endocardium than epicardium [30].

Using OS-CMR in patients with syndrome X (mean age 62 years), Karamitsos et al. found no evidence of decreased BOLD signal intensity following adenosine-induced vasodilation or quantitatively assessed myocardial perfusion compared to healthy controls with mean age of 58 years. The study patients with syndrome X were selected based on normal angiograms and no clinical history of diabetes, hypertension, dyslipidemia, left ventricular hypertrophy, or other cardiac or systemic disease[31]. However, all patients included in the study, as well as the two previously mentioned, were on various cardiac medications including beta-blockers, calcium channel blockers, statins, nitrates, and ACE inhibitors, indicating some degree of coronary risk like our matched controls. Our control patients, with similar mean age (52 years) to the controls in the study by Karamitsos et al, were predominantly on statins, suggesting the role of hypercholesteremia in the blunted signal intensity throughout the myocardium. Furthermore, one major contention was that Karamitsos et al. did not evaluate the subendocardium, which may have turned out to have abnormal BOLD ΔSI%.

3.7.3 Limitations

Firstly, the results on our study were based on a single, mid-ventricular slice in each patient, which may have underestimated more global disease, or some cases, overestimated focal disease limited to the apex. This study was more a proof-of-concept and further studies have aimed to use a global basal, mid, and apical approach to image patients. Secondly, given the variety of management options for patients at risk for or

currently diagnosed with CAD, we were not able to control for the medications used in our study population which may have influenced the overall signal intensity. Patients with higher compliance may have exhibited better reserve and oxygenation during hyperemia, which we did not account for. Thirdly, we did not compare our findings using OS-CMR to any other imaging modality to more definitively rule out or rule in evidence of arterial stenoses. However, based on clinical judgement and patient medical histories, we were able to ascertain that the controls with coronary risk factors were never indicated for coronary angiography and likely would have negative angiograms. Finally, in our control cohort, we looked specifically at evidence for CAD and included patients with any risk factors for CAD, including diabetes. This may have added a confounding effect, as we did not have a large enough sample size of patients with only diabetes to truly ascertain its role in disease progression in the subendocardial vasculature. Similarly, it would be valuable to recruit participants without coronary risk factors to further assess the role of aging alone in tissue oxygenation.

3.8 Conclusion

To our knowledge, our study is the first to examine tissue oxygenation using OS-CMR in the different myocardial layers, demonstrating regional transmurality not only in patients with CAD, but in matched controls with only risk factors for CAD. Importantly, decreased BOLD signal intensity percent change following adenosine-induced vasodilation in the subendocardium may be predicted by diastolic blood pressure and age, with younger participants demonstrating a robust, homogenous BOLD response

throughout the subendocardium to subepicardium following vasodilation. Therefore, assessment of the subendocardium provides further information into the understanding of ischemic heart disease, particularly microvascular dysfunction, and may potentially provide additional diagnostic information not easily detectable by current imaging modalities.

3.9 References

1. Hoffman JI, Buckberg GD. Pathophysiology of subendocardial ischaemia. *Br Med J.* 1975; 1: 76-79.

2. Reddy KG, Nair RN, Sheehan HM, Hodgson JM. Evidence that selective endothelial dysfunction may occur in the absence of angiographic or ultrasound atherosclerosis in patients with risk factors for atherosclerosis. *J Am Coll Cardiol.* 1994; 23: 833-843.

3. Toutouzas PC, Tousoulis D, Davies GJ. Nitric oxide synthesis in atherosclerosis. *Eur Heart J.* 1998; 19: 1504-1511.

4. Friedrich MG, Karamitsos TD. Oxygenation-sensitive cardiovascular magnetic resonance. *J Cardiovasc Magn Reson.* 2013; 15: 43-429X-15-43.

5. Zheng J, Wang J, Rowold FE, Gropler RJ, Woodard PK. Relationship of apparent myocardial T2 and oxygenation: towards quantification of myocardial oxygen extraction fraction. *J Magn Reson Imaging.* 2004; 20: 233-241.

6. Li D, Waight DJ, Wang Y. In vivo correlation between blood T2* and oxygen saturation. *J Magn Reson Imaging.* 1998; 8: 1236-1239.

7. Dharmakumar R, Qi X, Hong J, Wright GA. Detecting microcirculatory changes in blood oxygen state with steady-state free precession imaging. *Magn Reson Med.* 2006; 55: 1372-1380.

8. Luu J, Friedrich M, Harker J, Dwyer N, Guensch D, Hare J. Relationship of Vasodilator-Induced Changes of Myocardial Oxygenation with the Severity of Coronary Artery Stenosis – a Study using Oxygenation-Sensitive Cardiovascular Magnetic Resonance. 2014.

9. Hallgren KA. Computing Inter-Rater Reliability for Observational Data: An Overview and Tutorial. *Tutor Quant Methods Psychol.* 2012; 8: 23-34.

10. Vohringer M, Flewitt JA, Green JD, Dharmakumar R, Wang J,Jr, Tyberg JV, Friedrich MG. Oxygenation-sensitive CMR for assessing vasodilator-induced changes of myocardial oxygenation. *J Cardiovasc Magn Reson.* 2010; 12: 20.

11. Wacker CM, Hartlep AW, Pfleger S, Schad LR, Ertl G, Bauer WR. Susceptibility-sensitive magnetic resonance imaging detects human myocardium supplied by a stenotic coronary artery without a contrast agent. *J Am Coll Cardiol.* 2003; 41: 834-840.

12. Li D, Dhawale P, Rubin PJ, Haacke EM, Gropler RJ. Myocardial signal response to dipyridamole and dobutamine: demonstration of the BOLD effect using a double-echo gradient-echo sequence. *Magn Reson Med.* 1996; 36: 16-20.

13. Egred M, Waiter GD, Al-Mohammad A, Semple SI, Redpath TW, Walton S. Blood oxygen level dependent (BOLD) MRI: A novel technique for the detection of myocardial ischemia. *Eur J Intern Med.* 2006; 17: 551-555.

14. Walcher T, Manzke R, Hombach V, Rottbauer W, Wohrle J, Bernhardt P. Myocardial perfusion reserve assessed by T2-prepared steady-state free precession blood oxygen level-dependent magnetic resonance imaging in comparison to fractional flow reserve. *Circ Cardiovasc Imaging.* 2012; 5: 580-586.

15. Zeiher AM, Drexler H, Saurbier B, Just H. Endothelium-mediated coronary blood flow modulation in humans. Effects of age, atherosclerosis, hypercholesterolemia, and hypertension. *J Clin Invest.* 1993; 92: 652-662.

16. Egashira K, Inou T, Hirooka Y, Kai H, Sugimachi M, Suzuki S, Kuga T, Urabe Y, Takeshita A. Effects of age on endothelium-dependent vasodilation of resistance coronary artery by acetylcholine in humans. *Circulation.* 1993; 88: 77-81.

17. Arnold JR, Karamitsos TD, Bhamra-Ariza P, Francis JM, Searle N, Robson MD, Howells RK, Choudhury RP, Rimoldi OE, Camici PG, Banning AP, Neubauer S, Jerosch-Herold M, Selvanayagam JB. Myocardial oxygenation in coronary artery disease: insights from blood oxygen level-dependent magnetic resonance imaging at 3 tesla. *J Am Coll Cardiol.* 2012; 59: 1954-1964.

18. Benetos A, Zureik M, Morcet J, Thomas F, Bean K, Safar M, Ducimetiere P, Guize L. A decrease in diastolic blood pressure combined with an increase in systolic blood pressure is associated with a higher cardiovascular mortality in men. *J Am Coll Cardiol.* 2000; 35: 673-680.

19. Sleight P. Lowering of blood pressure and artery stiffness. *Lancet.* 1997; 349: 362.

20. Cecelja M, Chowienczyk P. Role of arterial stiffness in cardiovascular disease. *JRSM Cardiovasc Dis.* 2012; 1: cvd.2012.012016. eCollection 2012.

21. Janic M, Lunder M, Sabovic M. Arterial stiffness and cardiovascular therapy. *Biomed Res Int.* 2014; 2014: 621437.

22. Coutinho T, Goel K, Correa de Sa D, Kragelund C, Kanaya AM, Zeller M, Park JS, Kober L, Torp-Pedersen C, Cottin Y, Lorgis L, Lee SH, Kim YJ, Thomas R, Roger VL, Somers VK, Lopez-Jimenez F. Central obesity and survival in subjects with coronary artery disease: a systematic review of the literature and collaborative analysis with individual subject data. *J Am Coll Cardiol.* 2011; 57: 1877-1886.

23. Uren NG, Marraccini P, Gistri R, de Silva R, Camici PG. Altered coronary vasodilator reserve and metabolism in myocardium subtended by normal arteries in patients with coronary artery disease. *J Am Coll Cardiol.* 1993; 22: 650-658.

24. Karamitsos TD, Leccisotti L, Arnold JR, Recio-Mayoral A, Bhamra-Ariza P, Howells RK, Searle N, Robson MD, Rimoldi OE, Camici PG, Neubauer S, Selvanayagam JB. Relationship between regional myocardial oxygenation and perfusion in patients with coronary artery disease: insights from cardiovascular magnetic resonance and positron emission tomography. *Circ Cardiovasc Imaging.* 2010; 3: 32-40.

25. Vita JA, Treasure CB, Nabel EG, McLenachan JM, Fish RD, Yeung AC, Vekshtein VI, Selwyn AP, Ganz P. Coronary vasomotor response to acetylcholine relates to risk factors for coronary artery disease. *Circulation.* 1990; 81: 491-497.

26. Crea F, Camici PG, Bairey Merz CN. Coronary microvascular dysfunction: an update. *Eur Heart J.* 2013; .

27. Young LH, Wackers FJ, Chyun DA, Davey JA, Barrett EJ, Taillefer R, Heller GV, Iskandrian AE, Wittlin SD, Filipchuk N, Ratner RE, Inzucchi SE, DIAD Investigators. Cardiac outcomes after screening for asymptomatic coronary artery disease in patients with type 2 diabetes: the DIAD study: a randomized controlled trial. *JAMA.* 2009; 301: 1547-1555.

28. Panting JR, Gatehouse PD, Yang GZ, Grothues F, Firmin DN, Collins P, Pennell DJ. Abnormal subendocardial perfusion in cardiac syndrome X detected by cardiovascular magnetic resonance imaging. *N Engl J Med.* 2002; 346: 1948-1953.

29. Lanza GA, Buffon A, Sestito A, Natale L, Sgueglia GA, Galiuto L, Infusino F, Mariani L, Centola A, Crea F. Relation between stress-induced myocardial perfusion defects on cardiovascular magnetic resonance and coronary microvascular dysfunction in patients with cardiac syndrome X. *J Am Coll Cardiol.* 2008; 51: 466-472.

30. Rhoades R, Bell D. Medical Physiology: Principles for Clinical Medicine. 4th ed. Philadelphia: Wolters Kluwer; 2013.

31. Karamitsos TD, Arnold JR, Pegg TJ, Francis JM, Birks J, Jerosch-Herold M, Neubauer S, Selvanayagam JB. Patients with syndrome X have normal transmural myocardial perfusion and oxygenation: a 3-T cardiovascular magnetic resonance imaging study. *Circ Cardiovasc Imaging.* 2012; 5: 194-200.

Chapter Four: RESULTS – SECOND MANUSCRIPT

4.1 Title: Relationship of Vasodilator-Induced Changes of Myocardial Oxygenation with the Severity of Coronary Artery Stenosis – a Study using Oxygenation-Sensitive Cardiovascular Magnetic Resonance

Judy M. Luu[1], Matthias G. Friedrich[1,2], Jodi Harker[1,3], Nathan Dwyer[4], Dominik Guensch[1,5], Yoko Mikami[1], Peter Faris[6], and James L. Hare[1,7]

[1]: Stephenson CMR Centre at the Libin Cardiovascular Institute of Alberta, University of Calgary, Calgary AB, Canada; [2]: Philippa and Marvin Carsley Cardiovascular MR Centre at the Montreal Heart Institute/Université de Montréal, Montreal QC, Canada; [3]: Heart Care Partners, Brisbane, Australia; [4]: Royal Hobart Hospital, Hobart, TAS, Australia;[5]: Inselspital Bern, Switzerland; [6]: Alberta Bone and Joint Health Institute, University of Calgary, Calgary AB; [7]: Alfred Hospital & Baker IDI Research Institute, Melbourne, VIC, Australia

Key words: cardiovascular magnetic resonance, fractional flow reserve, oxygenation-sensitive imaging, ischemia, coronary artery disease.

4.2 Abstract

Background

Oxygenation-sensitive cardiovascular magnetic resonance (CMR) uses the signal generated by deoxygenated haemoglobin to measure tissue oxygenation and may represent a non-invasive method to assess myocardial ischemia in patients with coronary artery disease (CAD). The aim of this study was to validate whether OS-CMR can detect and quantify alterations in myocardial oxygenation in CAD.

Methods

OS-CMR scans were performed in patients that had evidence of ischemia on a prior myocardial stress test. Images were captured during rest and adenosine-induced coronary hyperaemia. The mean signal intensity (SI) percent changes were calculated between rest and hyperemia and were compared to intracoronary fractional flow reserve (FFR) assessed on angiography. FFR is the current reference standard to assess the extent of coronary occlusion (FFR <0.80 indicates significant stenosis). Complementary comparisons were also performed with quantitative coronary angiography (QCA), CMR first-pass perfusion, and late gadolinium enhancement (LGE) imaging.

Results

37 patients had both CMR assessment and a corresponding FFR evaluation. OS-CMR measurements of mean signal intensity percent changes were shown for a range of FFR values, where an FFR of less than 0.54 identified myocardium with a complete lack of change in oxygenation following adenosine-induced vasodilation. An OS-CMR threshold of 4.8% was shown to predict functionally significant stenoses with FFR

<0.80, with sensitivity of 86% and specificity of 93%. Measurements of mean signal intensity percent changes using OS-CMR had weak correlation with QCA stenosis diameter. OS-CMR showed a trend towards decreased mean signal intensity percent changes in myocardial segments with abnormal perfusion and in areas with LGE.

Conclusion

OS-CMR measures of tissue oxygenation can identify myocardium subtended by coronary arteries with functionally significant stenoses, supporting the role of OS-CMR in the evaluation of myocardial ischemia. Weak correlation to anatomical stenosis severity and myocardial perfusion warrants further research to elucidate the mechanistic components of oxygen-sensitive contrast generation.

4.3 Abbreviations:

AUC:	area under the curve
BOLD:	blood-oxygen level dependent
CAD:	coronary artery disease
CTO:	chronic total occlusion
FFR:	fractional flow reserve
LAD:	left anterior descending
LCx:	left circumflex
LGE:	late gadolinium enhancement
LV:	left ventricular
NPV:	negative predictive value
OS-CMR:	oxygenation-sensitive cardiovascular magnetic resonance
PPV:	positive predictive value
QCA:	quantitative coronary angiography
RCA:	right coronary artery
SI:	signal intensity
ΔSI%:	mean signal intensity percent change
TE:	echo time
TR:	repetition time

4.4 Background

The presence and extent of myocardial ischemia are important determinants of risks for patients with coronary artery disease. Subsequently, studies have shown that ischemia reduction driven by optimal medical therapy and/or revascularization can limit adverse outcomes [1]. To optimally guide revascularization, it is now established that measurement of Fractional Flow Reserve during coronary angiography more reliably predict hemodynamically limiting epicardial stenoses compared to angiography alone[2-5]. However, FFR is limited by the use of contrast medium and invasive methodology.

Over the last several years, there has been growing evidence to support the value of a non-invasive approach for the assessment of myocardial oxygenation using Cardiovascular Magnetic Resonance [6]. Without the need for contrast agents or radiation, Oxygenation-Sensitive CMR (OS-CMR) exploits the inherent magnetic properties of deoxygenated hemoglobin such that signal intensity (SI) is directly dependent on tissue oxygenation in the myocardium [7,8]. The potential clinical application of OS-CMR has been shown in various human studies, including comparisons against nuclear SPECT (single photon emission computed tomography)[9], positron emission tomography[10], CMR myocardial perfusion[11], and quantitative coronary angiography[12]. In these studies, researchers have shown dissociation between myocardial hypoperfusion from tissue oxygenation, suggesting that OS-CMR may reflect a complex interaction between myocardial oxygen supply and demand, deoxyhemoglobin content, and possibly aspects of microvasculature function.

Recently, in patients with coronary artery disease, Walcher et al. compared BOLD-CMR to the reference standard of FFR and showed sensitivity and specificity of 88.2% and 89.5%, respectively. As there is such limited data available comparing OS-CMR to FFR, we sought to further explore the relationship between myocardial tissue oxygenation and the functional significance of a coronary stenosis as measured by FFR to determine an optimal threshold value for OS-CMR[13]. We also sought to further expand on the previous study by exploring the relationship of tissue oxygenation to coronary anatomy, myocardial perfusion, and late-gadolinium enhancement.

4.5 Methods

4.5.1 Study population

We prospectively recruited patients with suspected or known CAD referred for clinically indicated diagnostic angiography or who had already undergone angiography with FFR (without intervention) within the preceding four weeks. Exclusion criteria included previous coronary bypass surgery as well as the presence of contraindications to MRI, adenosine or gadolinium contrast administration. Xanthine or dipyridamole use within 24 hours before the CMR scan was not permitted. Ethics approval was obtained from the University of Calgary Conjoint Health Research Ethics Board and full written informed consent was obtained from all subjects.

4.5.2 CMR imaging protocol

CMR was performed with the patient in supine position using 1.5T MRI System (Magnetom Avanto®, Siemens Healthcare, Erlangen, Germany) with a 32-channel chest coil. Image acquisition was during breath-holds, using retrospective electrocardiogram (ECG)-gated sequences. Steady state free precession (SSFP) cine images were initially acquired for LV volume and functional scanning (TR: 67, TE: 1.15, Flip angle: 74, Slice thickness: 10 mm). Subsequently, three sets of oxygenation-sensitive CMR images were acquired in short axis views at baseline in the basal, mid, and apical regions using a T2* oxygenation-sensitive, ECG-triggered steady-state free precession (SSFP) sequence with a long TR, as previously reported [14]. Scan parameters were: field of view 400 x 400 mm; matrix size 128 x 128, bandwidth 273 Hz/Pixel, TR/TE = 5.4/2.7ms, flip angle 90°, slice thickness 15mm for basal and mid, 10mm for apical slices. Typical breath-hold length was 10-15 seconds. Data acquisition was repeated during intravenous administration (at least 2 minutes after starting the infusion) of 140mcg/kg/min adenosine.

Immediately following acquisition of OS-CMR images, first pass-perfusion imaging was acquired in the same short-axis planes using an ECG-gated saturation recovery prepared gradient echo sequence after iv administration of 0.075 mmol/kg gadopentetate dimeglumine contrast administration (Magnevist®, Bayer, Germany) (Scan parameters: voxel size 4.3 x 3.4 x 10.0mm repetition time very R-R interval, TE = 0.99ms, inversion time = 115ms, flip angle 20°, and slice thickness 10.0mm). After 15 minutes, resting perfusion images were acquired without adenosine using the same sequence.

Late gadolinium enhancement (LGE) images were acquired using a standard inversion recovery gradient echo pulse sequence 10 minutes after injection of gadopentetate dimeglumine (Gd-DTPA, 0.15mmol/kg BW Magnevist, Schering, Germany) for visualisation of myocardial fibrosis. Segments with transmural infarction (>75% extent) were excluded from analysis.

4.5.3 Analysis of Oxygenation-Sensitive Images

CMR images were analyzed offline by a blinded reader using certified software (cmr[42], CIRCLE Cardiovascular Imaging Inc., Calgary, Canada). For images acquired with the oxygenation-sensitive SSFP cine sequence, the images at end-systole were used for each slice in basal, mid, and apical regions. Segments were excluded if image quality precluded accurate analysis - this was done blinded to the FFR results and according to pre-specified criteria. Image quality criteria used included the presence of significant partial volume effect, the presence of inhomogeneity artefact, or any other significant image problem such as discordance in slice position between rest and stress due to extensive respiratory motion. Epicardial and endocardial contours were defined for each short axis slice. The software automatically segmented the whole myocardium according to the American Heart Association guidelines. The change in mean signal intensity (ΔSI%) was calculated as the SI at rest subtracted from SI at maximal hyperemia during adenosine infusion, divided by the SI at rest and expressed as a percentage.

4.5.4 Analysis of First-Pass Perfusion and Late-Gadolinium Enhancement Imaging

Perfusion images were qualitatively analysed by an experienced reader blinded to other imaging data. Rest and stress images of the same slice were aligned side by side using certified software (cmr[42], CIRCLE Cardiovascular Imaging Inc., Calgary, Canada) on an offline workstation. Perfusion images were evaluated by manually scrolling through each phase. Images were analysed according to the major coronary territory assignments outlined by the American Heart Association (LAD, LCx, or RCA). A perfusion defect on MR images was defined as any focal region of myocardium with diminished contrast enhancement during stress and/or rest images, when compared to normal myocardium.

LGE images were visually evaluated on a per-coronary territory analysis according to AHA guidelines in both short-axis and long-axis views. Areas of LGE were defined as regions with subendocardial contrast uptake with associated regional wall motion abnormalities.

4.5.5 Assessment of Fractional Flow Reserve (FFR)

Conventional invasive coronary angiography was performed. Following acquisition of diagnostic images, coronary guide catheters were introduced and a specialized pressure wire (Pressure Wire 5, Radi Medical Systems, Uppsala, Sweden) was calibrated and electronically equalized with the aortic pressure before being placed in the coronary artery, distal to the lesion being investigated. Intracoronary glyceryl trinitrate 200μg was given to reduce vasospasm. To induce maximal vasodilation, a bolus of intracoronary adenosine (48 μg for right coronary artery, 98 μg for left coronary artery) was then administered. Under hyperemia, the ratio of the pressure distal to the stenosis to the

aortic pressure was then used to calculate the FFR. FFR was measured in vessels with visually assessed stenosis of at least intermediate severity (lesion ≥50%). In the case of a chronic total occlusion (CTO) where FFR could not be measured prior to intervention, a FFR of 0.50 was arbitrarily assigned[2]. These data were used in a separate analysis. Coronary artery supply for myocardial segments was defined according to a validated jeopardy score (the APPROACH score) [15], which took into account individual coronary anatomy (including dominance) and which can be applied to a conventional bulls-eye plot using semi-automated software (Coronary Artery Reporting and Archiving Tool, CARAT)[16]. Both per-segment and per-coronary territory analyses were performed following image quality exclusions. Per-coronary territory was analyzed by averaging the segments that corresponded to the coronary artery using the American Heart Association 16-segment model. For the analysis using FFR as the reference standard, myocardial segments with known FFR were classified according to the measured value as ischemic (FFR<0.80) or non-ischemic (FFR≥ 0.80).

4.5.6 Quantitative Coronary Angiography

Quantitative coronary angiography (QCA) was performed offline using QAngio XA Version 7.1.40 (Medis Medical Imaging Systems, Leiden, The Netherlands) by an independent operator blinded to the results of OS-CMR, pressure wire results, and patient outcome. End-diastolic cine frames in which the lesion was most severe without any vessel overlap were used. Within a coronary artery, the reader marked the region of interest. The software was then used to calculate the minimal luminal diameter, reference vessel diameter (before the stenosis), lesion length, and ideal vessel diameter

at stenosis. From these measurements, the percent diameter stenosis was derived. The independent reader then repeated these calculations in coronary arteries they deemed were diseased in each patient. Myocardial segments were assigned to the supplying coronary artery based on the APPROACH lesion score as described above.

4.5.7 Statistical Analysis

Data analysis was performed using statistical software (IBM SPSS Statistics for Mac version 20.0. Armonk, NY: IBM Corp). Continuous variables were presented as mean +/- SD and categorical variables as percentages. To account for the statistical dependence of observations made from multiple segments per patient, we used Generalized Estimating Equations (GEE) for tests of significance [17]. We used restricted cubic splines with 95% confidence intervals from a GEE model to examine the relationship between FFR and change in OS-CMR signal intensity [18]. For comparisons among ischemic and non-ischemic segments, we report group means and 95% confidence from a GEE model. The diagnostic performance of OS-CMR was assessed using the receiver-operating characteristic (ROC) curve analysis using all available segments for each patient. For the per-coronary territory ROC curve analysis, the average of segments corresponding to the appropriate coronary territory measured for each patient was used. The threshold value was selected that maximized the sum of the sensitivity and specificity. A Pearson's correlation was performed to determine the correlation between QCA and OS-CMR signal intensity.

4.6 Results

Out of a total of 64 patients recruited, 37 patients had both CMR assessment and a corresponding FFR evaluation (Figure 1). Of these, 10 patients had a total occlusion and the subtended segments were assigned an FFR of 0.5. Separate analyses with and without these data were performed. Of the myocardial segments assessed with both CMR and FFR, 70% of segments were subtended by the LAD coronary artery (n=155), 21% by the RCA (n=47) and 9% by the LCx (n=20). CMR image quality was a major issue, with 41% of segments excluded by the blinded reviewer, leaving 29 patients for analysis. The majority of excluded segments (50%) were from the apical region, 26% from the mid slice, and 24% from the basal slice. Of the excluded segments, 75% were in the LAD territory, 9% in the LCx territory, and 16% in the RCA territory. One patient had to be excluded entirely because of extensive transmural late gadolinium enhancement. Other patients with regional myocardial scarring had those segments excluded. Segments were primarily excluded due to respiratory motion artefact, especially within the first 10 patients of the study. Segments in the basal region were excluded due to outflow tract interference. Finally, apical segments were often excluded due to poor coverage of the apex and poor delineation of myocardial borders in the apex following adenosine stress imaging. The average number of segments per patient included in the primary analysis was 4.5 segments. In a secondary intention-to-treat analysis, where all segments from 37 patients were included irrespective of image quality, an average of 6 segments were included per patient. A summary of patient demographics and baseline clinical characteristics is shown in Table 1.

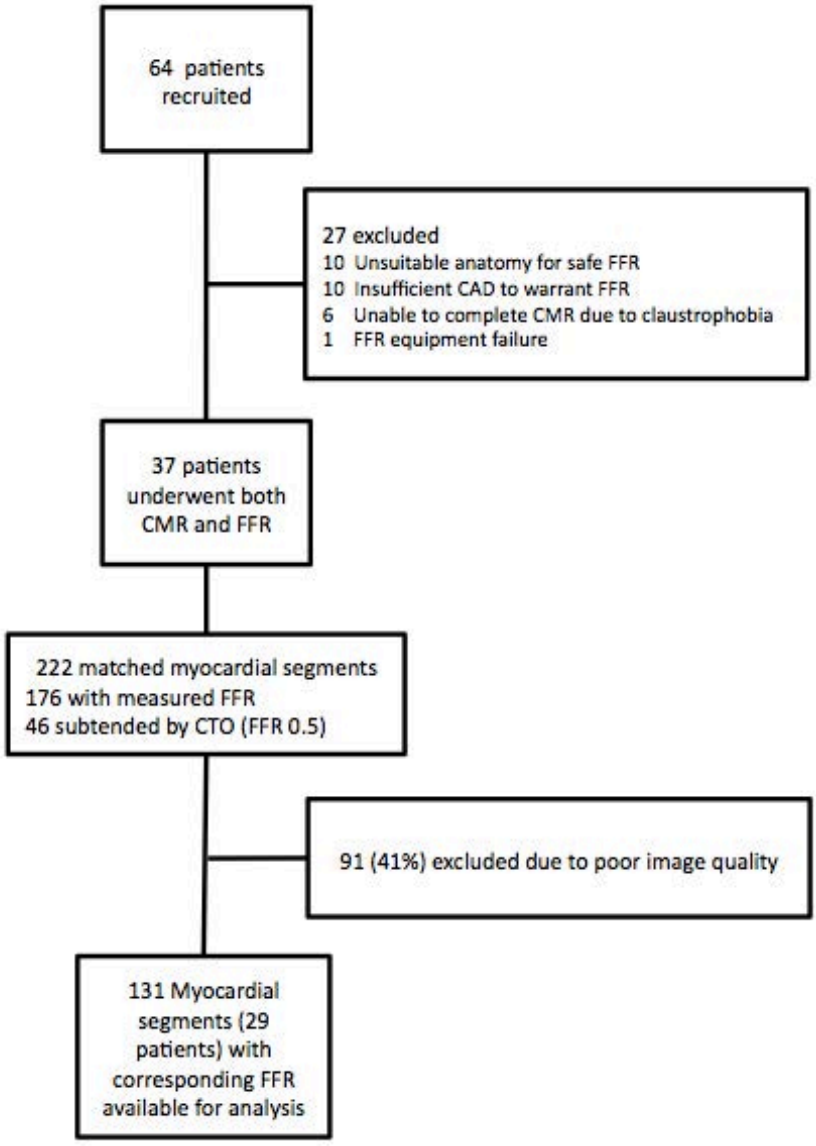

Figure 4-1: Flow of patients through the study.

Table 4-1: Patient Demographics and Baseline Clinical Data.

	Subjects undergoing CMR and FFR (n=37)	Other subjects (FFR or CMR not performed) (n=27)	p-value
Age	61.0±8.5	61.1±8.6	p=0.96
Male	31 (78%)	21 (88%)	p=0.33
Weight (kg)	89.9±14.6	84.8±16.8	p=0.20
BMI	29.4±5.1	29.2±5.4	p=0.87
Diastolic Blood Pressure	77.4±8.3	78.1±8.9	p=0.74
CAD Clinical Risk Factors, N(%)			
Past/present smoker	28 (70%)	10 (42%)	p=0.027
Hypertension	21 (53%)	15 (63%)	p=0.44
Dyslipidemia	30 (75%)	18 (75%)	p=1.00
Diabetes Mellitus	10 (25%)	8 (33%)	p=0.48
Family History	31 (78%)	75%)	p=0.78
Prior CAD	17 (43%)	3 (13%)	p=0.013
CMR Volumetric indices			
LVEDVi (ml/m^2)	88.1	86.2	p=0.70
LVESVi (ml/m^2)	37.0	36.9	p=0.98
LVEF (%)	58.8%	55.5%	p=0.24
LGE present (%)	9 (24%)	7 (26%)	p=0.75

CAD, coronary artery disease; MI, myocardial infarction; CMR, cardiac magnetic resonance; LVEDV, left ventricular end-diastolic volume index; LVESVi, left ventricular end-systolic volume index; LVEF, left ventricular ejection fraction; LGE, late gadolinium enhancement.

4.6.1 Relationship of Vasodilator-Induced Myocardial Oxygenation Changes with FFR

Figure 2 (See Appendix Figure A-6 for absolute changes) shows the relationship of change in OS-CMR signal intensity according to FFR including segments subtended by a totally occluded vessel (panel A), and then also with this data excluded (panel B). There was a modest but significant overall correlation between OS-CMR ΔSI% and FFR with r=0.35, p<0.001. There was a clear attenuation in the increase in OS-CMR ΔSI% once the FFR was <0.80. Furthermore, there was a reduction in OS-CMR signal intensity for segments subtended by a severe stenosis (FFR <0.6), suggesting that vasodilation with adenosine resulted in a net reduction of tissue oxygenation in these segments. This result was evident with or without inclusion of segments subtended by a totally occluded vessel.

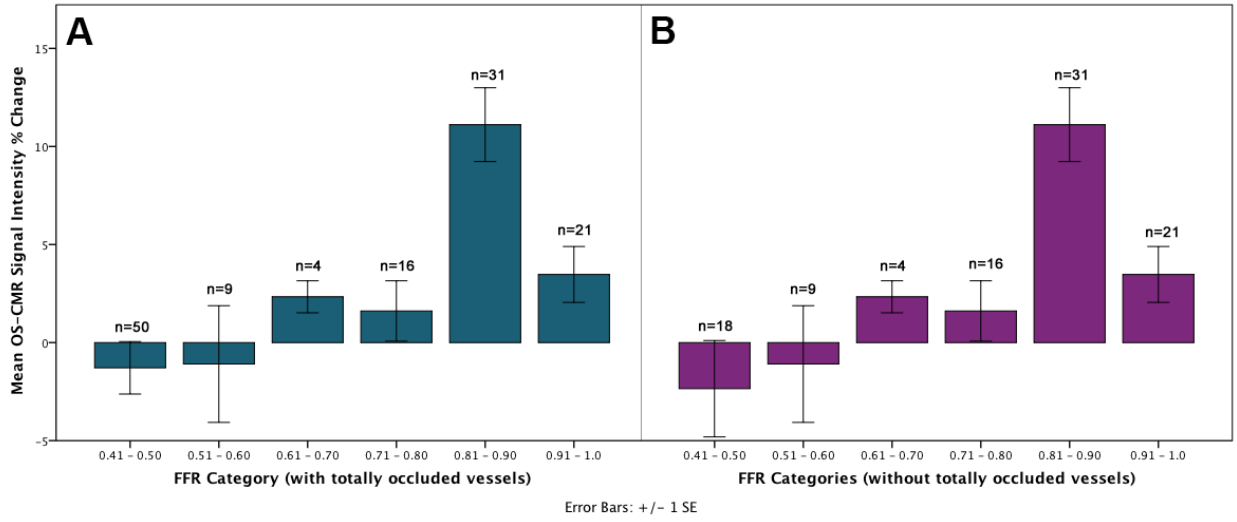

Figure 4-2: OS-CMR versus FFR ranges.

Relationship of myocardial signal intensity changes (segmental analysis) in oxygenation-sensitive CMR (OS-CMR) images with fractional flow reserve (FFR) with segments subtended by occluded vessels included (Panel A) and excluded (Panel B). Occluded vessels were assigned an FFR value of 0.5.

When using FFR as the reference standard of truth, pooled segments with an FFR of less than 0.80 showed no significant increase of myocardial oxygenation (mean change -0.20%, 95% CI -2.09 to 1.68) compared to segments perfused by coronary arteries with non-significant lesions (mean signal increase of 6.5%; 95% CI 4.10 to 8.94; $p<0.001$; Figure 3). This was also the case with exclusion of segments subtended by total occlusion with a mean ΔSI% of -0.36% (95% CI -2.61 to 1.89; $p=0.001$ compared to coronary arteries with non-significant lesions). In the per-coronary artery territory analysis, there was a significant difference between the mean ΔSI% of regions with significant (FFR<0.8) stenoses (-0.49%; 95% CI -3.78 to 2.78) compared to coronaries with non-significant lesions identified with FFR≥0.80 (7.36%; 95% CI 4.08 to 10.64; $p<0.001$).

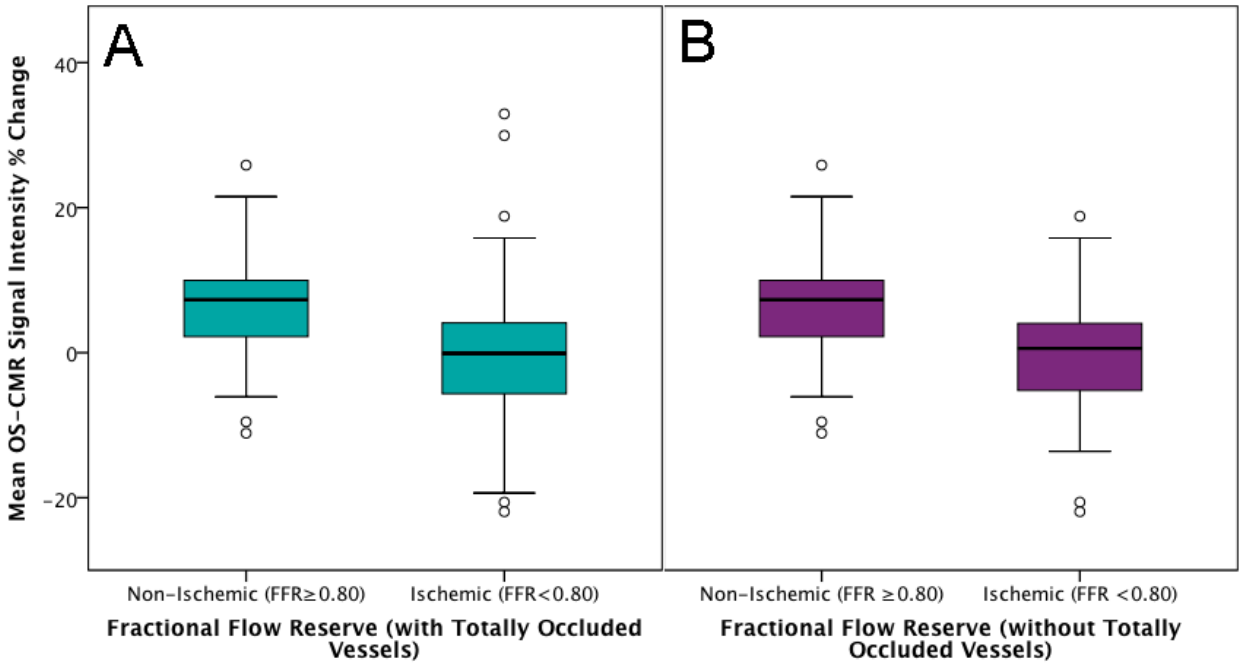

Figure 4-3: Relationship of OS-CMR to FFR, with or without CTOs.

Box and whisker plots of myocardial signal intensity changes between significant (FFR<0.8) and non-significant coronary stenosis. Panel A shows data with inclusion of totally occluded vessels and Panel B with these segments excluded.

When OS-CMR was used as the reference standard, segments showing a complete lack of an increase in tissue oxygenation during vasodilatation (ΔSI BOLD ≤0%) had a mean FFR of 0.59 (95% CI 0.55 to 0.64) compared with a mean FFR of 0.75 (95% CI 0.71 to 0.78; p<0.001) in segments with any vasodilator-associated increase in oxygenation (ΔSI BOLD >0%). Similar results were seen in the per-coronary territory analysis, with a mean FFR of 0.61 (95% CI 0.47 to 0.74) of coronary territories showing a complete lack of vasodilator response versus a mean FFR of 0.78 (95% CI 0.70 to 0.86; p=0.013) for coronary territories showing a positive vasodilator response to adenosine.

4.6.2 Relationship of Myocardial Oxygenation with Conventional QCA, CMR First-Pass Perfusion Imaging, and Late Enhancement

Similar patterns were also seen when comparing net changes of myocardial oxygenation with coronary disease severity as assessed by conventional QCA (Figure 4). Excluding those with poor image quality, there were 335 available segments on CMR subtended by stenoses identified using QCA by a blinded reader. Of these, 156 (47%) myocardial segments were supplied by the LAD, 101 (30%) supplied by the RCA, 64 (19%) supplied by the LCx, and 14 (4%) stenotic segments found in the left main. OS-CMR SI % change showed a weak negative correlation with stenoses diameters ($r = -0.212$; $p < 0.001$). An imaging example of OS-CMR in comparison to coronary angiography is seen in Figure 5.

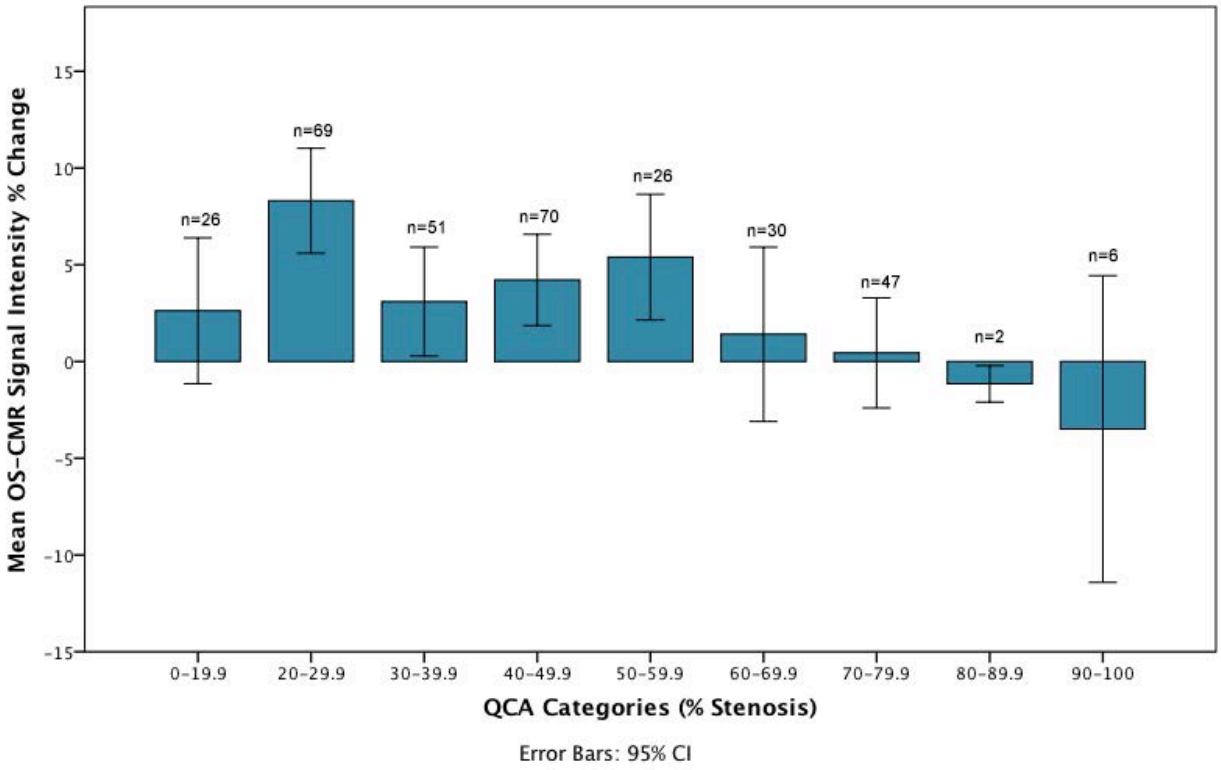

Figure 4-4: OS-CMR versus QCA.

Relationship of oxygenation-sensitive CMR (OS-CMR) signal intensity (segmental analysis) according to QCA assessment of lesion severity (population as a whole).

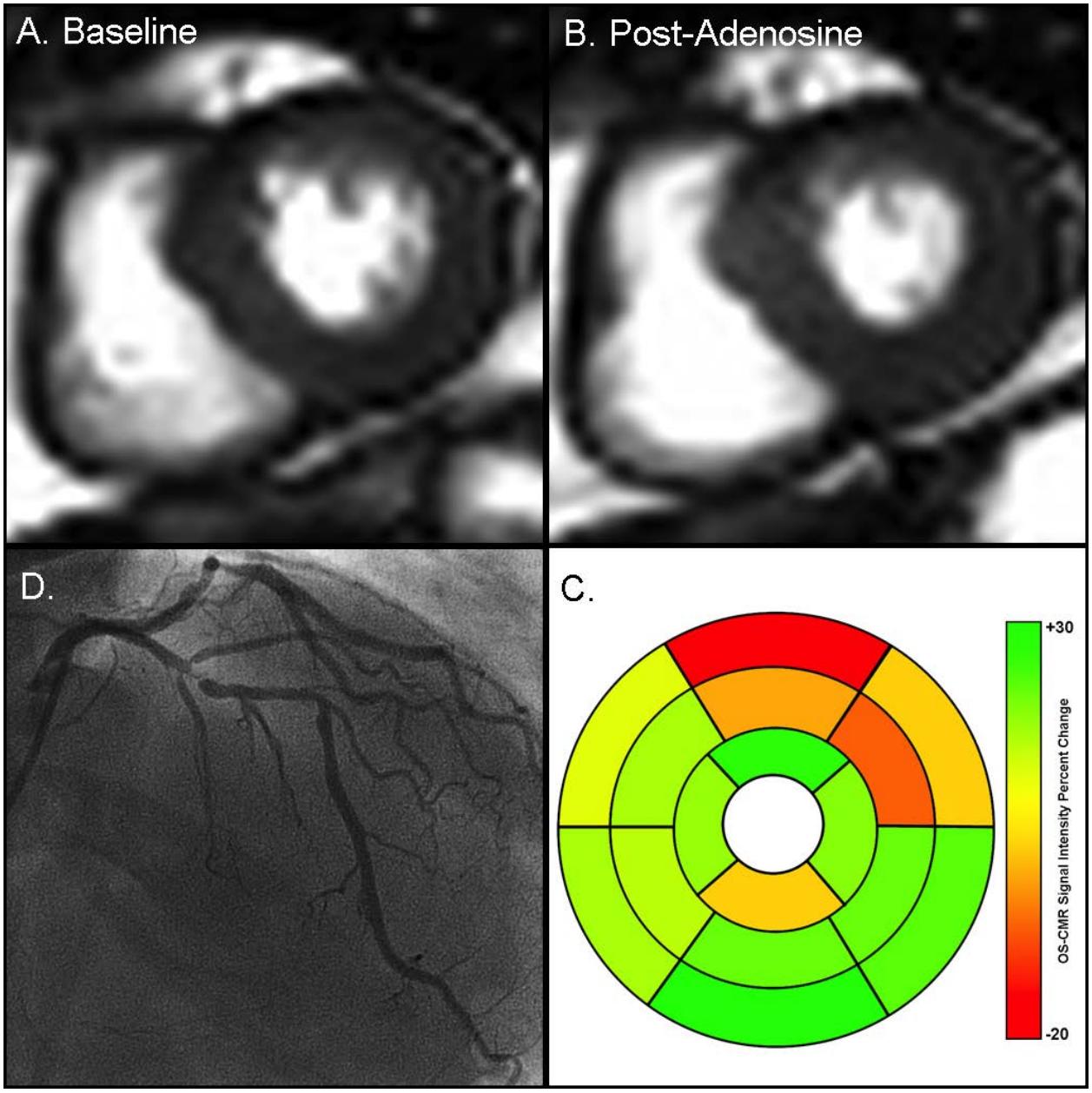

Figure 4-5: Patient image example.

Raw images of OS-CMR at A) baseline and B) post-adenosine are seen in the upper rows, with a C) representative polar map illustrating decreased signal intensity percent change in the anterior/anterolateral myocardial segments. D) Invasive coronary angiography identified severe stenosis of the left anterior descending artery (QCA 75%). FFR in the LAD was measured at 0.49 (not shown).

OS-CMR was compared to the qualitative assessment of first-pass perfusion images in 43 patients that had both OS-CMR and first-pass perfusion images available on a per-coronary territory basis. Mean OS-CMR showed a trend to less positive response in coronary territories with abnormal stress perfusion images (ΔSI% 0.95, 95% CI -2.42 to 4.33) compared to those with normal perfusion patterns (ΔSI% of 4.73, 95% CI 2.95 to 6.50, p=0.052).

In coronary territories with evidence of subendocardial LGE, the mean OS-CMR SI percent change was 0.50% (95% CI -4.47 to 4.89) compared to remote myocardium with no evidence of LGE with mean SI% change of 4.25% (95% CI 2.57 to 5.93); p=NS. Areas with subendocardial LGE also had reduced FFR of 0.61 (95% CI 0.40 to 0.82) compared to remote myocardium without evidence of LGE (mean FFR 0.74; 95% CI 0.68 to 0.81); p=NS).

4.6.3 Association of FFR Values with Inducible Increases of Myocardial Oxygenation

Using OS-CMR SI % change of less than or equal to zero as the standard of reference, an FFR of less than 0.62 optimally identified segments without an increase of oxygenation following vasodilation (AUC = 0.71; 95% CI 0.62 to 0.79; sensitivity 71%, specificity 75%, PPV 60%, NPV of 83%, LR+ of 2.61 and LR- 0.34). Similarly, for the per-coronary territory analysis, an FFR of less than 0.54 identified myocardium with a complete lack of oxygenation following adenosine-induced vasodilation with a sensitivity of 82% and specificity of 70% (AUC = 0.74, 95% CI 0.54 to 0.95).

4.6.4 Diagnostic Performance of Oxygenation-Sensitive CMR for Detecting Coronary Artery Stenosis With an FFR of <0.80

Using data for all included patients from a GEE-fitted logistic regression model for the optimal OS-CMR cut-off to identify a coronary artery stenosis with an FFR of less than 0.8, a net signal intensity change of less than 5.4% identified segments subtended by a coronary artery with a functionally significant stenosis (AUC = 0.78; 95% CI 0.69 to 0.86; sensitivity 85%, specificity 65%, PPV 74%, NPV 79%, LR+ of 2.45 and LR- of 0.23. In a per-coronary territory analysis with combined FFR measurements and CTO, an OS-CMR signal intensity change of less than 4.78% identified subjects with an FFR of less than 0.8 with a sensitivity of 86% and specificity of 93% (AUC = 0.86; 95% CI 0.70 to 1.0). This is similar to the diagnostic accuracy based on per-coronary territory analysis of QCA, where a percent stenosis greater than 51.9% identified subjects with an FFR <0.80 with sensitivity of 83% and specificity 89% (AUC = 0.90; 95% CI 0.80 – 1.0). Figure 6 illustrates the mean differences between FFR measurements of coronary territories with OS-CMR threshold of 4.8% or less.

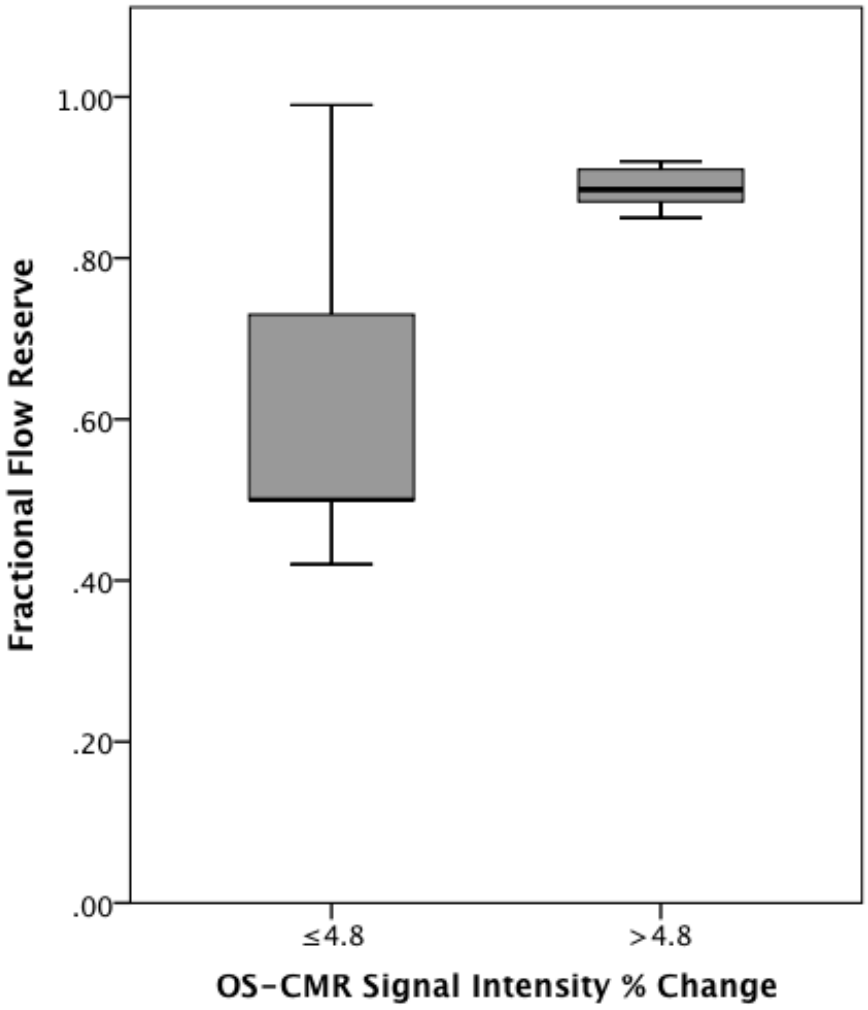

Figure 4-6: Relationship of FFR to OS-CMR, using threshold cut-off of 4.8%.

Box and whisker plots of FFR measurements between myocardium with decreased oxygenation following vasodilation (ROC curve-derived threshold of ≤4.8%) and myocardium with increased oxygenation (>4.8% change) as based on per-coronary territory analysis.

4.7 Discussion

Using OS-CMR at 1.5T, we have demonstrated an associated reduction in myocardial oxygenation following adenosine-induced vasodilation with the functional severity of a coronary stenosis. However, this translated to a weaker relationship between myocardial perfusion and stenosis diameter, as assessed by CMR perfusion imaging and coronary angiography, respectively. Specifically, a complete lack of change or decrease of myocardial oxygenation during adenosine-induced vasodilation was demonstrated at coronary stenoses with FFR of 0.54 or less. Similarly, an OS-CMR mean percent change signal intensity threshold value of 4.8% adequately predicts functionally significant stenoses with FFR<0.80.

4.7.1 OS-CMR as a Marker for Myocardial Ischemia

Previous studies have shown the relative change in signal intensity using OS-CMR is a function of volume percentage of deoxyhemoglobin following pharmacologically induced vasodilation, reflecting the balance between supply and demand of perfusion of the myocardium [6,11,19]. In myocardium supplied by normal coronary arteries, there is an increase in oxygen saturation with a relative decrease in deoxyhemoglobin under hyperaemic conditions. Conversely, in myocardium supplied by narrowed coronary arteries, there is a blunted hyperaemic response in the capillary bed with pharmacology-induced vasodilation, resulting in a smaller decrease of deoxyhemoglobin. The corresponding decrease in signal intensity on OS-CMR images has been shown to be a direct indicator of a vasodilation-induced myocardial ischemic reaction [12,20].

Nearly over a decade ago, the theoretical foundation of FFR was established through dog studies and later confirmed in humans, demonstrating that pressure measurements for FFR at maximal pharmacologically-induced hyperemia takes into account the flow reserve of the epicardial coronary artery, myocardium, and collateral flow [21,22]. Importantly, an FFR of 66% or 0.66 was determined to be the most accurate in predicting abnormal ECG signs of myocardial ischemia, characterized by ST-segment depression in patients with normal systolic function and isolated coronary artery stenoses, with no patients found to have an abnormal ECG above the threshold FFR 72% [23]. In the present study, we demonstrated consistent results, with a complete lack of an increase or even a decrease in myocardial oxygenation seen at FFR 0.54 (per-coronary territory analysis) and FFR 0.62 (per-segmental analysis). In addition, FFR 0.75 was seen in myocardium showing any vasodilator-associated increase in oxygenation, validating OS-CMR measures of tissue oxygenation as a reasonable marker of myocardial ischemia and functional severity of coronary stenosis.

In a recent study, Walcher et al. also compared BOLD-CMR to that of FFR, showing a very modest significant signal decrease in segments supplied by coronary arteries with FFR≤0.80 compared to those segments perfused by a coronary artery with FFR>0.80. Undoubtedly, with only a 0.4% difference detected by BOLD-CMR, the study by Walcher et al. may not have captured the true physiological response of adenosine-induced myocardial ischemia at a threshold of FFR≤0.80 compared to the threshold found in our study at FFR 0.54 [13].

Keeping in mind that an FFR of 0.54 correlates with a complete lack of change in tissue oxygenation following adenosine-induced vasodilation, which may indicate a

more serious clinical presentation. Our data reveals that a mean BOLD SI% change of threshold 4.8% adequately predicts functionally significant stenoses with FFR≤0.80. Therefore, from a clinical perspective, a threshold of 4.8% may be a more practical threshold at which medical management should be intervened and a threshold of 0% or complete lack of relative increase in signal intensity following vasodilation, suggests serious ischemia that may require more aggressive management. Further studies will need to be conducted to elucidate the overall prognostic value of the newly established OS-CMR signal intensity threshold.

In our study, we found a smaller increase in signal intensity change following adenosine-induced vasodilation in the FFR>0.80 group. The first possible explanation was alluded to earlier from the study by Arnold et al, where areas of myocardium remote from ischemia and subtended by vessels with minimal or no disease was found to exhibit varying ranges of signal intensities in keeping with hypoperfused myocardium, demonstrating a possible uncoupling between epicardial flow and microvascular function[11]. Another possible explanation for this discrepancy may be paradoxically explained as follows:

FFR 0.91 to 1.0:

$$= \Delta SI\% = [(\text{Stress-Rest})/\text{Rest}] \times 100$$

$$= (6\text{-}5)/5$$

$$= 0.20 \text{ or } 20\%$$

VERSUS

FFR 0.81 to 0.90:

$$= \Delta SI\% = [(\text{Stress-Rest})/\text{Rest}] \times 100$$

$$= (6\text{-}4)/4$$

$$= 0.50 \text{ or } 50\%$$

Figure A-6 in the Appendix illustrates the absolute change from baseline to hyperemia in the various FFR categories. In the FFR 0.91 to 1.0 subgroup, there is a visually less pronounced change from baseline to hyperemia, as the signal intensity is likely already high at baseline, relative to those specific myocardium segments. It is important, however, to realize that baseline signal intensity is specific to each individual, such that the intrinsic myocardial/tissue composition and inhomogeneities each influence the local magnetic field differently. Hence, the methodology for OS-CMR relies heavily on relative change, rather than absolute change.

4.7.2 Limitations of FFR

Despite comparing our data to a proven reference standard of FFR, it is important to understand that FFR also has its limitations. FFR measures the difference in pressure across an epicardial stenosis and has been shown to be independent of hemodynamic changes in heart rate, blood pressure, and contractility[24]. Measurements of distal coronary pressure, as de Bruyne and colleagues have proposed, integrates all possible changes in vessel diameter that could affect absolute coronary blood flow. Furthermore, by measuring FFR during maximal vasodilation with adenosine, de Bruyne et al. argues that FFR measures are extremely reproducible due to the "extraordinary capability of the microvasculature to repeatedly vasodilate to exactly the same extent" [25]. However, this would only be valid if maximal vasodilation was always achieved and if the

microvasculature was functionally intact. Theoretically in the case of microvascular disease, baseline epicardial blood flow would be lower than it would be in cases with normal functioning microvasculature. FFR measurements in this case, would be overestimated and one would presume that a normal FFR indicated that the epicardial stenosis was not a major contributing factor to perfusion impairment [26]. However, the patient would still have diseased myocardium not recognized by the FFR. By assessing both FFR and coronary flow reserve in the cardiac catheterization lab in 150 intermediate coronary lesions in 126 patients, Meuwissen et al. have shown discordant results in 27% cases, largely due to the variability in microvascular resistance that exist across individuals patients and across perfusion territories [27]. Furthermore, adenosine has been shown to be an effective vasodilator, lowering systemic vascular resistance and blood pressure, and when used in patients with CAD, development of perfusion defects by nuclear SPECT was seen in 94% of patients [28]. However in the case of diabetic patients with presence of microvascular disease, maximal coronary vasodilation by adenosine was reduced in comparison to non-diabetic patients with CAD [29]. Because OS-CMR is a reflection of the intracapillary deoxygenated hemoglobin in the myocardium, measures of ΔSI% may be more susceptible to changes in the microcirculation. Therefore, direct head-to-head comparison to FFR as the reference standard, while necessary to establish the utility of OS-CMR, may not be appropriate in patients with underlying microvascular disease.

4.7.3 Exploring the Components Contributing to Tissue Oxygenation

While routinely used to guide patient management, stenosis severity by anatomical percent diameter has been shown to be a poor predictor of maximum flow capacity in CAD patients, not accounting for factors such as diffuse atherosclerosis and extent of arterial remodelling [30]. Similarly, we found a weak correlation between myocardial oxygenation to that of stenosis diameter measured by QCA. This is consistent with previous studies comparing OS-CMR to QCA[11]. Arnold et al. also reported an uncoupling between microvascular perfusion to tissue oxygenation, most prominent in areas with myocardial scar, where perfusion was reduced but did not have associated deoxygenation or decreasing mean SI% change. In our analysis of late-gadolinium enhancement, we found a trend towards decreased mean SI% change in areas with scar versus remote myocardium that was not significant, suggesting that there was in fact, no real difference in deoxygenation between areas with scar and remote myocardium, as reported by Arnold et al. Conversely, we may have been limited by overall sample size to achieve statistical significant, as most of our patients had stable CAD with no previous myocardial infarctions.

We also found a weak relationship and dissociation between myocardial perfusion and tissue oxygenation, with large scatter in the areas with abnormal versus normal perfusion. This is likely due to the quantitative analysis of the perfusion images, which may not have truly reflected the perfusion bed and related components to myocardial blood volume and myocardial blood flow. Previous studies that compared first-pass perfusion to BOLD-CMR in patients with CAD and have shown similar findings, whereby 50% of hypoperfused segments demonstrated no evidence of

deoxygenation. In addition, Spearman correlation between mean BOLD SI% change and absolute myocardial blood flow measured by first-pass perfusion was only ρ=0.26. Furthermore, the authors in the same study showed no significant difference in the BOLD SI% change between segments with or without late enhancement, as was found in our study[11]. Because we analyzed the CMR images using a total myocardium approach, perhaps areas of non-ischemic but viable epicardium averaged out the signal intensity in the subendocardium with a normal BOLD response. Equally, as postulated by Arnold et al, certain areas of myocardium may down-regulate energy-using processes, similar to hypocontractile myocardium, in order to prevent ischemia. Hence, while there may be hypoperfusion seen, tissue oxygenation remains adequate through ongoing physiological adaptation in the form of hibernation[11].

The persistent finding of a dissociation between anatomical stenosis severity at the epicardial level, perfusion at the microvascular level, and tissue oxygenation suggests that OS-CMR measures of mean SI% change may reflect more than the deoxyhemoglobin content in the capillary bed in response to perfusion supply and demand. With ongoing studies, we may be able to determine the relative roles microvascular function and even collateral circulation play in establishing the OS-CMR signal intensity.

4.7.4 Limitations

In the present study, we analyzed patients with FFR measurements of only one coronary vessel as compared to QCA and perfusion, which had all coronary territories measured. This is a limitation as we were not able to actively compare remote myocardium

subtended by normal coronaries in the same patient to myocardium perfused by stenotic coronaries, which also further limited our sample size of segments and coronary territories with FFR measurements. However, the decision to proceed with invasive FFR measurements was based on the clinical judgement of experienced interventional cardiologists, prioritizing the safety of the patients first. In addition, our study was designed not to provide a clinical protocol, but instead to increase the knowledge related to vasodilation-induced changes in myocardial oxygenation and hemodynamic significance of coronary stenoses. Therefore, a large portion of segments was excluded to limit the influence of artefacts or image quality, which were mostly found in the apical segments.

4.8 Conclusion

The present study demonstrates the relationship between vasodilator-induced changes of myocardial oxygenation using OS-CMR at different levels of FFR thresholds. An OS-CMR signal intensity threshold of 4.8% identified segments subtended functionally significant stenoses. In comparison, a complete lack of vasodilator-induced increase in tissue oxygenation was associated with more severe coronary stenoses identified with FFR of less than 0.54. Complementary comparisons with QCA, CMR perfusion, and late-enhancement studies demonstrate the complexity of tissue oxygenation measurements that warrants further investigation. Future studies are needed to assess the long-term prognostic value of OS-CMR in patients with CAD.

4.9 References

1. Shaw LJ, Berman DS, Maron DJ, Mancini GB, Hayes SW, Hartigan PM, Weintraub WS, O'Rourke RA, Dada M, Spertus JA, Chaitman BR, Friedman J, Slomka P, Heller GV, Germano G, Gosselin G, Berger P, Kostuk WJ, Schwartz RG, Knudtson M, Veledar E, Bates ER, McCallister B, Teo KK, Boden WE, COURAGE Investigators. Optimal medical therapy with or without percutaneous coronary intervention to reduce ischemic burden: results from the Clinical Outcomes Utilizing Revascularization and Aggressive Drug Evaluation (COURAGE) trial nuclear substudy. *Circulation.* 2008; 117: 1283-1291.

2. Tonino PA, De Bruyne B, Pijls NH, Siebert U, Ikeno F, van't Veer M, Klauss V, Manoharan G, Engstrom T, Oldroyd KG, Ver Lee PN, MacCarthy PA, Fearon WF, FAME Study Investigators. Fractional flow reserve versus angiography for guiding percutaneous coronary intervention. *N Engl J Med.* 2009; 360: 213-224.

3. Tonino PA, Fearon WF, De Bruyne B, Oldroyd KG, Leesar MA, Ver Lee PN, Maccarthy PA, Van't Veer M, Pijls NH. Angiographic versus functional severity of coronary artery stenoses in the FAME study fractional flow reserve versus angiography in multivessel evaluation. *J Am Coll Cardiol.* 2010; 55: 2816-2821.

4. Pijls NH, Fearon WF, Tonino PA, Siebert U, Ikeno F, Bornschein B, van't Veer M, Klauss V, Manoharan G, Engstrom T, Oldroyd KG, Ver Lee PN, MacCarthy PA, De Bruyne B, FAME Study Investigators. Fractional flow reserve versus angiography for guiding percutaneous coronary intervention in patients with multivessel coronary artery disease: 2-year follow-up of the FAME (Fractional Flow Reserve Versus Angiography for Multivessel Evaluation) study. *J Am Coll Cardiol.* 2010; 56: 177-184.

5. Pijls NH, van Schaardenburgh P, Manoharan G, Boersma E, Bech JW, van't Veer M, Bar F, Hoorntje J, Koolen J, Wijns W, de Bruyne B. Percutaneous coronary intervention of functionally nonsignificant stenosis: 5-year follow-up of the DEFER Study. *J Am Coll Cardiol.* 2007; 49: 2105-2111.

6. Friedrich MG, Karamitsos TD. Oxygenation-sensitive cardiovascular magnetic resonance. *J Cardiovasc Magn Reson.* 2013; 15: 43-429X-15-43.

7. Zheng J, Wang J, Rowold FE, Gropler RJ, Woodard PK. Relationship of apparent myocardial T2 and oxygenation: towards quantification of myocardial oxygen extraction fraction. *J Magn Reson Imaging.* 2004; 20: 233-241.

8. Li D, Waight DJ, Wang Y. In vivo correlation between blood T2* and oxygen saturation. *J Magn Reson Imaging.* 1998; 8: 1236-1239.

9. Friedrich MG, Niendorf T, Schulz-Menger J, Gross CM, Dietz R. Blood oxygen level-dependent magnetic resonance imaging in patients with stress-induced angina. *Circulation.* 2003; 108: 2219-2223.

10. Karamitsos TD, Leccisotti L, Arnold JR, Recio-Mayoral A, Bhamra-Ariza P, Howells RK, Searle N, Robson MD, Rimoldi OE, Camici PG, Neubauer S, Selvanayagam JB. Relationship between regional myocardial oxygenation and perfusion in patients with coronary artery disease: insights from cardiovascular magnetic resonance and positron emission tomography. *Circ Cardiovasc Imaging.* 2010; 3: 32-40.

11. Arnold JR, Karamitsos TD, Bhamra-Ariza P, Francis JM, Searle N, Robson MD, Howells RK, Choudhury RP, Rimoldi OE, Camici PG, Banning AP, Neubauer S, Jerosch-Herold M, Selvanayagam JB. Myocardial oxygenation in coronary artery disease: insights from blood oxygen level-dependent magnetic resonance imaging at 3 tesla. *J Am Coll Cardiol.* 2012; 59: 1954-1964.

12. Jahnke C, Gebker R, Manka R, Schnackenburg B, Fleck E, Paetsch I. Navigator-gated 3D blood oxygen level-dependent CMR at 3.0-T for detection of stress-induced myocardial ischemic reactions. *JACC Cardiovasc Imaging.* 2010; 3: 375-384.

13. Walcher T, Manzke R, Hombach V, Rottbauer W, Wohrle J, Bernhardt P. Myocardial perfusion reserve assessed by T2-prepared steady-state free precession blood oxygen level-dependent magnetic resonance imaging in comparison to fractional flow reserve. *Circ Cardiovasc Imaging.* 2012; 5: 580-586.

14. Hare J, Luu J, Friedrich M. Functional significance of blood oxygen level dependent (BOLD) imaging in patients with coronary artery disease – a validation study using fractional flow reserve. (Operating Grant Submission to CIHR). March 2010.

15. Graham MM, Faris PD, Ghali WA, Galbraith PD, Norris CM, Badry JT, Mitchell LB, Curtis MJ, Knudtson ML, APPROACH Investigators (Alberta Provincial Project for Outcome Assessment in Coronary Heart Disease. Validation of three myocardial jeopardy scores in a population-based cardiac catheterization cohort. *Am Heart J.* 2001; 142: 254-261.

16. APPROACH Team. Alberta Provincial Project for Outcome Assessment in Coronary Heart Disease. Available at: http://www.approach.org/. Accessed 03/04, 2012.

17. Zeger S, Liang K, Albert P. Models for longitudinal data: a generalized estimating equations approach. *Biometrics.* 1988; 44: 1049-1060.

18. Hastie T. Generalized additive models. In: Chambers J, Hastie T, eds. Statistical Models in S. Wadworth & Brooks/Cole; 1992.

19. Egred M, Waiter GD, Al-Mohammad A, Semple SI, Redpath TW, Walton S. Blood oxygen level dependent (BOLD) MRI: A novel technique for the detection of myocardial ischemia. *Eur J Intern Med.* 2006; 17: 551-555.

20. Wacker CM, Hartlep AW, Pfleger S, Schad LR, Ertl G, Bauer WR. Susceptibility-sensitive magnetic resonance imaging detects human myocardium supplied by a stenotic coronary artery without a contrast agent. *J Am Coll Cardiol.* 2003; 41: 834-840.

21. Pijls NH, van Son JA, Kirkeeide RL, De Bruyne B, Gould KL. Experimental basis of determining maximum coronary, myocardial, and collateral blood flow by pressure measurements for assessing functional stenosis severity before and after percutaneous transluminal coronary angioplasty. *Circulation.* 1993; 87: 1354-1367.

22. De Bruyne B, Baudhuin T, Melin JA, Pijls NH, Sys SU, Bol A, Paulus WJ, Heyndrickx GR, Wijns W. Coronary flow reserve calculated from pressure measurements in humans. Validation with positron emission tomography. *Circulation.* 1994; 89: 1013-1022.

23. De Bruyne B, Bartunek J, Sys SU, Heyndrickx GR. Relation between myocardial fractional flow reserve calculated from coronary pressure measurements and exercise-induced myocardial ischemia. *Circulation.* 1995; 92: 39-46.

24. de Bruyne B, Bartunek J, Sys SU, Pijls NH, Heyndrickx GR, Wijns W. Simultaneous coronary pressure and flow velocity measurements in humans. Feasibility, reproducibility, and hemodynamic dependence of coronary flow velocity reserve, hyperemic flow versus pressure slope index, and fractional flow reserve. *Circulation.* 1996; 94: 1842-1849.

25. De Bruyne B, Sarma J. Fractional flow reserve: a review: invasive imaging. *Heart.* 2008; 94: 949-959.

26. Kern MJ. Coronary physiology revisited : practical insights from the cardiac catheterization laboratory. *Circulation.* 2000; 101: 1344-1351.

27. Meuwissen M, Chamuleau SA, Siebes M, Schotborgh CE, Koch KT, de Winter RJ, Bax M, de Jong A, Spaan JA, Piek JJ. Role of variability in microvascular resistance on fractional flow reserve and coronary blood flow velocity reserve in intermediate coronary lesions. *Circulation.* 2001; 103: 184-187.

28. Ogilby JD, Iskandrian AS, Untereker WJ, Heo J, Nguyen TN, Mercuro J. Effect of intravenous adenosine infusion on myocardial perfusion and function. Hemodynamic/angiographic and scintigraphic study. *Circulation.* 1992; 86: 887-895.

29. Nahser PJ,Jr, Brown RE, Oskarsson H, Winniford MD, Rossen JD. Maximal coronary flow reserve and metabolic coronary vasodilation in patients with diabetes mellitus. *Circulation.* 1995; 91: 635-640.

30. Gould KL. Does coronary flow trump coronary anatomy? *JACC Cardiovasc Imaging.* 2009; 2: 1009-1023.

Chapter Five: RESULTS – THIRD MANUSCRIPT

5.1 Title: Impact of Medical Management with or without Percutaneous Coronary Intervention on Myocardial Oxygenation as assessed by OS-CMR

Judy M. Luu[1], James Hare[2], Jodi Harker[3], Yoko Mikami[1], Henk Ter Keurs, and Matthias G. Friedrich[4]

[1]: Stephenson CMR Centre at the Libin Cardiovascular Institute of Alberta, University of Calgary, Calgary AB, Canada; [2]: Alfred Hospital & Baker IDI Research Institute, Melbourne, VIC, Australia; [3]: Heart Care Partners, Brisbane, Australia; [4]: Philippa and Marvin Carsley Cardiovascular MR Centre at the Montreal Heart Institute/Université de Montréal, Montreal QC, Canada

Keywords: Myocardial oxygenation, oxygenation-sensitive CMR, medical management, PCI, coronary artery disease

5.2 Abstract

Background

Oxygenation-sensitive cardiovascular magnetic resonance (CMR) has previously been shown to identify ischemic myocardium supplied by functionally significant coronary stenoses. To investigate the role of OS-CMR in the assessment of patients with stable CAD, the purpose of this study was to determine the impact of medical therapy versus PCI plus medical therapy on myocardial oxygenation after one-month follow-up.

Methods

OS-CMR scans were performed in patients with known or suspected of having CAD preceding coronary angiography. Based on the clinical expertise of the performing interventional cardiologists, patients were recommended to proceed with medical management versus percutaneous coronary internvention (PCI) plus medical management. CMR images were captured during rest and adenosine-induced coronary hyperaemia. The mean signal intensity percent changes (ΔSI%) were calculated between rest and adenosine-induced hyperemia. Repeat CMR scans were performed one month after the initial CMR scan.

Results

Images from 34 patients were available for follow-up analysis. 24 of which were recommended for medical management and 10 patients proceeded with PCI plus medical management. There was improved myocardial oxygenation at one-month follow-up, particularly in the subendocardium in patients who underwent PCI in combination with ongoing medical therapy (ΔSI% 4.02; 95% CI 2.06 – 5.98%)

compared to baseline (ΔSI% of -0.38%; 95% CI -2.32 – 1.55%)(p=0.001). In patients managed by medical therapy alone, there was reduction in OS-CMR myocardial oxygenation at follow-up (ΔSI% 0.44; 95% CI -0.73 – 1.62%) compared to baseline (ΔSI% 3.45; 95% CI 2.01 – 4.88%) most notable in the subendocardium (p=0.003).

Conclusion

PCI plus medical therapy improved myocardial oxygenation at one-month follow-up compared to patients managed by medical therapy alone. OS-CMR assessment of regional myocardial oxygenation may play a role in guiding management in the stable CAD population. Further research is needed to ascertain the prognostic significance of reduced myocardial oxygenation in the long-term.

5.3 Abbreviations

BOLD:	Blood-Oxygen Level Dependent
CAD:	Coronary Artery Disease
FFR:	Fractional Flow Reserve
LV:	Left Ventricular
OMT:	Optimal Medical Therapy
OS-CMR:	Oxygen-sensitive Cardiovascular Magnetic Resonance
PCI:	Percutaneous Coronary Intervention
ΔSI%:	Mean signal intensity percent change from rest to stress
SI:	Signal Intensity
SSFP:	Steady State Free Precession
TE:	Echo time
TR:	Repetition time

5.4 Background

Despite ongoing improvements in diagnostic and treatment management, cardiovascular disease remains one of the leading causes of death in Canada, with a myocardial infarction estimated to occur every seven minutes [1]. The extent and severity of ischemia is targeted as a potential modifiable risk factor for patients with suspected coronary artery disease, with studies demonstrating improved outcomes of myocardial infarction and death with ischemia reduction [2]. A cornerstone of management of patients with stable coronary artery disease (CAD) is coronary revascularization using percutaneous coronary intervention (PCI). However, previous multi-centre, randomized controlled studies have shown inconclusive data regarding the additional benefit of PCI with optimal medical therapy (OMT) in the reduction of ischemia compared to OMT alone[2-4]. In these studies, optimal medical therapy implies trial of intensive pharmacotherapy, lifestyle modifications, and secondary prevention.

With the advent of Fractional Flow Reserve (FFR), epicardial coronary lesions meeting the FFR cut-off of less than 0.80 were shown to be hemodynamically significant to cause ischemia and therefore, can appropriately undergo PCI. In the FAME trial (Fractional Flow Reserve versus Angiography for Multivessel Evaluation), FFR was shown to be more accurate than angiography in identifying ischemia-producing lesions between 50% to 90% angiographic severity [5]. However, although FFR is currently the reference standard, it is still an invasive procedure that has potential risks for the patient related to coronary catheterization, including risk of vessel dissection or perforation, embolism, and arrhythmias.

A promising modality has recently emerged in recent years, which utilizes MRI to non-invasively evaluate patients with ischemic heart disease [6]. A recent study conducted by Luu et al. has shown the ability of oxygen-sensitive CMR (OS-CMR) to identify abnormal myocardium supplied by coronary territories with functionally significant stenoses. Based on the study, a mean signal intensity percent change of less than 4.8% best predicted functionally significant stenoses with FFR≤0.80 [7]. Furthermore, previous data from Luu and colleagues have shown regional distribution of myocardial oxygenation, whereby the researchers demonstrated differential signal intensity responses following adenosine-induced vasodilation in the subendocardium compared to the subepicardium in patients with CAD [8]. To further investigate the possible use of OS-CMR in the assessment of patients with stable CAD, the purpose of this study was to determine the impact of medical therapy versus PCI plus medical therapy on myocardial oxygenation after one-month follow-up.

5.5 Methods

For this study, the same patient sample included in Chapter 4 was used. Therefore, similar methodologies were employed.

5.5.1 Study population

We prospectively recruited patients with suspected or known CAD referred for clinically indicated diagnostic angiography or who had already undergone angiography with FFR (without intervention) within the prior four weeks. Information was collected

regarding patients baseline characteristics, coronary risk factors and medications. Patients were then asked to return for a repeat CMR scan at one-month follow-up after undergoing coronary angiography with or without PCI. Xanthine or dipyridamole use within 24 hours of CMR scan was not permitted. Ethics approval was obtained from the University of Calgary Conjoint Health Research Ethics Board and full written informed consent was obtained from all subjects.

5.5.2 Coronary Angiography Recommendation

Conventional invasive coronary angiography was performed in each patient. Clinical records of the angiogram were collected offline using the CARAT software (Coronary Artery Reporting and Archiving Tool) [9]. Based on the clinical judgement of the interventionalist, patients were recommended to proceed with medical therapy, PCI, and or coronary artery bypass grafting (CABG). The angiograms provided information as to which coronary vessels were stented during the revascularization. Follow-up angiography was not required in the study patients.

5.5.3 CMR imaging protocol

The baseline and follow-up CMR scans were performed with the patient in supine position using 1.5T MRI System (Magnetom Avanto®, Siemens Healthcare, Erlangen, Germany) with a 32-channel cardiac coil. Image acquisition was performed during breath-holds, using retrospective electrocardiogram (ECG)-gated sequences. Steady state free precession (SSFP) cine images were initially acquired for left ventricular (LV) volume and functional scanning (TR: 67, TE: 1.15, Flip angle: 74, Slice thickness: 10

mm). Subsequently, three sets of oxygenation-sensitive CMR images were acquired in short axis views at baseline in the basal, mid, and apical regions using a T2* oxygenation-sensitive, ECG-triggered steady-state free precession (SSFP) sequence with a long TR, as previously reported [10]. Scan parameters were: field of view 400 x 400 mm; matrix size 128 x 128, bandwidth 273 Hz/Pixel, TR/TE = 5.4/2.7ms, flip angle 90°, slice thickness 15mm for basal and mid, 10mm for apical slices. Typical breath-hold length was 10-15 seconds. The data acquisition was repeated during intravenous administration (at least 2 minutes after starting the infusion) of 140mcg/kg/min adenosine.

5.5.4 Analysis of Oxygenation-Sensitive Images

CMR images were analyzed offline by a blinded reader using certified software (CVI[42], Circle Cardiovascular Imaging Inc., Calgary, Canada). The images at end-systole were used for each slice in basal, mid, and apical regions to allow for the thickest amount of myocardium to for contour drawing. End-systole images were used for both baseline and hyperemia analyses to minimize confounding effects of varying perfusion pressures during the cardiac cycle. Segments were excluded if image quality precluded accurate analysis - this was done blinded to the angiography results and according to pre-specified criteria. Image quality criteria used included the presence of significant partial volume effect, the presence of inhomogeneity artefact, or any other significant image problem such as discordance in slice position between rest and stress due to extensive respiratory motion. Epicardial and endocardial contours were defined for each short axis slice. The software automatically segmented and outputted the signal intensities (SI) for the whole myocardium, subepicardium, and subendocardium according to the

American Heart Association guidelines. The change in mean signal intensity (ΔSI%) was calculated as the SI at rest subtracted from SI at maximal hyperemia during adenosine infusion, divided by the SI at rest and expressed as a percentage. Based on previous findings from our research group, a mean ΔSI% of less than <4.8% indicated myocardium subtended by a functionally significant stenosis [7].

5.5.5 Statistical Analysis

Data analysis was performed using statistical software (IBM SPSS Statistics for Mac version 20.0. Armonk, NY: IBM Corp). Continuous variables were presented as mean +/- 95% confidence intervals and categorical variables as percentages of the indicated total sample size. Study patients were grouped into categories that were recommended for medical therapy versus those that were recommended for and subsequently received PCI with medical therapy. Mean differences in the myocardial layers between baseline and follow-up scans were calculated using Paired-Sample T-Tests, with consideration for patients recommended for medical management versus PCI and medical therapy. A per-coronary analysis was also performed, whereby the average of segments corresponding to the appropriate coronary territory measured for each patient was used. Catheterization recommendations were then allocated to each coronary territory based on the angiograms.

5.6 Results

In total, 64 patients were recruited to the study, with one patient excluded due to incompletion of the CMR protocol. 24 patients did not return for follow-up and one patient was excluded entirely due to poor image quality. Therefore, 38 patients were available with follow-up OS-CMR scans. However, four patients with severe CAD recommended for coronary artery bypass surgery were excluded from the final analysis. Of the remaining 34 patients, three patients with normal coronaries and 21 patients with mild stenoses on angiography were recommended for medical management. 10 patients proceeded with PCI and continued optimal medical therapy by the time of his/her CMR scan follow-up. In total, 264 segments were available for analysis from the 24 patients recommended for medical management, averaging 11 segments analysed per patient. Conversely, 128 segments were available for analysis from 10 patients recommended for percutaneous coronary intervention, averaging 12.8 segments analysed per patient. Patient demographics and baseline characteristics are listed in Table 1. Medications are listed in Table 2.

The mean OS-CMR ΔSI% for the baseline and follow-up scans for patients recommended for medical management versus PCI plus medical management are listed in Table 3 and Table 4, respectively. Relative signal intensity changes were overall significantly decreased in all myocardial layers at one-month follow-up in patients treated with medical therapy. Conversely, signal intensity percent changes were overall significantly increased in all myocardial layers in patients treated with PCI plus medical therapy (Figure 1).

Based on a per-coronary territory analysis of myocardium subtended by revascularized coronary arteries (n=10), the mean OS-CMR ΔSI% at baseline was 6.2% (95% CI 1.2 – 11.2%) in the subepicardium and 1.08% (95% CI -4.2 – 6.4%) in the subendocardium. At one-month follow-up after PCI, the mean OS-CMR ΔSI% was 6.5% (95% CI -3.0 – 15.9%) in the subepicardium and -0.11% (95% CI 7.0 – 6.7%) in the subendocardium. There was no statistical significance between the mean ΔSI% at baseline and at follow-up in the myocardium supplied by coronary arteries that underwent revascularization.

Table 5-1: Patient Demographics and Baseline CMR parameters.

	Medical Management (n=24)	PCI and Medical Therapy (n=10)	p Value[1]
Age	60±8	58±10	p=NS
Male, N (%)	20 (83%)	10 (100%)	p=0.04
BMI	27.9±4.7	28.3±3.8	p=NS
Systolic BP	133±15	126±12	p=NS
Diastolic BP	80±10	77±6	p=NS
CMR Baseline Parameters			
LVSVi (mL/m^2)	44.5±7	46.6±8	p=NS
LVEDVi (mL/m^2)	89.0±17	91.7±14	p=NS
LVESVi (mL/m^2)	32.3±11	32.9±8	p=NS
LVEF (%)	57.5±9.6	58.9±56.6	p=NS

Note: Values are presented as n (%) or mean ± SD.

LVSVi, left ventricular stroke volume index, LVEDVi, end-diastolic volume index;

LVESVi, end-systolic volume index; LVEF, ejection fraction

Table 5-2: Patient Coronary Risk Factors and Medications.

CAD Clinical Risk Factors, N (%)	Medical Management (n=24)	PCI and Medical Therapy (n=10)	p Value[1]
Past/present smoker,	16 (67%)	6 (60%)	p=NS
Hypertension	13 (54%)	4 (40%)	p=NS
Dyslipidemia	20 (83%)	7 (70%)	p=NS
Diabetes Mellitus	4 (17%)	3 (30%)	p=NS
Family History	20 (83%)	7 (70%)	p=NS
Prior CAD	8 (33%)	3 (30%)	p=NS
Medications, N (%)	**Medical Management (n=24)**	**PCI and Medical Therapy (n=10)**	**p Value[1]**
Antiplatelets	21 (88%)	10 (100%)	p=NS
Beta-Blockers	12 (50%)	8 (80%)	p=NS
Calcium Channel Blockers	2 (8%)	0 (0%)	p=NS
Statins	23 (96%)	8 (80%)	p=NS
ACE inhibitors or ARBs	15 (63%)	4 (40%)	p=NS
Diuretics	4 (17%)	0 (0%)	p=0.043

ACE Inhibitors: Angiotensin-converting-enzyme; ARBS: Angiotensin II receptor blockers

Table 5-3: OS-CMR signal intensity percent changes baseline and one-month follow-up CMR scans for patients recommended for medical management.

Myocardial Layer	CMR Scan	SI % Change	95% CI	Significance
Total Myocardium (n=264)	Baseline	5.65	4.28 – 7.02	P<0.001
	Follow-up	3.08	1.86 – 4.30	
Subepicardium (n=264)	Baseline	8.23	6.66 – 9.80	p=0.009
	Follow-up	5.57	4.07 – 7.06	
Subendocardium (n=264)	Baseline	3.45	2.01 – 4.88	p=0.003
	Follow-up	0.44	-0.73 – 1.62	

Table 5-4: OS-CMR signal intensity percent changes baseline and one-month follow-up CMR scans for patients recommended for and proceeded with PCI plus medical management.

Myocardial Layer	CMR Scan	SI % Change	95% CI	Significance
Total Myocardium (n=128)	Baseline	2.47	0.35 – 4.60	P<0.001
	Follow-up	7.66	5.61 – 9.70	
Subepicardium (n=128)	Baseline	5.61	3.02 – 8.19	p=0.002
	Follow-up	10.62	8.29 – 12.95	
Subendocardium (n=128)	Baseline	-0.38	-2.32 – 1.55	p=0.001
	Follow-up	4.02	2.06 – 5.98	

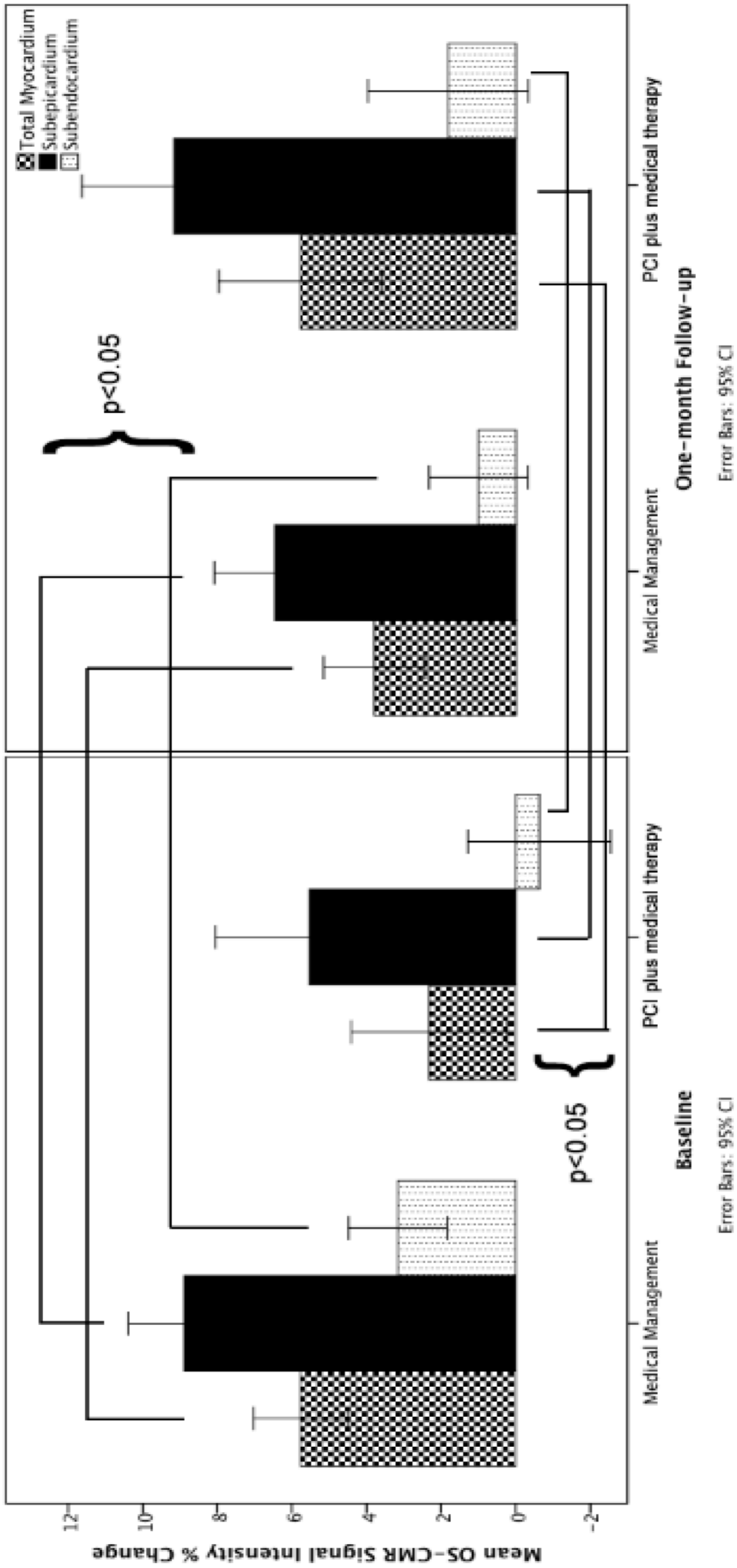

Figure 5-1: OS-CMR signal intensity percent changes at baseline and one-month follow-up CMR scans.

Mean signal intensity percent changes are shown for the two study groups: patients recommended for medical management versus patients who were treated with PCI and medical therapy.

5.7 Discussion

In this study, we have shown evidence for improved myocardial oxygenation at one-month follow-up, particularly in the subendocardium in a small group of patients who have underwent PCI in combination with ongoing medical therapy. In patients managed by medical therapy alone, which included stable CAD patients that did not require PCI and in patients with visually normal coronary angiograms, there was a reduction in OS-CMR signal intensity at follow-up, which was most notable in the subendocardium, suggesting that despite visual angiographic assessments of normal to mild coronary disease, evidence of decrease myocardial oxygenation still persists. Further research is needed to ascertain the prognostic significance of reduced myocardial oxygenation in the long-term.

5.7.1 Evidence for Benefit of PCI plus Optimal Medical Therapy

The decision regarding which are the most appropriate diagnostic and therapeutic measures for patients with stable CAD remains a complex issue. Recent evidence from a meta-analysis of 12 randomized controlled trials and over 7000 patients demonstrated no significant difference between PCI versus optimal medical therapy alone for the improvement of non-fatal myocardial infarction or all-cause cardiovascular mortality, based on coronary angiography[11]. The meta-analysis included such trials as the COURAGE trial (Clinical Outcomes Utilizing Revascularization and Aggressive Drug Evaluation)[12] and BARI 2D trial (Bypass Angioplasty Revascularization Investigation 2 Diabetes)[13], which used inclusion criteria based on angiographic findings, with or

without evidence of non-invasive testing for ischemia. The later FAME 2 trial, used FFR for careful selection of ischemia-inducing stenoses most suitable to yield benefit by revascularization in patients with stable CAD. The FAME 2 trial demonstrated that PCI plus optimal medical therapy decreases the need for urgent revascularization by angioplasty in patients shown to have functionally significant stenoses as indicated by FFR≤0.80 [14]. Furthermore, PCI was shown to provide greater angina relief compared to OMT alone [11]. Freedom from angina was noted at all follow-up points at less than one year, 1 to 5 years, and greater than 5 years. Current clinical opinion holds that aggressive medical therapy and lifestyle modifications without PCI are safe in the majority of patients with stable CAD as a first-line management approach. PCI is best reserved as an option for symptom relief and/or failed optimal medical therapy [15].

5.7.2 OS-CMR for the Evaluation of Stable CAD

Recent evidence from our research group comparing OS-CMR to FFR in patients with stable CAD has shown that a ΔSI% threshold of 4.8% adequately predicts myocardium supplied by functionally significant stenoses with FFR≤0.80. Although there are no randomized control trials using the recently established OS-CMR threshold, it may reasonable to suggest that patients with total myocardium ΔSI% >4.8% may be amenable to optimal medical therapy. Previous studies using OS-CMR by Wacker et al. have qualitatively demonstrated in a limited number of patients, improved T2* signal as evident by visual observation of less pronounced differences between regions with reduced T2* and regions of normal myocardium in patients before and after percutaneous transluminal coronary angioplasty [16,17]. However, to date, there are very

limited data available providing evidence of OS-CMR signal intensity changes in follow-up patients after intervention, particularly evaluating regional myocardial oxygenation changes in the different myocardial layers. Hence, while the period of follow-up in our study is relatively limited (1 month), the results from this study may provide preliminary insight into this area of research.

In the current study, we have obtained evidence for reduced ΔSI% below 4.8% to suggest ischemic subendocardium at the time of the baseline CMR scan, despite having relatively normal oxygenation in the total myocardium and subepicardium in patients recommended for medical management. At one-month follow-up, further reduction in the ΔSI% is seen in the subendocardium, while the ΔSI%, although decreased in the subepicardium, continues to be within 'normal' OS-CMR ΔSI% ranges. These results, while may be interpreted as limited due to the small degree of change, suggests that patients with visually normal to mild coronary disease on angiography may have increased risk from having unidentified reduced subendocardial oxygenation. In fact, previous studies have demonstrated that plaque rupture in acute coronary syndromes commonly occur in mild, non-flow limiting coronary stenosis or non-culprit lesions [3,18]. More serious consequences including sudden cardiac death are also shown to occur more likely in patients with mild stenoses not causing ischemia, particularly after a thrombus occlusion develops. These studies demonstrate the already well-established understanding that anatomical severity by angiography does not indicate hemodynamic severity[19] nor does it imply a strong correlation with myocardial oxygenation[20]. Therefore, there may be an increasing role for OS-CMR in the evaluation of CAD.

Secondly, we found improvement in regional ΔSI% in both the subepicardium and subendocardium following revascularization plus medical management at the one-month follow-up interval, with the most pronounced increase seen in the subendocardium, where mean ΔSI% approached ranges near normal myocardium. We were cautious to interpret and compare the data fully as there was a wide confidence interval, suggesting a large scatter in the baseline scans and follow-up scans of the patients who underwent PCI. The large scatter may be due to a number of factors, including the small sample size, confounding effects of medications, compliance, and single versus multi-vessel disease. However, the trend towards improved subendocardial signal intensity following PCI plus medical management is consistent with previous data using quantitative CMR, where researchers have shown improved hyperaemic myocardial blood flow and contractility in patients undergoing PCI of chronic total occlusions (CTO) and stenosed, but non-occluded coronary arteries, at 24 hours post-procedure and at 6 months follow-up. Whereas in patients with medically-managed CTO, hyperaemic blood flow and wall thickening of the affected segments continued to show no improvement even at six months compared to CTO segments in patients who underwent revascularization [21]. In the current study, we did not find improved ΔSI% in myocardium specifically supplied by coronary arteries that underwent revascularization. However, this is likely related to the very limited and under-powered sample size. Further studies are needed with a larger number of participants to more conclusively determine the effect of PCI on intracapillary myocardial oxygenation.

This study further supports the role of CMR to guide revascularization in patients with stable CAD. CMR assessment using myocardial perfusion imaging and

late gadolinium enhancement has been shown to provide additional information including prognostic information and alternative diagnoses [22]. Data from the European CMR Registry demonstrated that in patients undergoing a CMR study for suspected CAD or ischemia assessment, a new, unsuspected diagnosis came about in 19.6% of patients. Equally, based on the CMR study, patient management was influenced in over 70% of the patients [22,23]. Therefore, rather than identifying patients with markedly reduced epicardial blood flow as is the current standard protocol using coronary angiography and FFR, perhaps we may be able to identify patients at risk for subendocardial injury, which is known to be more prone towards ischemic damage.

5.7.3 Limitations

This study was limited by a lack of a reference standard against angiography. Ideally, FFR would have been appropriate to determine the hemodynamic significance of the coronaries in the two study populations in order more appropriately guide therapy, as previously shown in literature. Furthermore, FFR performed in all coronaries would have allowed for accurate evaluation of all myocardial territories in relation to the oxygenation status. Therefore, validation of the study findings with hemodynamic pressure-wire studies is a critical goal for the future. Secondly, we were limited by a small sample size and lack of randomization. We suspect with a larger number of patients in both study cohorts allowing for randomization, a clearer conclusion may be drawn as to whether medical management alone or medical management with revascularization improves outcome. Finally, we did not record patient compliance with medications or regimes taken to modify lifestyle habits. This information was rather

difficult to obtain and would not have altered the inclusion of our patients at follow-up. In keeping with future prospective studies looking at the prognostic impact of OS-CMR, further quality of life and symptom relief measures should be recorded to provide a more complete patient assessment.

5.8 Conclusion

In the current study, we demonstrated the improvement of myocardial oxygenation at one-month follow-up in patients who underwent PCI with medical therapy. Conversely, we saw a reduction in myocardial oxygenation, most prominent in the subendocardium in patients treated with medical therapy alone. While it is difficult to assess the impact of our findings due to limited prognostic and outcome data, it is still reasonable to anticipate the future potential diagnostic role of OS-CMR in the stable CAD population.

5.9 References

1. Heart and Stroke Foundation of Canada. Statistics. Available at: http://www.heartandstroke.com/site/c.ikIQLcMWJtE/b.3483991/k.34A8/Statistics.htm#references. Accessed April/16, 2014.

2. Shaw LJ, Berman DS, Maron DJ, Mancini GB, Hayes SW, Hartigan PM, Weintraub WS, O'Rourke RA, Dada M, Spertus JA, Chaitman BR, Friedman J, Slomka P, Heller GV, Germano G, Gosselin G, Berger P, Kostuk WJ, Schwartz RG, Knudtson M, Veledar E, Bates ER, McCallister B, Teo KK, Boden WE, COURAGE Investigators. Optimal medical therapy with or without percutaneous coronary intervention to reduce ischemic burden: results from the Clinical Outcomes Utilizing Revascularization and Aggressive Drug Evaluation (COURAGE) trial nuclear substudy. *Circulation.* 2008; 117: 1283-1291.

3. Epstein SE, Waksman R, Pichard AD, Kent KM, Panza JA. Percutaneous coronary intervention versus medical therapy in stable coronary artery disease: the unresolved conundrum. *JACC Cardiovasc Interv.* 2013; 6: 993-998.

4. Boden WE, O'Rourke RA, Teo KK, Maron DJ, Hartigan PM, Sedlis SP, Dada M, Labedi M, Spertus JA, Kostuk WJ, Berman DS, Shaw LJ, Chaitman BR, Mancini GB, Weintraub WS, COURAGE Trial Investigators. Impact of optimal medical therapy with or without percutaneous coronary intervention on long-term cardiovascular end points in patients with stable coronary artery disease (from the COURAGE Trial). *Am J Cardiol.* 2009; 104: 1-4.

5. Tonino PA, Fearon WF, De Bruyne B, Oldroyd KG, Leesar MA, Ver Lee PN, Maccarthy PA, Van't Veer M, Pijls NH. Angiographic versus functional severity of coronary artery stenoses in the FAME study fractional flow reserve versus angiography in multivessel evaluation. *J Am Coll Cardiol.* 2010; 55: 2816-2821.

6. Friedrich MG, Karamitsos TD. Oxygenation-sensitive cardiovascular magnetic resonance. *J Cardiovasc Magn Reson.* 2013; 15: 43-429X-15-43.

7. Luu J, Friedrich M, Harker J, Dwyer N, Guensch D, Hare J. Relationship of Vasodilator-Induced Changes of Myocardial Oxygenation with the Severity of Coronary Artery Stenosis – a Study using Oxygenation-Sensitive Cardiovascular Magnetic Resonance. 2014.

8. Luu J, Schmidt A, Flewitt J, Mikami Y, Ter Keurs H, Friedrich MG. Regional assessment of myocardial oxygenation using Oxygen-Sensitive Cardiovascular Magnetic Resonance. 2014.

9. APPROACH Team. Alberta Provincial Project for Outcome Assessment in Coronary Heart Disease. Available at: http://www.approach.org/. Accessed 03/04, 2012.

10. Hare J, Luu J, Friedrich M. Functional significance of blood oxygen level dependent (BOLD) imaging in patients with coronary artery disease – a validation study using fractional flow reserve. (Operating Grant Submission to CIHR). March 2010.

11. Pursnani S, Korley F, Gopaul R, Kanade P, Chandra N, Shaw RE, Bangalore S. Percutaneous coronary intervention versus optimal medical therapy in stable coronary artery disease: a systematic review and meta-analysis of randomized clinical trials. *Circ Cardiovasc Interv.* 2012; 5: 476-490.

12. Boden WE, O'Rourke RA, Teo KK, Hartigan PM, Maron DJ, Kostuk WJ, Knudtson M, Dada M, Casperson P, Harris CL, Chaitman BR, Shaw L, Gosselin G, Nawaz S, Title LM, Gau G, Blaustein AS, Booth DC, Bates ER, Spertus JA, Berman DS, Mancini GB, Weintraub WS, COURAGE Trial Research Group. Optimal medical therapy with or without PCI for stable coronary disease. *N Engl J Med.* 2007; 356: 1503-1516.

13. BARI 2D Study Group, Frye RL, August P, Brooks MM, Hardison RM, Kelsey SF, MacGregor JM, Orchard TJ, Chaitman BR, Genuth SM, Goldberg SH, Hlatky MA, Jones TL, Molitch ME, Nesto RW, Sako EY, Sobel BE. A randomized trial of therapies for type 2 diabetes and coronary artery disease. *N Engl J Med.* 2009; 360: 2503-2515.

14. De Bruyne B, Pijls NH, Kalesan B, Barbato E, Tonino PA, Piroth Z, Jagic N, Mobius-Winkler S, Rioufol G, Witt N, Kala P, MacCarthy P, Engstrom T, Oldroyd KG, Mavromatis K, Manoharan G, Verlee P, Frobert O, Curzen N, Johnson JB, Juni P, Fearon WF, FAME 2 Trial Investigators. Fractional flow reserve-guided PCI versus medical therapy in stable coronary disease. *N Engl J Med.* 2012; 367: 991-1001.

15. American College of Cardiology. OMT Looks Better and Better for Stable Ischemic Heart Disease *(ACCEL) - One challenge: patients' overwhelming 'therapeutic misconception' about PCI.* Available at: http://www.cardiosource.org/News-Media/Publications/CardioSource-World-News/2013/July/OMT-Looks-Better-and-Better-for-Stable-Ischemic-Heart-Disease.aspx. Accessed April/20, 2014.

16. Wacker CM, Bock M, Hartlep AW, Bauer WR, van Kaick G, Pfleger S, Ertl G, Schad LR. BOLD-MRI in ten patients with coronary artery disease: evidence for imaging of capillary recruitment in myocardium supplied by the stenotic artery. *MAGMA.* 1999; 8: 48-54.

17. Wacker CM, Hartlep AW, Pfleger S, Schad LR, Ertl G, Bauer WR. Susceptibility-sensitive magnetic resonance imaging detects human myocardium supplied by a stenotic coronary artery without a contrast agent. *J Am Coll Cardiol.* 2003; 41: 834-840.

18. Stone GW, Maehara A, Lansky AJ, de Bruyne B, Cristea E, Mintz GS, Mehran R, McPherson J, Farhat N, Marso SP, Parise H, Templin B, White R, Zhang Z, Serruys PW, PROSPECT Investigators. A prospective natural-history study of coronary atherosclerosis. *N Engl J Med.* 2011; 364: 226-235.

19. Gould KL. Does coronary flow trump coronary anatomy? *JACC Cardiovasc Imaging.* 2009; 2: 1009-1023.

20. Arnold JR, Karamitsos TD, Bhamra-Ariza P, Francis JM, Searle N, Robson MD, Howells RK, Choudhury RP, Rimoldi OE, Camici PG, Banning AP, Neubauer S, Jerosch-Herold M, Selvanayagam JB. Myocardial oxygenation in coronary artery disease: insights from blood oxygen level-dependent magnetic resonance imaging at 3 tesla. *J Am Coll Cardiol.* 2012; 59: 1954-1964.

21. Cheng AS, Selvanayagam JB, Jerosch-Herold M, van Gaal WJ, Karamitsos TD, Neubauer S, Banning AP. Percutaneous treatment of chronic total coronary occlusions improves regional hyperemic myocardial blood flow and contractility: insights from quantitative cardiovascular magnetic resonance imaging. *JACC Cardiovasc Interv.* 2008; 1: 44-53.

22. Morton G, Schuster A, Perera D, Nagel E. Cardiac magnetic resonance imaging to guide complex revascularization in stable coronary artery disease. *Eur Heart J.* 2010; 31: 2209-2215.

23. Bruder O, Schneider S, Nothnagel D, Dill T, Hombach V, Schulz-Menger J, Nagel E, Lombardi M, van Rossum AC, Wagner A, Schwitter J, Senges J, Sabin GV, Sechtem U, Mahrholdt H. EuroCMR (European Cardiovascular Magnetic Resonance) registry: results of the German pilot phase. *J Am Coll Cardiol.* 2009; 54: 1457-1466.

Chapter Six: DISCUSSION

6.1 Synopsis

Oxygenation-sensitive CMR is a technique that exploits the paramagnetic properties of intracapillary deoxygenated hemoglobin in order to generate endogenous contrast without necessity for IV contrast agents or ionizing radiation. Myocardial oxygenation is measured by a relative change from baseline to pharmacologically induced hyperemia. In order to achieve oxygen-sensitive contrast, we utilized the SSFP approach to allow for high signal-to-noise ratio, better image quality, and dynamic visualization of the cardiac phases (cine imaging).

The work presented in this thesis aimed to enhance the understanding of myocardial oxygenation using CMR. By studying a population, which included patients with coronary artery, participants with only coronary risk factors but no established clinical disease, and young, healthy volunteers, we demonstrated that the signal intensity changes in response to adenosine-induced vasodilation measured by OS-CMR may be a function of both advancing age and decreasing diastolic blood pressure. Furthermore, for the first time, we were able to analyze the myocardium in such a way that exposed the differential features of the ΔSI% captured by OS-CMR, whereby the ΔSI% was less in the subendocardium compared to the subepicardium in both patients with CAD and in individuals with only risk factors for cardiovascular disease. We hypothesized that this finding may reflect dysfunction of the microcirculation and its capacity to vasodilate and compensate in the face of increasing oxygen demands. This may be akin to dysfunction of the microcirculation's ability to autoregulate flow when faced with pressure changes.

From there, we compared our imaging technique to the reference standard of FFR and demonstrated the ability of OS-CMR to identify abnormal myocardium supplied by coronary arteries with hemodynamically limiting stenoses. Because FFR has been established as a useful prognosticator to effectively diagnose and guide appropriate management in patients with CAD, we hypothesized that measures of ΔSI% in response to adenosine-vasodilation may reflect myocardial ischemia. However, we found that the relationship was not as consistent when compared to other measures of myocardial ischemia like stenosis diameter or myocardial perfusion.

Finally, in patients with stable CAD, we sought to determine the impact of revascularization plus medical therapy versus medical therapy alone on myocardial oxygenation by assessing patients after a follow-up time period of one-month. Limited by sample size and lack of randomization, we demonstrated a trend towards improved myocardial oxygenation as measured by OS-CMR in the cohort of patients who received PCI plus medical therapy. Conversely, patients treated with medical therapy alone exhibited worsened ΔSI%, which was most profound in the subendocardium.

6.2 A Case for Dysfunctional Autoregulation or Vasodilatory Capacity

OS-CMR measurements of myocardial oxygenation provide additional insight to the knowledge of the ischemic cascade. We know from previous data that evaluations of areas of myocardial scar with hypoperfusion using PET imaging show dissociation to myocardial deoxygenation[1]. We also know from our own data and those previously published that there is a persistent weak relationship between epicardial stenosis severity

and the downstream measurement of myocardial oxygenation, such that in patients having only coronary risk factors and no clinical evidence of CAD, there was evidence of deoxygenation present in the subendocardium. These findings highlight how assessment of myocardial oxygenation may be a separate marker of disease in the development and pathophysiology of CAD.

With that notion, the relative changes in signal intensity following adenosine-induced hyperemia may reflect the potential role of OS-CMR in assessing the capacity of microvasculature to vasodilate or autoregulate. Vasodilator-induced hyperemia and the corresponding changes in myocardial oxygenation are theoretically different than those induced by physical exercise. With the administration of adenosine, the resistance in the vasculature of areas subtended by normal coronary arteries dilate, decreasing the coronary resistance to increase blood flow four to five times above basal levels. However, in vessels subtended by a stenotic epicardial artery, coronary resistance is diminished as the endogenous vasodilator reserve has already been utilized. Therefore, minor to no further reductions in coronary microvascular resistance can occur in the arteriole bed and myocardial blood flow in such areas may not change or even decrease[2]. With exercise, there is overall higher metabolic oxygen demand and increased cardiac output such that the limited increase in coronary blood flow in a stenotic territory can result in an imbalance in regional supply/demand that may induce myocardial ischemia. On the contrary, the regional changes in coronary blood flow during adenosine-induced vasodilation are not associated with significant changes in myocardial oxygen demand. Hence, the hemodynamic effects and perfusion defect, if present, is likely a reflection of abnormal coronary flow reserve rather than true

ischemia[2,3]. Dysfunctional autoregulation or vasodilating capacity of the microcirculation is however, still closely linked to myocardial ischemia. For instance, during exercise, increased oxygen demand is met with increase blood flow through effective autoregulation of the coronary circulation. However, if the resistance vessels of the microcirculation were unable to fully vasodilate to meet the oxygen demand, then the secondary outcome would ultimately result in myocardial ischemia.

From there, we have evidence to suggest that advancing age and decreasing blood pressure may influence myocardial oxygenation, factors which are both shown to be associated with arterial integrity. Advancing age has been shown to lead to arterial stiffening, impairing the ability of the microvasculature to mediate flow. As mentioned earlier, over time, arterial stiffening may also result in the paradoxical increase in systolic blood pressure due to reduced capacitance, and decrease in diastolic blood pressure due to reduced elastic recoil supporting the diastolic pressure[4]. Age and diastolic blood pressure were the two risk factors most strongly correlated to measures of ΔSI% and also predicted abnormal myocardial ΔSI%. Further research is needed to confirm these findings and further elucidate the role of myocardial oxygenation in evaluating dysfunctional vasodilator capacity.

6.2.1 Confounders of Oxygen-Sensitive Contrast

In the current thesis, we were not able to directly evaluate the role of the collateral circulation in augmenting myocardial oxygenation. However, previous researchers have suggested the role of collaterals in measurements of myocardial oxygenation, where in a study published by Jahnke et al, large variability of ΔSI% values ranging from -15% to

30% was seen in myocardial segments supplied by a coronary artery with no angiographic evidence of stenosis. Similarly, the variability ranged from -30% to 10% in myocardial segments supplied by an occluded coronary artery with 100% diameter stenosis but no late gadolinium enhancement[5]. Such variability in measurements of ΔSI% may be attributed to the compensatory effect of the collateral circulation, augmenting flow for areas with total occlusions. In a study of 36 patients who underwent elective angioplasty, researchers demonstrated quantitative relationship between lesion severity and collateral development, whereby with stenosis diameter at a threshold of 70% or more, there was increased collateral development in the coronary vasculature [6]. This may be a potential reason as to why contrary to seeing deoxygenation with increasing stenosis diameter, there was often a large variability in OS-CMR signal intensities in our data. Theoretically, the presence or development of collateral arteries would improve myocardial oxygenation, as there would be a greater reserve during pharmacologically induced vasodilation from the microvasculature. Referring back to Figure 1-11, with increased collaterals and myocardial blood flow, there would be a concomitant decrease in volume percentage of deoxygenated hemoglobin, creating less distortion of the local magnetic field to generate of a stronger signal from reduced T2* decay.

Secondly, we did not directly draw blood samples to measure the pH or oxygen saturation. However, valuable data from previous research can help elucidate the effect of pH changes on measurements of myocardial oxygenation. Current studies by Guensch et al. suggest that arterial changes in pH and partial pressure of oxygen (paO_2) have minimal influence on myocardial oxygenation. These researchers effectively

decreased the hemoglobin oxygen affinity by manipulating the partial pressure of carbon dioxide ($paCO_2$) and tested the impact on myocardial oxygenation. T2*-weighted SSFP OS-CMR at 1.5T was performed in nine anesthesized and ventilated pigs. 60-second breathholds were induced and changes in myocardial and blood pool oxygenation were monitored. The long breathholds led to increases in $paCO_2$, resulting in a trend towards increased myocardial signal intensity, despite parallel decreases in paO_2 and pH in the blood pool. The authors hypothesized that the CO_2-mediated increase in coronary vasodilation and perfusion likely allowed for adequate compensation of the drop in arterial hemoglobin saturation during the long breathhold [7].

6.3 Relation of the Present Work to Previously Published Studies

To date, OS-CMR has been compared to multiple modalities, including nuclear SPECT[8], PET[9], QCA[1,10], CMR perfusion[1,10], and recently one study comparing OS-CMR to the invasive reference standard of FFR[11] With these studies, the diagnostic accuracy of BOLD-CMR has been reported to range from 47-81% specificity and 67-88% sensitivity. At 3.0T, Jahnke et al. demonstrated a specificity of 81% and sensitivity of 85% to detect stenosis ≥50% at a BOLD threshold value of signal intensity change at 2.7%. Other researchers have also identified a role for OS-CMR in hypertensive LV hypertrophy, whereby there was a 3-fold reduction in oxygenation-dependent vasodilator response to dipyridamole using BOLD-CMR[12].

Previous studies reported moderate diagnostic accuracy for OS-CMR for potentially two main reasons—non-optimal reference standard or non-optimal oxygen-

sensitive contrast generation. Until recently, OS-CMR was compared head to head with another imaging modality such as PET or nuclear SPECT, with coronary angiography as the reference standard. Significant CAD was often defined as the presence of at least one stenosis ≥50% diameter in any of the epicardial arteries or associated branches. While angiography is commonly performed in the clinical setting, we now know that anatomical measures of stenoses may not truly reflect the underlying pathophysiology due to the presence of diffuse atherosclerosis and extent of arterial remodeling in humans. Studies performed in canine models have previously shown a characteristic decrease in coronary flow reserve with increasing percent diameter stenosis of at least 50% and 85% at which resting coronary flow began to fall [13]. However, the correlation between anatomy and hemodynamic severity of a stenosis in humans has been proven to be very weak[14], with discrepancies between angiography and FFR in 50% to 70% stenoses and 70% to 91% stenoses[15]. By comparing OS-CMR to coronary angiography over multiples studies, researchers were beginning to document the dissociation and weak correlation between the two measures. Interpreting our own data, we are now more confident that the assessment of epicardial stenosis by angiography does not reflect the overall impact of reduced flow, diffuse atherosclerosis, microvascular dysfunction, or collateralization in the myocardium.

From a clinical perspective, when a physician is faced with the question of how best to identify ischemic myocardium or determine the optimal therapy for patients with CAD, OS-CMR's potential role in the armamentarium of imaging modalities is that it offers the benefit of being contrast and radiation free. Also, more importantly, with

ongoing advancement, OS-CMR has the potential to provide a unifying assessment of LV function, coronary disease, and microcirculatory vasodilator reserve.

6.4 Troubleshooting

One issue to be addressed was the sub-optimal image quality, since a large number of segments or coronary territories were excluded due to poor image quality, especially in the first 10 patients of the study. We attributed the poor image quality to a learning curve for training of the breath holds. Patients were instructed to hold his/her breaths at the end of expiration because the diaphragm at end-expiration maintains that position for a longer duration and are more stable over time compared to end-inspiration[16]. Previous studies at performed at 1.5T using a segmented gradient echo demonstrated reproducible susceptibility artefacts occurring in the phrenico-mediastinal recess and superimposed onto the inferolateral sections of the myocardium. The researchers also confirmed that imaging in end-expiratory helped diminish those susceptibility artefacts[17]. However, while our scan times for each breath hold was relatively short (within 10-15 seconds), the first few patients were not fully aware of the proper breath hold, resulting in respiratory motion artefacts.

Keeping in mind also that the SSFP technique, while generally faster and allowing for a higher signal-to-noise ratio, is inherently prone to off-resonance artifacts. In their experimental animal validation study, Dharmakumar et al. mentioned the importance of manually shimming the field to identify the optimum center frequency to prevent the banding artifacts, especially with the long repetition time required with the

SSFP sequence[18]. As a result of magnetic susceptibility, the magnetic field is far from homogenous and inherently has areas where signal will drop, causing artefacts or image distortions. With shimming using resistant coils, field corrections are produced that will help make the magnetic field more homogenous. We found that a combination of better instructions on proper breath-holding techniques and adequate shimming allowed for improved image quality as the study progressed.

In general, the reproducibility of OS-CMR was excellent, with great agreement between intraobserver and interobserver variability. We noted interclass correlation for inter- and intraobserver variability to be 0.93 (CI 0.90 – 0.95) and 0.88 (CI 0.83 – 0.92), respectively. Equally, previous authors have noted similar values for reader variability, with intraclass correlation coefficient at 0.84 and interobserver at 0.87 [11]. To further improve on the image analysis, automatic computer software contouring would allow for more reproducible results and reduced analysis time.

6.4.1 BOLD-CMR at Higher Field Strengths

To overcome some of the challenges present at 1.5T, Jahnke and colleagues used a 3D T2-prepared segmented gradient echo technique with cine capabilities to image the entire cardiac phase and real-time free breathing navigator-gated techniques at 3.0T. As the field strength increases, more energy is applied to align the hydrogen nuclei with the magnetic field. The number of spin-up nuclei increases in proportion to the number of spin-down nuclei, allowing for an increased net magnetization during patient imaging [19]. Thus, it is expected that with a doubling of field strength causes a doubling of signal to

noise ratio (SNR). Furthermore, at 3.0T, there is also the advantage of having decreased imaging time and increased resolution[20].

This study was advantageous in multiples perspectives in that it was able to achieve an increased signal-to-noise ratio and reduced breathing artefacts by allowing patients to breath freely without necessity for breath holds [10]. Using an SSFP-based BOLD-CMR sequence, researchers have previously validated the advantage of oxygenation-sensitive cardiac imaging at 3.0T in dog models, achieving a 2.5 fold increase in BOLD sensitivity relative to 1.5T to identify various levels of coronary artery stenoses in the LCx of canines [21]. With an increased signal-to-noise ratio at 3.0T, one draw-back due to the inherent inhomogeneities in the magnetic field is that subsequent off-resonant transverse magnetizations can destructively cancel out creating dark-banding artefacts on the images, which may be even more pronounced with an SSFP sequence [22]. To overcome these challenges, Karamitsos et. al ensured careful pre-scanning preparations with shimming and center frequency adjustments using a T2-prepared SSFP sequence at 3.0T in CAD patients and normal volunteers (Figure 6-1). Overall, very good image quality was noted, with off-resonance artefacts present in nine of the 32 subjects and occurring mostly in the anterior wall heart-lung interface, then the inferior wall [9].

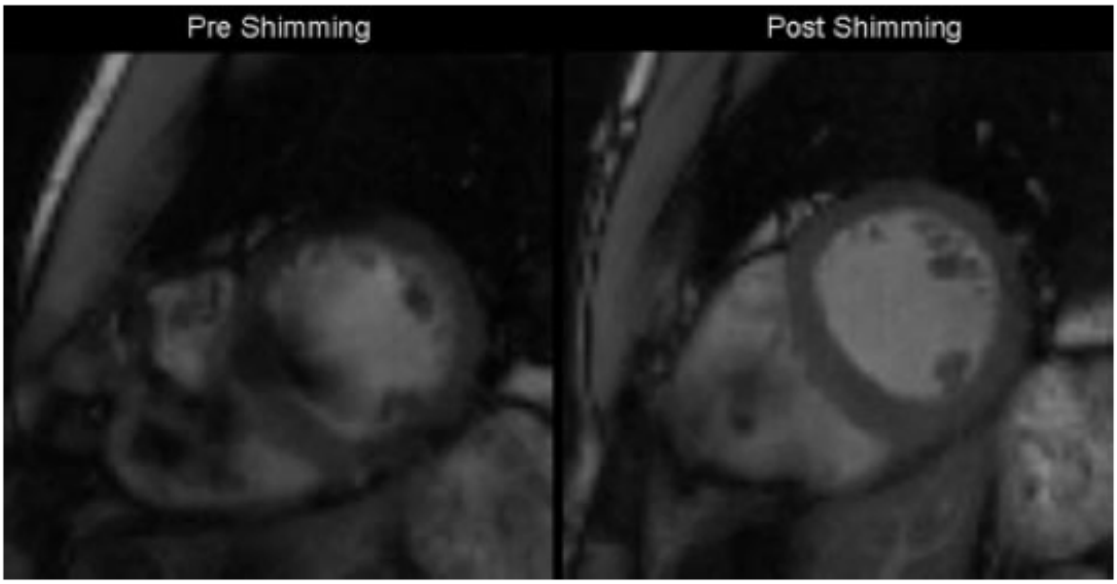

Figure 6-1: Example of the effect of shimming in short-axis slice of a patient with CAD.

Shimming effectively corrects for the inhomogeneities in the magnetic field. Image on the left was acquired before shimming with significant artifacts in the septum, anterior wall, and blood pool. Image quality (right image) was much improved after shimming adjustments. Adapted from Karamitosos et al. 2010 [9].

6.5 Future Directions

Recent pilot data have shown the ability of SSFP BOLD-CMR to identify ischemic territories with severe (flow limiting) stenosis at resting conditions in dog models, with further validation in patients to be performed [23]. This is promising as future OS-CMR scans may not require the use of pharmacological vasodilating agents altogether.

As previously mentioned above, Guensch and colleagues have also demonstrated the potential role of carbon dioxide (CO_2) as a coronary vasodilator. In 14 healthy volunteers, two different breathing protocols were performed. In eight of the participants, long breath-holds with one and two minutes of hyperventilation were done and in six aquatic athletes, 60-seconds long breath-holds were done. Breath-holds lasted

between 35 to 117 seconds and periods of hyperventilation lasts for 60 to 120 seconds. Interestingly, a decreased in signal intensity (deoxygenation) was noted in the left ventricular blood pool, while tissue oxygenation in the myocardium increased by 8.2% during the long breath-holds. Hyperventilation resulted in a decrease in capillary $PaCO_2$, which corresponded to a significant drop by 7.5% in the myocardial signal intensity (oxygenation)[24]. Therefore, by using CO_2-mediated breathing maneuvers to alter myocardial oxygenation in vivo with OS-CMR, the inherent problem of having to use adenosine as a pharmacological vasodilator may soon to be resolved. Ongoing research will need to be performed, however, to further establish the role of endogenous vasodilators in patients with ischemic heart disease.

In the immediate future, one major question remains as to determining the prognostic impact of abnormal myocardial oxygenation. To date, there are no studies that have addressed this area. However, from our small sample study of 34 patients with follow-up OS-CMR scans following coronary angiography. By directly measuring the signal intensity in the subendocardium, we were able to demonstrate improved tissue oxygenation, most notable in the subendocardium, following PCI plus medical therapy. Furthermore, on medical therapy alone, at one-month follow-up, there was evidence to suggest reduced signal intensity in the total myocardium, subepicardium, and subendocardium. Of note, researchers looked at follow-up after 10 weeks PCI with stenting and after 20 weeks following CABG in two patients total and found improved homogeneity in T2* signal intensity between treated and normal myocardium[25]. While outside the scope of this thesis, the next step would potentially be to follow these

patients at intervals of one-year and upward of two-years to determine if any, adverse outcomes resulted in both groups.

Ongoing research is currently being performed in the latest multi-centre ISCHEMIA trial (International Study of Comparative Health Effectiveness with Medical and Invasive Approaches) to determine the optimal management for patients with stable ischemic heart disease prior to cardiac catheterization, with randomization to be performed based on evidence of moderate ischemia on stress imaging using other non-invasive modalities, including echocardiography, nuclear and CMR myocardial perfusion imaging. As a sub-study, OS-CMR is being used to guide revascularization in patients with moderate to severe ischemia [26] and with such a large study population (goal of 8000 patients), valuable data will be gathered to elucidate the prognostic role of OS-CMR in the anticipated 4-year follow-up period.

6.6 References

1. Arnold JR, Karamitsos TD, Bhamra-Ariza P, Francis JM, Searle N, Robson MD, Howells RK, Choudhury RP, Rimoldi OE, Camici PG, Banning AP, Neubauer S, Jerosch-Herold M, Selvanayagam JB. Myocardial oxygenation in coronary artery disease: insights from blood oxygen level-dependent magnetic resonance imaging at 3 tesla. *J Am Coll Cardiol.* 2012; 59: 1954-1964.

2. Braunwald E, Libby P, Bonow R, Mann D, Zipes D. Braunwald's Heart Disease: A Textbook of Cardiovascular Medicine. 8th ed. Philadelphia, PA: Saunders Elsevier; 2008.

3. Iskandrian AS, Verani MS, Heo J. Pharmacologic stress testing: mechanism of action, hemodynamic responses, and results in detection of coronary artery disease. *J Nucl Cardiol.* 1994; 1: 94-111.

4. Sleight P. Lowering of blood pressure and artery stiffness. *Lancet.* 1997; 349: 362.

5. Jahnke C, Kozerke S, Schnackenburg B, Marx N, Paetsch I. Three-dimensional contrast-enhanced and non-contrast-enhanced cardiac magnetic resonance imaging for the assessment of myocardial ischemic reactions: the practice of looking deeply into the myocardium. *J Nucl Cardiol.* 2011; 18: 937-951.

6. Rentrop KP, Thornton JC, Feit F, Van Buskirk M. Determinants and protective potential of coronary arterial collaterals as assessed by an angioplasty model. *Am J Cardiol.* 1988; 61: 677-684.

7. Guensch DP, Fischer K, Flewitt JA, Friedrich MG. Impact of intermittent apnea on myocardial tissue oxygenation--a study using oxygenation-sensitive cardiovascular magnetic resonance. *PLoS One.* 2013; 8: e53282.

8. Friedrich MG, Niendorf T, Schulz-Menger J, Gross CM, Dietz R. Blood oxygen level-dependent magnetic resonance imaging in patients with stress-induced angina. *Circulation.* 2003; 108: 2219-2223.

9. Karamitsos TD, Leccisotti L, Arnold JR, Recio-Mayoral A, Bhamra-Ariza P, Howells RK, Searle N, Robson MD, Rimoldi OE, Camici PG, Neubauer S, Selvanayagam JB. Relationship between regional myocardial oxygenation and perfusion in patients with coronary artery disease: insights from cardiovascular magnetic resonance and positron emission tomography. *Circ Cardiovasc Imaging.* 2010; 3: 32-40.

10. Jahnke C, Gebker R, Manka R, Schnackenburg B, Fleck E, Paetsch I. Navigator-gated 3D blood oxygen level-dependent CMR at 3.0-T for detection of stress-induced myocardial ischemic reactions. *JACC Cardiovasc Imaging.* 2010; 3: 375-384.

11. Walcher T, Manzke R, Hombach V, Rottbauer W, Wohrle J, Bernhardt P. Myocardial perfusion reserve assessed by T2-prepared steady-state free precession blood oxygen level-dependent magnetic resonance imaging in comparison to fractional flow reserve. *Circ Cardiovasc Imaging.* 2012; 5: 580-586.

12. Beache GM, Herzka DA, Boxerman JL, Post WS, Gupta SN, Faranesh AZ, Solaiyappan M, Bottomley PA, Weiss JL, Shapiro EP, Hill MN. Attenuated myocardial vasodilator response in patients with hypertensive hypertrophy revealed by oxygenation-dependent magnetic resonance imaging. *Circulation.* 2001; 104: 1214-1217.

13. Gould KL, Lipscomb K, Hamilton GW. Physiologic basis for assessing critical coronary stenosis. Instantaneous flow response and regional distribution during coronary hyperemia as measures of coronary flow reserve. *Am J Cardiol.* 1974; 33: 87-94.

14. Gould KL. Does coronary flow trump coronary anatomy? *JACC Cardiovasc Imaging.* 2009; 2: 1009-1023.

15. Tonino PA, Fearon WF, De Bruyne B, Oldroyd KG, Leesar MA, Ver Lee PN, Maccarthy PA, Van't Veer M, Pijls NH. Angiographic versus functional severity of coronary artery stenoses in the FAME study fractional flow reserve versus angiography in multivessel evaluation. *J Am Coll Cardiol.* 2010; 55: 2816-2821.

16. Taylor AM, Jhooti P, Wiesmann F, Keegan J, Firmin DN, Pennell DJ. MR navigator-echo monitoring of temporal changes in diaphragm position: implications for MR coronary angiography. *J Magn Reson Imaging.* 1997; 7: 629-636.

17. Wacker CM, Hartlep AW, Pfleger S, Schad LR, Ertl G, Bauer WR. Susceptibility-sensitive magnetic resonance imaging detects human myocardium supplied by a stenotic coronary artery without a contrast agent. *J Am Coll Cardiol.* 2003; 41: 834-840.

18. Dharmakumar R, Arumana JM, Larson AC, Chung Y, Wright GA, Li D. Cardiac phase-resolved blood oxygen-sensitive steady-state free precession MRI for evaluating the functional significance of coronary artery stenosis. *Invest Radiol.* 2007; 42: 180-188.

19. Westbrook C, Roth C, Talbot J. MRI in Practice. Fourth Edition ed. West Sussex, UK: Wiley-Blackwell; 2011.

20. Voss HU, Zevin JD, McCandliss BD. Functional MR imaging at 3.0 T versus 1.5 T: a practical review. *Neuroimaging Clin N Am.* 2006; 16: 285-97, x.

21. Dharmakumar R, Arumana JM, Tang R, Harris K, Zhang Z, Li D. Assessment of regional myocardial oxygenation changes in the presence of coronary artery stenosis with balanced SSFP imaging at 3.0 T: theory and experimental evaluation in canines. *J Magn Reson Imaging.* 2008; 27: 1037-1045.

22. Kelle S, Nagel E. Cardiovascular MRI at 3 T. *Eur Radiol.* 2007; 17 Suppl 6: F42-7.

23. Tsaftaris SA, Zhou X, Tang R, Li D, Dharmakumar R. Detecting myocardial ischemia at rest with cardiac phase-resolved blood oxygen level-dependent cardiovascular magnetic resonance. *Circ Cardiovasc Imaging.* 2013; 6: 311-319.

24. Guensch DP, Fischer K, Flewitt JA, Yu J, Lukic R, Friedrich JA, Friedrich MG. Breathing manoeuvre-dependent changes in myocardial oxygenation in healthy humans. *Eur Heart J Cardiovasc Imaging.* 2014; 15: 409-414.

25. Wacker CM, Hartlep AW, Pfleger S, Schad LR, Ertl G, Bauer WR. Susceptibility-sensitive magnetic resonance imaging detects human myocardium supplied by a stenotic coronary artery without a contrast agent. *J Am Coll Cardiol.* 2003; 41: 834-840.

26. ISCHEMIA Study Organizers. ISCHEMIA trial - For Physicians. Available at: https://ischemiatrial.org/. Accessed April/21, 2014.

Chapter Seven: CONCLUSION AND CLOSING REMARKS

Ischemic heart disease is a complex condition that has multiple pathways through which pathological alterations in the human body can be identified. Measurements of myocardial oxygenation by OS-CMR is just one of the many diagnostic imaging approaches that build upon the foundation of years of research in this field, including angiography, nuclear SPECT, and perfusion imaging. The Holy Grail undoubtedly, would be to find the best technique or approach that confers little risk to the patient, is cost effective, is accurate in its assessment, and can predict long-term outcomes in patients at risk for ischemic heart disease. While the current research available for OS-CMR necessitates that the technique is not quite ready to be incorporated into the routine assessment of patients at risk for heart disease, the future however, is promising. New advances in MRI hardware will allow for stronger signal and more reproducible imaging that is non-invasive without the need for radiation. Furthermore, developments to improve imaging protocols will one day allow for assessment of myocardial oxygenation without use of pharmacological vasodilating agents. Therefore, OS-CMR, although still in the validation period, will one day be used as part of the routine armamentarium against cardiovascular disease. It is with the hope that the data from this thesis will contribute valuable information into the understanding and advancement of OS-CMR.

Chapter Eight: APPENDIX

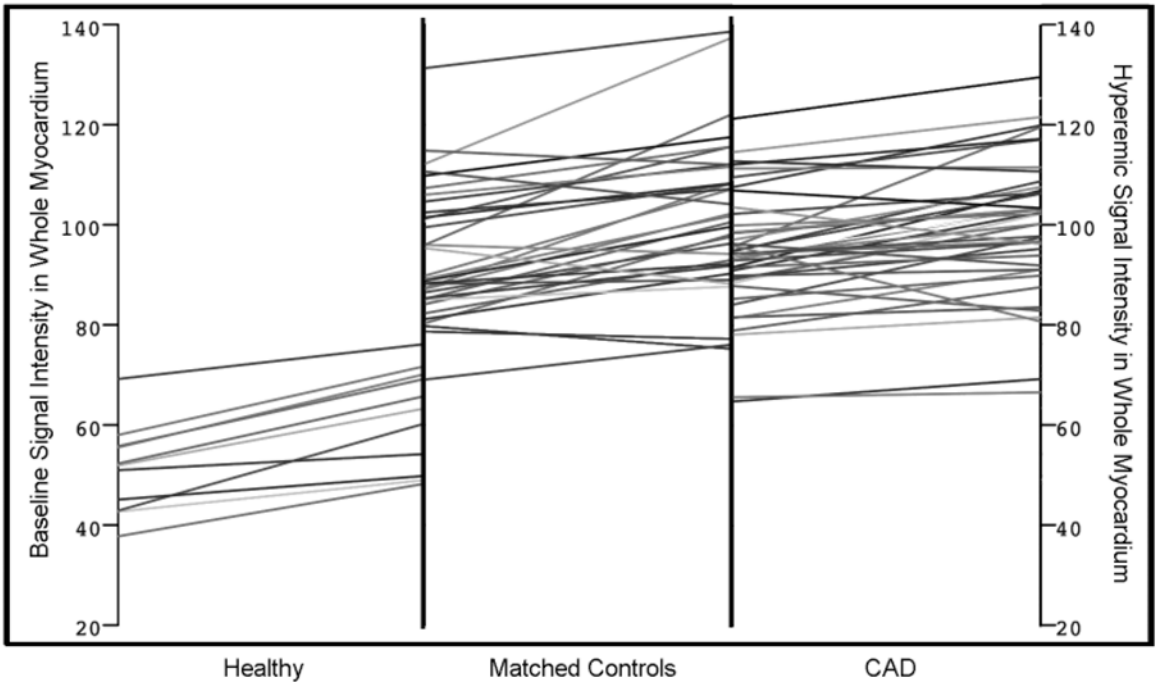

Figure A-1: Absolute OS-CMR signal intensity changes from baseline to hyperemia in whole myocardium (See Figure 3-2 in Chapter 3 Results – Regional assessment of myocardial oxygenation using Oxygen-Sensitive Cardiovascular CMR).

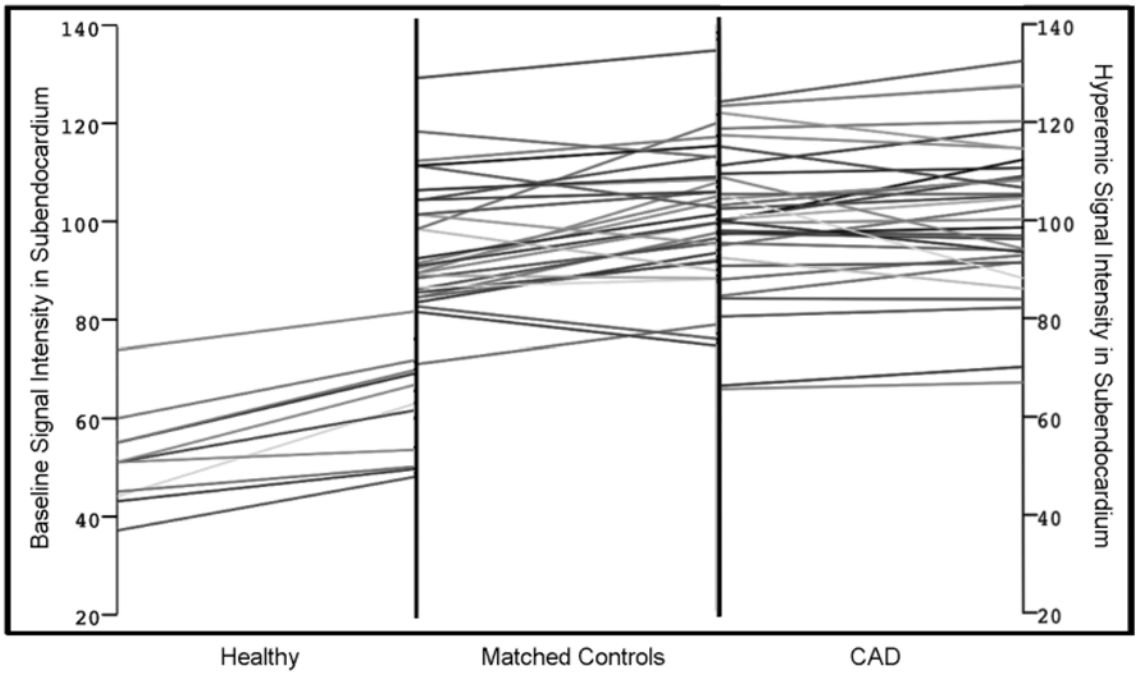

Figure A-2: Absolute OS-CMR signal intensity changes from baseline to hyperemia in subendocardium (See Figure 3-2 in Chapter 3 Results – Regional assessment of myocardial oxygenation using Oxygen-Sensitive Cardiovascular CMR).

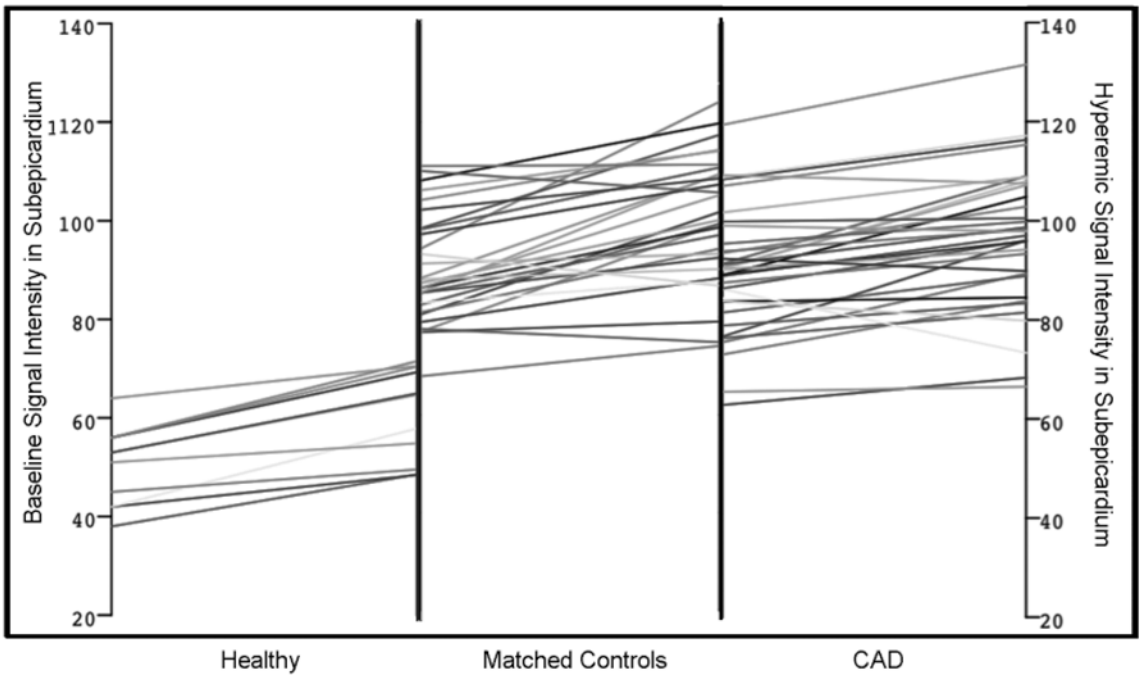

Figure A-3: Absolute OS-CMR signal intensity changes from baseline to hyperemia in subepicardium (See Figure 3-2 in Chapter 3 Results – Regional assessment of myocardial oxygenation using Oxygen-Sensitive Cardiovascular CMR).

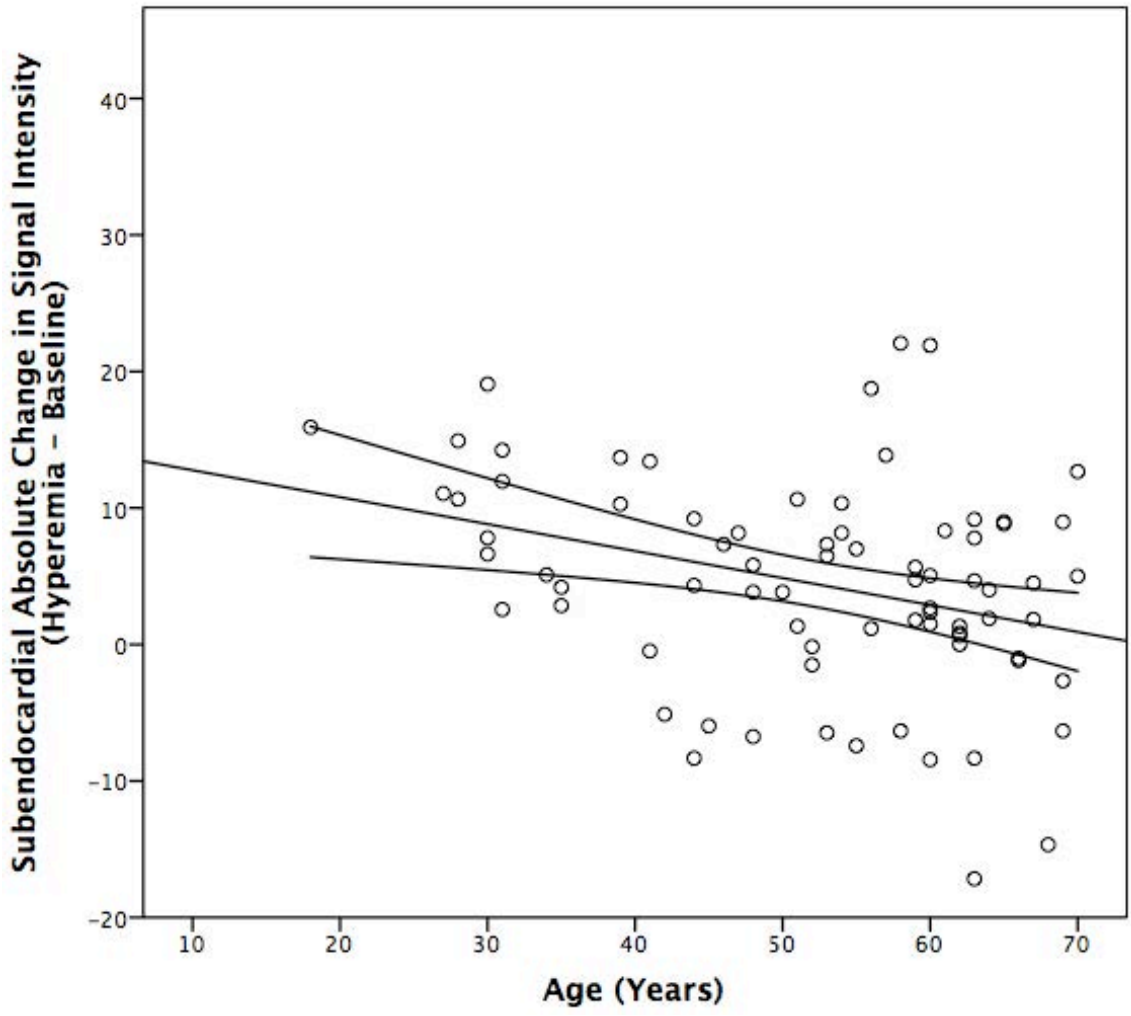

Figure A-4: Absolute OS-CMR signal intensity changes from baseline to hyperemia in subendocardium correlated to predictive variable, age (See Figure 3-5 in Chapter 3 Results – Regional assessment of myocardial oxygenation using Oxygen-Sensitive Cardiovascular CMR).

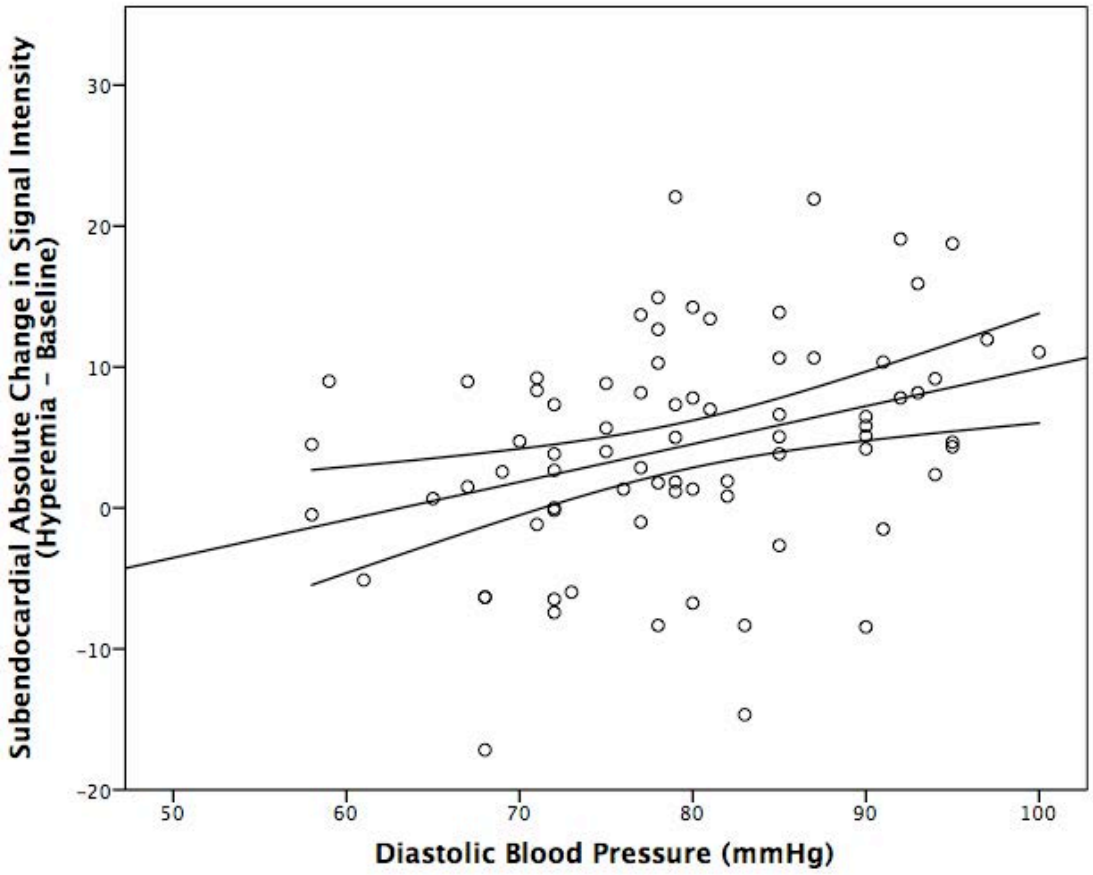

Figure A-5: Absolute OS-CMR signal intensity changes from baseline to hyperemia in subendocardium correlated to predictive variable, diastolic blood pressure (See Figure 3-6 in Chapter 3 Results – Regional assessment of myocardial oxygenation using Oxygen-Sensitive Cardiovascular CMR).
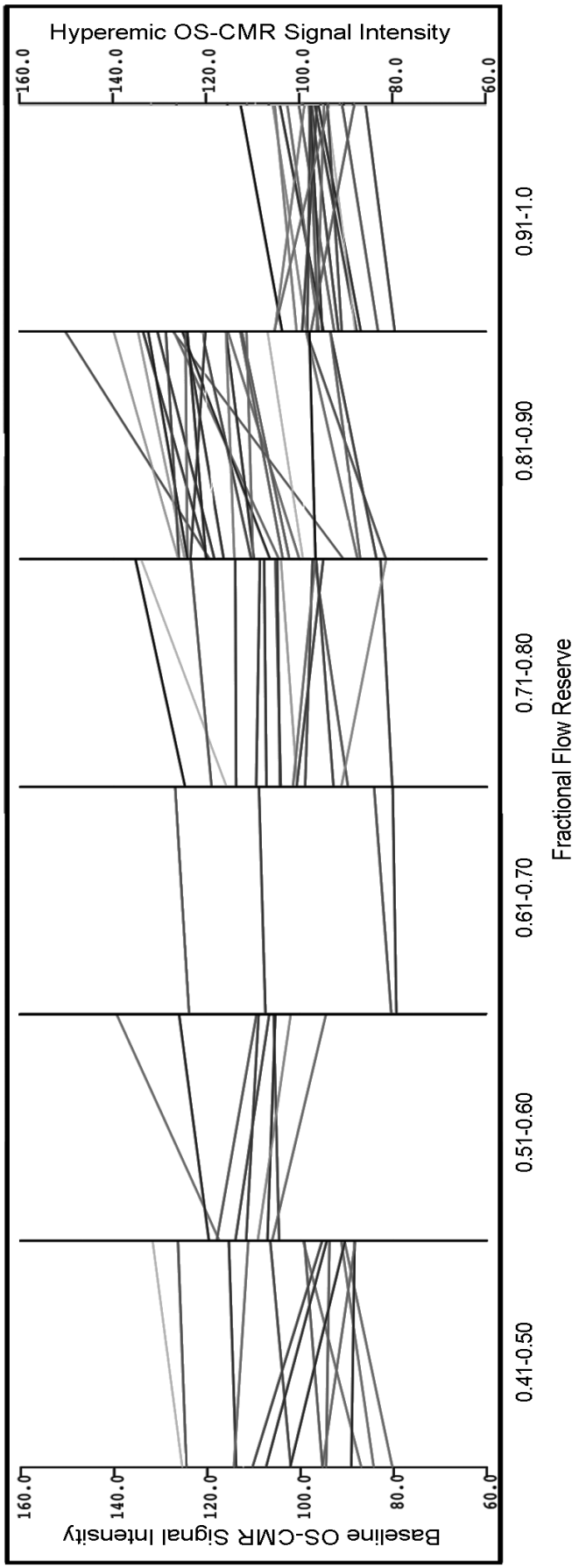
Figure A-6: Absolute changes from baseline to hyperemia of OS-CMR signal intensity as a function of FFR ranges (see Figure 4-2; Chapter 4 Results: Relationship of Vasodilator-Induced Changes of Myocardial Oxygenation with the Severity of Coronary Artery Stenosis…).